REVIEWS OF GEOPHYSICS, VOL. 24, NO. 2, PAGES 217–284, MAY 1986

Relations Among Subduction Parameters

RICHARD D. JARRARD

Lamont-Doherty Geological Observatory, Palisades, New York

Clues to the dynamics of the subduction process are found in the many measurable parameters of modern subduction zones. Based on a critical appraisal of the geophysical and geological literature, 26 parameters are estimated for each of 39 modern subduction zones. To isolate causal relationships among these parameters, multivariate analysis is applied to this data set. This analysis yields empirical quantitative relations that predict strain regime and strike-slip faulting in the overriding plate, maximum earthquake magnitude, Benioff zone length, slab dip, arc-trench gap, and maximum trench depth. Excellent correlation is found between length of the Benioff zone and the product of convergence rate and age of the downgoing slab. This relationship is consistent with the conductive heating model of Molnar et al. (1979), if the model is modified in one respect. The rate of heating of the slab is not constant; it is substantially slower during passage of the slab beneath the accretionary prism and overriding plate. The structural style in the overriding plate is determined by its stress state. Though the stress state of overriding plates cannot be quantified, one can classify each individual subduction zone into one of seven semiquantitative strain classes that form a continuum from strongly extensional (class 1, back-arc spreading) to strongly compressional (class 7, active folding and thrusting). This analysis indicates that strain class is probably determined by a linear combination of convergence rate, slab age, and shallow slab dip. Interplate coupling, controlled by convergence rate and slab age, is an important control on strain regime and the primary control on earthquake magnitude. Arc-parallel strike-slip faulting is a common feature of convergent margins, forming a forearc sliver between the strike-slip fault and trench. Optimum conditions for the development of forearc slivers are oblique convergence, a compressional environment, and a continental overriding plate. The primary factor controlling presence of strike-slip faulting is coupling; strongly oblique convergence is not required. The rate of strike-slip faulting is affected by both convergence obliquity and convergence rate. Maximum trench depth is a response to flexure of the underthrusting plate. The amount of flexural deflection at the trench depends on the vertical component of slab pull force, which is very sensitive to slab age and shallow slab dip. Shallow slab dip conforms to the cross-sectional shape of the overriding plate, which is controlled by width of the accretionary prism and duration of subduction. Deep slab dip is affected by the mantle trajectory established at shallow depth but may be modified by mantle flow. Much of the structural complexity of convergent margins is probably attributable to terrane juxtaposition associated with temporal changes in both forearc strike-slip faulting and strain regime. Empirical equations relating subduction parameters can provide both a focus for future theoretical studies and a conceptual and kinematic link between plate tectonics and the geology of subduction zones.

CONTENTS

Paper number 5R0903.
8755-1209/86/005R-0903$15.00

INTRODUCTION

The subduction process involves a complex interplay of forces that affect plate motions and determine the structural style behind trenches. Clues to the dynamics of the subduction process are found in the many measurable parameters that

describe modern subduction zones. Traditionally, the major causal relationships within subduction zones have been sought through either theoretical or qualitative analyses. Quantitative physical models have been unable to establish these relationships with confidence, due to uncertainties in essential physical quantities (e.g., mantle viscosity and shear stress) and physical complexity of the subduction process. Many qualitative relationships have been proposed, usually based on a plausible causal relationship and an apparent correlation between two subduction parameters for modern subduction zones. Often these proposed relationships are mutually exclusive.

The variety of structural environments and plate interactions at convergent margins is well illustrated by a brief comparison of the Marianas and Peru-Chile plate boundaries. The Marianas is characterized by slowly converging, old oceanic crust that is underthrusting a tensional overriding plate at an almost vertical dip, accompanied by relatively modest maximum earthquakes ($M_w = 7.2$). In contrast, the Peru-Chile plate boundary is characterized by rapidly converging, younger oceanic crust that is underthrusting a compressional overriding plate at a nearly horizontal dip, accompanied by very large ($M_w = 8.6$–9.5) earthquakes. Most other current convergent margins can be described as lying somewhere on a continuum between the Marianas and Peru-Chile extremes [*Uyeda and Kanamori*, 1979].

This apparent continuum is as much a disadvantage as an advantage in the search for quantitative models that will allow the use of some characteristics of convergent margins to predict others. Some parameters (e.g., convergence rate, absolute motion, age of the arc, and age of the underthrusting plate) can be thought of as independent variables, which will not necessarily occupy similar positions on a continuum of trench styles. Other parameters (e.g., length and dip of the slab, compression or tension in the overriding plate, trench depth, and maximum earthquake magnitude) are dependent variables which are probably controlled by the independent variables but usually not in a manner predictable on theoretical grounds.

The purpose of this paper is to evaluate and possibly revise models relating the dependent and independent parameters above. First, however, it is necessary to compile our present best estimates of these parameters for as many modern subduction zones as possible. Often at least one parameter is not reliably known for a subduction zone, but relationships among some of the other parameters for that trench can still be utilized. Empirical equations relating independent and dependent variables are derived through multiple regression analysis. These empirical equations, in conjunction with theoretical studies, may help us to isolate the primary cause-and-effect relationships between subduction parameters. Given the coefficients of this set of equations, one can also estimate values for unknown or poorly known variables from well-known variables for the same subduction zones.

For times prior to the Tertiary, empirical equations may permit the estimation of plate tectonic variables (convergence rate, crustal age, absolute motion) from geologic variables (compression/extension, arc curvature, arc-trench gap) that are decipherable from the rock record. An example is the history of the vanished Tethyan Ocean. The correlation coefficients for the equations provide estimates of the reliability with which modern trench parameters can be predicted from other parameters. It does not necessarily follow that ancient trench parameters can be predicted with equal reliability. Thus an important step preceding application of the relationships to the prediction of past unknown parameters is the testing of the models on the histories of relatively well known regions (e.g., western North America).

The Pacific margins are now known to be largely a mosaic of displaced terranes, with complex geologic histories somehow related to changing rates and directions of convergence. Progress in describing the kinematics of plate convergence, both Pliocene-Pleistocene [*Le Pichon*, 1968; *Minster et al.*, 1974; *Chase*, 1978*a*; *Minster and Jordan*, 1978] and Tertiary [*Atwater and Molnar*, 1973; *Engebretson*, 1982], has not been accompanied by comparable progress in predicting terrane motions [e.g., *Stone et al.*, 1982; *Alvarez et al.*, 1980]. In this paper I consider only one group of terrane motions: those occurring within the overriding plate. Two other types of terrane motion are beyond the scope of this paper: accretion resulting from buoyant portions of the underriding plate colliding with the trench [e.g., *Nur*, 1983] and the diffuse deformation behind trenches that results from continent-continent collision [*Dewey and Bird*, 1970]. Instead, the emphasis is on relationships during "normal" subduction.

The scope of this project is necessarily more limited than the entire range of relations among subduction parameters. Discussion of the tectonics of the accretionary prism is beyond the scope of this paper; some of the recent advances in this subject are summarized by *Davis et al.* [1983], *von Huene* [1984], and *Hilde* [1983]. Implications of subduction parameters for the driving force of plate motions [e.g., *Forsyth and Uyeda*, 1975], mineralization [*Uyeda and Nishiwaki*, 1980], uplift in the overriding plate [*McGetchin et al.*, 1980; *Parrish*, 1983], sea level changes [*Malumián and Ramos*, 1984], and arc geochemistry [*Green*, 1980] are similarly beyond the scope of this paper.

THE DATA

The subduction zones considered in this analysis are shown in Figure 1. Table 1 indicates preferred values for the key parameters for these subduction zones; values shown in parentheses are considered to be too poorly known for inclusion in statistical analyses. Some parameters are not listed because they can be simply derived from a combination of other listed parameters. Table 2 lists all variables considered and their units.

It must be emphasized that assignment of a value for some parameters is based on a subjective evaluation of sometimes conflicting evidence; this is particularly true for strain classes. Consequently, one may anticipate that some of the data of Table 1 will be subject to substantial revision. Because of the large number of subduction zones analyzed, such revisions are unlikely to have a major impact on the results of statistical analyses.

Choice of Subduction Zones

Selection of the subduction zones in Table 1 is partially influenced by the concept of slab segmentation. For example, four trench segments are used for the Peru-Chile Trench, corresponding to the segments seismically determined by *Isacks and Barazangi* [1977]. Segmentation on the lateral scale of 500 to 1500 km seems well established for South America and Central America [*Isacks and Barazangi*, 1977; *Burbach et al.*, 1984]. The boundaries of these segments are zones of slab warping rather than tearing [*Hasegawa and Sacks*, 1980; *Grange et al.*, 1984; *Bevis and Isacks*, 1984]. Much smaller

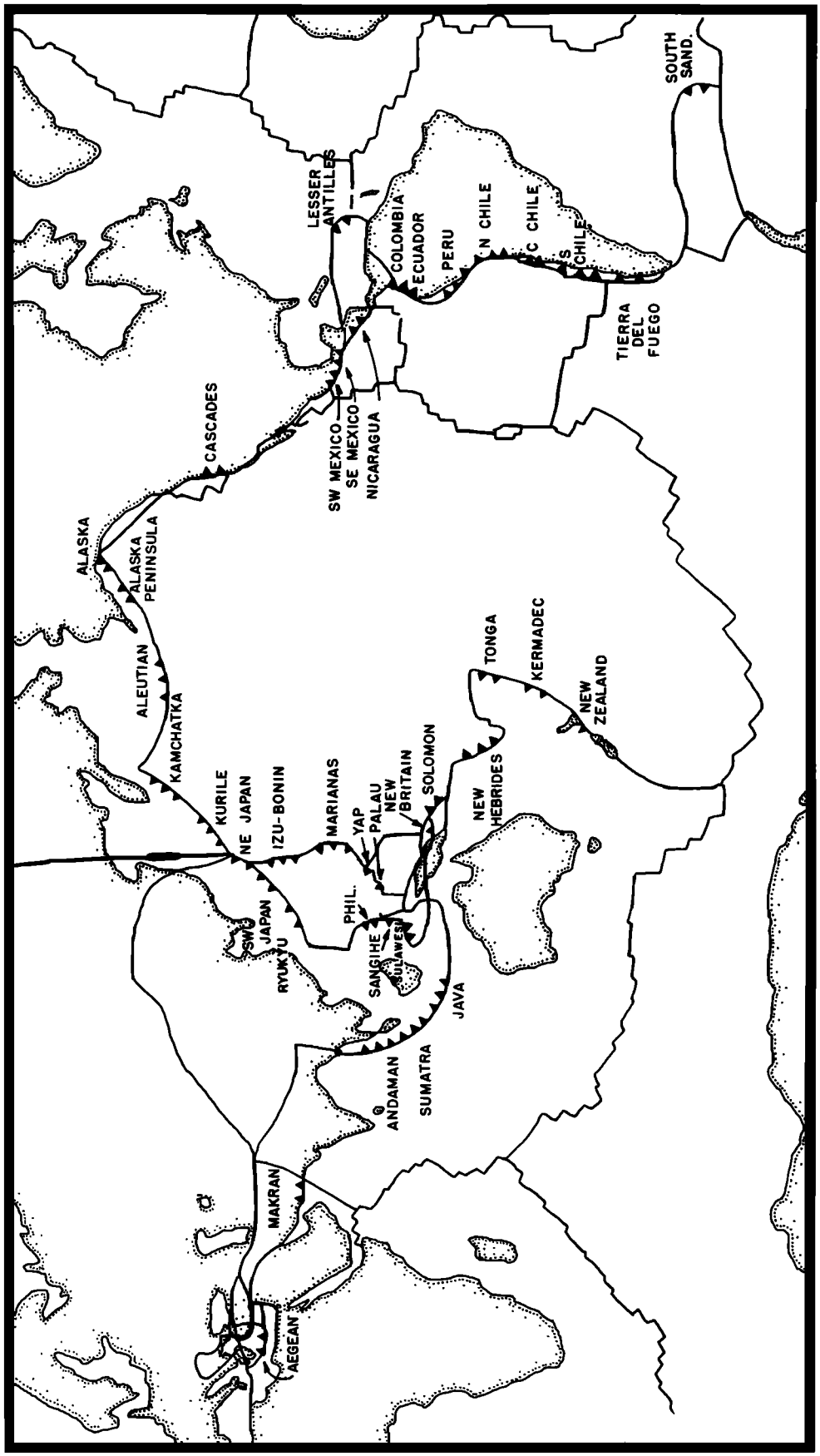

Fig. 1. Mercator projection of present continental outlines and major plate boundaries. Subduction zones considered in this analysis are labeled and indicated by solid triangles.

TABLE 1.

Symbol	Subduction Zone: Segment Name	Reference Position Lat., Long.	Upper Plate: Azimuth Perpendicular Trench	Crust	Strain Class	Slab: DipS	Slab: DipI	Slab: DipD	M_w'	Trench: Depth	Trench: Δd	Slab Extent: Horizontal	Slab Extent: Depth	Length Slab
AEG	Aegean	36, 22	49	C	1	20 ± 3	25 ± 3	43	...	...	...	290	180	340
MAK	Makran	24, 60	6	C	...	8	12	...	...	...	...	430	80	440
AND	Andaman	9, 92	84	C	1	19	22	...	...	...	...	270	140	310
SUM	Sumatra	−2, 98	53	C	5	16	19	50 ± 5	7.9	5.9	0.7	370	170	380
JAV	Java	−11, 112	8	T	5	16	21	63	7.1	7.45	2.15	570	630	870
SUL	North Sulawesi	2, 122	185	O	2	18	26	68	...	...	...	290	300	460
SAN	Sangihe	3, 126	280	O	...	...	...	56	...	...	...	620 ± 20	670	920
PHL	Philippine	8, 127	258	T	...	43	41	...	...	10.06	4.10	100	130 ± 20	170
RYK	Ryukyu	25, 128	318	C	2	19	23	45	8.0	7.51	1.97	300	280	440
SJP	SW Japan	33, 135	329	C	5	10	...	...	8.6	4.8	0.19	330	75	345
NZL	New Zealand	−40, 178	300	C	3	12	18	50	7.8	...	...	440	270	540
KER	Kermadec	−34, −178	289	O	1	23	30	71	8.1	10.05	4.49	330	500	640
TON	Tonga	−22, −174	290	O	1	23	28	57	8.3	10.8	5.24	670	650	940
NHB	New Hebrides	−17, 167	73	O	1	36	44	73	7.9	7.07	2.56	190	280	330
SOL	Solomon	−7, 155	40	O	4	35 ± 5	42 ± 5	84 ± 4	...	8.94	4.42	300	520	600
NBR	New Britain	−6, 150	338	O	1	30 ± 5	35 ± 5	58	...	8.24	3.73	250	290	390
PAL	Palau	7, 135	315	O	(4)	...	...	...	...	8.05	3.55	...	...	...
YAP	Yap	8, 138	295	O	(4)	...	...	...	...	8.53	...	...	...	...
MAR	Marianas	17, 148	270	O	1	19	24	81	7.2	9.66	4.95	310	700	860
IZU	Izu-Bonin	30, 143	262	O	2	22	28	65 ± 9	7.2	9.70	3.54	580	600	860
NJP	NE Japan	39, 144	282	C	6	15	19	27	8.35	8.0	1.95	1340	600	1480
KUR	Kurile	45, 152	320	C	(5)	22	28	50	8.8	9.78	4.27	650 ± 40	600 ± 40	890
KAM	Kamchatka	53, 162	301	C	(5)	19	25	54	9.0	7.5	2.0	580 ± 30	600 ± 30	860
ALU	Central Aleutians	50.5, 180	0	O	4	25	31	64	8.7	7.14	1.64	250	270	370
AKP	Alaska Peninsula	60, −152	285	C	4	9	13	51	...	...	...	470	155	530
ALA	Alaska	62, −149	328	C	6	7	10	...	9.1	...	...	620	160	650
CAS	Cascades	45, −125.5	87	C	4	9 ± 4	...	...	...	...	...	97	34	103
WMX	SW Mexico	17, −103	23	C	6	19	25	...	...	5.29	1.79	210	90	230
SMX	SE Mexico	15.5, −97	19	C	6	14	18	53	...	5.12	1.62	400	210	480
NIC	Middle America	12.5, −91	24	C	3	30	38	65	8.4	6.66	2.56	170	210	280
ANT	Lesser Antilles	16, −59	250	O	4	16	22	51	7.5	7.0	1.8	320	200	410
COL	Colombia	5, −78	105	C	6	22	26	38	8.8	4.0	0.8	315	215	390
ECU	Ecuador	−2, −81	101	C	6	...	(31)	(32)	...	...	...	...	210	...
PER	Peru	−10, −80	55	C	6	14	13	(5)	8.6	6.3	1.6	710	190	730
NCH	North Chile	−21, −71	67	C	7	20	21	30	8.65	8.05	3.35	810	600	1040
CCH	Central Chile	−30, −72	100	C	7	16	14	(5)	8.65	6.4	2.2	720	180	730
SCH	South Chile	−38, −74	105	C	5	13	16	30	9.5	4.7	0.6	490	170	520
TDF	Tierra del Fuego	−49, −77	93	C	(3)	...	...	...	...	...	...	...	...	...
SCO	South Sandwich	−58, −24	270	O	1	31	38	67	7.0	8.26	3.81	220	250	350

*C, *Chase* [1978*a*]. M, *Minster and Jordan* [1978].

scale segmentation has also been proposed, often on the basis of apparent offsets in the volcanic arc, but is not assumed in this analysis. For example, proposed slab segmentation on the lateral scale of 100–300 km in Central America [*Stoiber and Carr*, 1973] and Makran [*Dykstra and Birnie*, 1979] is not detected seismically [*Burbach et al.*, 1984; *Jacob and Quittmeyer*, 1979].

Many subduction zones are not included in Table 1 or subsequent discussions, generally because current subduction is incipient, waning, or unknown. Most of these excluded subduction zones are in Southeast Asia, a region of rapid Neogene transitions in plate interactions [e.g., *Hamilton*, 1979]. In the Philippines region, the Manila, North Philippine, Halmahera, and Cotabato trenches are excluded. Subduction in the North Philippines appears to be changing polarity from eastward subduction at the Manila Trench to westward subduction at the northern Philippine Trench. Differing opinions on the timing of arc polarity changes in this region are summarized by *Uyeda and McCabe* [1983]. Just south of the Philippines are the Halmahera and Cotabato subduction zones. The Halmahera Trench is undergoing arc polarity reversal; its Benioff zone is very limited in both along-strike and vertical extent [*Hamilton*, 1979; *Cardwell et al.*, 1980]. Both current and past activity of the nearby Cotabato Trench are unknown, and no Benioff zone has been resolved [*Hamilton*, 1979; *Cardwell et al.*, 1980]. Farther south, the Banda and Seram subduction zones are excluded because of continental collision, unknown slab age, and uncertain convergence rates and directions [*Cardwell and Isacks*, 1978; *Bowin et al.*, 1980]. Farther east, the New Guinea, West Melanesian, and Trobriand trenches are excluded because of uncertain present and past activities [*Fitch*, 1972; *Hamilton*, 1979; *Ripper*, 1982; *Weissel et al.*, 1982]. The nearby Mussau Trench is excluded because subduction appears to have begun only about 1 million years ago [*Hegarty et al.*, 1982]. The region between the Solomon and New Hebrides subduction zones is potentially usable but has received little study, except in the South Solomon region which is complicated by ridge subduction and has only shallow seismicity [*Weissel et al.*, 1982].

Several subduction zones outside Southeast Asia are also excluded. The Benioff zone of southwest New Zealand exhibits possible breakage and rotation, probably caused by the rapid changes in subduction history here [*Smith and Davey*, 1984]. The "Bucaranga segment" of Venezuela has a detectable Be-

Subduction Parameters

Age Slab	Age Tip	Time Since Tip Subducted C	Time Since Tip Subducted M	Descent Angle C	Descent Angle M	Arc Age Arc	Arc Gap $a-t$	Arc RC	Rate Perpendicular to Trench* V_c C	V_c M	V_{cba} C	V_{cba} M	V_{oa} C	V_{oa} M	Rollback C	Rollback M
...	...	8.9	10.0	73	100	11 ± 1	210	2	0.7	0.4	3.8	3.4	−1.1	−0.1	2.0	2.9
97	87	11.9	11.9	...	...	46	480	...	3.7	3.7	3.7	3.7	−0.3	−0.4	−0.3	−0.4
72 ± 5	51 ± 7	9.7	11.9	...	...	100 ± 40	270	7	2.1	1.4	3.2	2.6	−0.5	−0.1	0.6	1.1
55 ± 5	45 ± 7	6.1	6.8	50	48	27 ± 3	300	22	6.2	5.6	6.2	5.6	0.0	−0.2	0.0	−0.2
138 ± 10	107 ± 10	10.6	10.7	68	61	27 ± 3	300	39	8.2	8.1	8.2	8.1	0.7	−0.3	0.7	−0.3
38	9 ± 6	15.3	15.3	...	...	7 ± 4	150	6	3.0	3.0	3.0	3.0	...	...	...	...
...	...	...	...	...	...	13 ± 5	...	7	...	...	...	...	0.6	0.0	...	...
...	...	3.7	2.1	...	...	6 ± 4	250	18	4.6	8.0	4.6	8.0	0.3	0.1	0.3	0.1
49	37 ± 7	14.7	9.2	64	45	55 ± 5	150	14	3.0	4.8	3.0	4.8	1.1	0.0	1.1	0.0
21	3 ± 3	26.5	17.2	...	...	175 ± 5	300	4	1.3	2.0	1.3	2.0	1.2	0.0	1.2	0.0
98	97 ± 5	16.4	18.0	24	18	21 ± 3	280	50	3.3	3.0	3.3	3.0	−3.7	−5.3	−3.7	−5.3
113	114	10.4	11.3	87	79	30 ± 2	165	50	5.1	4.7	10.5	10.1	−2.5	−4.0	2.9	1.4
120 ± 20	110 ± 30	9.6	10.0	74	67	24 ± 7	185	45	7.5	7.2	12.5	12.2	−1.2	−2.7	3.8	2.3
52	45	...	...	...	...	8 ± 3	140	30	(8.8)	(8.4)	(9.0)	(8.6)	(6.3)	(6.7)	(6.8)	(6.9)
50 ± 10	45 ± 16	5.0	5.1	98	96	8 ± 3	100	12	12.0	11.8	12.0	11.8	3.0	2.5	3.0	2.5
50 ± 10	47 ± 14	2.7	2.6	76	70	8 ± 3	125	6	4.3	4.5	14.7	14.9	−5.8	−7.1	4.6	3.3
31 ± 3	...	...	...	...	...	45 ± 5	...	3	0.6	0.6	0.6	0.6	−3.2	−7.1	−3.2	−7.1
33	...	...	...	...	...	45 ± 5	...	4.5	1.2	1.2	1.2	1.2	−3.9	−8.1	−3.9	−8.1
155	134	9.4	17.1	87	66	45 ± 5	225	8	6.0	3.4	10.3	7.7	−3.3	−6.5	1.0	−2.2
146	122	11.3	13.6	57	45	45 ± 5	210	85	7.6	6.3	7.6	6.3	−1.2	−3.0	−1.2	−3.0
130	94	14.9	14.5	29	28	115 ± 5	300	11	9.9	10.2	9.9	10.2	0.7	0.2	0.7	0.2
119	89	10.2	10.4	56	49	82 ± 16	190	15	8.7	8.6	8.7	8.6	1.1	−0.2	1.1	−0.2
90 ± 15	72 ± 18	9.8	10.0	60	54	153 ± 10	225	15	8.8	8.6	8.8	8.6	1.0	0.0	1.0	0.0
54	48 ± 15	6.2	6.3	84	72	56 ± 6	190	14	6.0	5.9	6.0	5.9	2.1	0.9	2.1	0.9
46	50 ± 10	12.9	13.6	46	48	160 ± 10	400	14	4.1	3.9	4.1	3.9	−0.5	−0.3	−0.5	−0.3
46	48 ± 10	10.3	10.7	...	...	160 ± 10	470	...	6.3	6.1	6.3	6.1	1.2	0.8	1.2	0.8
8	9	3.0	3.0	...	...	175 ± 10	280	90	3.4	3.4	3.4	3.4	2.2	1.8	2.2	1.8
15	14	3.9	4.1	...	...	90 ± 3	240	15	5.9	5.6	5.9	5.6	1.9	2.1	1.9	2.1
14	14	6.7	6.9	65	68	90 ± 3	380	15	7.2	7.0	7.2	7.0	1.6	1.9	1.6	1.9
23 ± 5	23 ± 5	4.3	4.4	59	63	100 ± 10	150	10	6.5	6.4	6.5	6.4	−0.8	−0.3	−0.8	−0.3
68	78	11.1	11.1	80	67	48 ± 4	260	5.5	3.7	3.7	3.7	3.7	1.8	1.1	1.8	1.1
15 ± 10	8 ± 10	5.7	5.6	56	59	242 ± 5	270	173	6.8	6.9	6.8	6.9	2.5	2.9	2.5	2.9
32	...	...	...	...	...	226 ± 19	275	6	7.9	7.7	7.9	7.7	2.5	3.0	2.5	3.0
45	57	8.9	9.5	...	...	226 ± 19	...	19	8.2	7.7	8.2	7.7	1.5	2.7	1.5	2.7
82	112	10.4	11.7	35	43	226 ± 19	300	140	10.0	8.9	10.0	8.9	1.6	2.9	1.6	2.9
48	68	7.4	8.6	...	...	226 ± 19	...	10	9.8	8.5	9.8	8.5	2.0	2.8	2.0	2.8
26 ± 5	30 ± 6	5.4	6.3	36	42	226 ± 19	300	55	9.7	8.2	9.7	8.2	1.7	2.5	1.7	2.5
20	...	...	...	...	...	150 ± 6	230	7	2.3	2.1	2.3	2.1	1.2	2.3	1.2	2.3
49	74	4.6	4.6	116	111	30	150	3	0.9	0.9	7.9	7.9	−0.4	−1.1	6.6	5.9

nioff zone, but it has a poorly known slab age, a complex history of plate interactions, and possibly anomalously thick crust in the slab [*Pennington*, 1981]. A very short trench segment in the West Scotia region may have active back-arc spreading but is otherwise poorly known [*Barker and Hill*, 1981]. The western portion of the Aleutian subduction zone is excluded because it is almost purely strike-slip [e.g., *Chase*, 1978*a*; *Minster and Jordan*, 1978]. The Wrangell segment of Alaska is excluded because it is uncertain whether the short Benioff zone is part of the Pacific plate or Yakutat block [*Stephens et al.*, 1984]. All regions of continent-continent collision are excluded (e.g., Burma, Hindu Kush, Romania, and Spain).

Several subduction zones are described in the literature by various names. The South Sandwich zone is also called the Scotia Arc. Southwest Japan is also referred to as Shikoku or as Nankai Trough. Java, Sumatra, and Andaman are collectively called the Sunda Arc. The Aegean zone is also called Hellenic Trench or Greece. The portion of the Middle America Trench considered here is Nicaragua. The portion of the West Indies (Caribbean Trench) considered here is the Lesser Antilles.

Arc Curvature

Nearly all subduction zones are segmented into arc-shaped portions in plan view. On the overriding plate a similar arcuate band of active volcanoes is almost always present, usually located above that portion of the down going slab that is 100 to 125 km deep. The geometry of most volcanic arcs and trenches can be closely fit by a portion of a small circle on the earth's surface [*Frank*, 1968], defining a radius of curvature for the arc or trench. Radii of curvature for arcs are tabulated in Table 1; most have been determined by *Tovish and Schubert* [1978] and are not remeasured here. Virtually all arc curvatures are convex with respect to the underthrusting plate.

Although the radius of curvature of either the arc or the trench could be utilized as a clue to subduction zone dynamics, arc curvature is preferable for two reasons. First, arc curvature is more readily estimated for ancient subduction zones in the rock record than is trench curvature. Second, trench location and curvature are easily modified by regional variations in forearc accretion [*Karig et al.*, 1976]. In contrast, continental and island arcs generally closely follow a Benioff zone contour, usually about 100 to 125 km. Trench radii of

TABLE 2. Subduction Parameters Considered

	Variable	Symbol	Units
Slab	length of Benioff zone	L_s	km
	horizontal extent of Benioff zone	...	km
	maximum depth of Benioff zone	...	km
	shallow dip (to 60-km depth)	DipS	deg
	intermediate dip (to 100-km depth)	DipI	deg
	deep dip (150–400 km)	DipD	deg
	descent angle of slab into mantle	DipU	deg
	slab age at trench	A_s	m.y.
	age of slab tip	A_t	m.y.
	time since slab tip subducted	T_{st}	m.y.
	trench depth	d	km
	relative trench depth	Δd	km
	slab pull force	F_s	N/m
Upper plate	duration of subduction (arc age)	A_a	m.y.
	arc-trench gap	gap	km
	arc radius of curvature	RC	deg
	strain regime	strain	class
	modern strike-slip direction	...	...
Relative motion (rates perpendicular to trench)	convergence rate	V_c	cm/yr
	convergence rate including back-arc spreading	V_{cba}	cm/yr
	rollback (absolute motion, forearc)	V_{sa}	cm/yr
	absolute motion, overriding plate	V_{oa}	cm/yr
	absolute motion, underriding plate	V_{ua}	cm/yr
	obliquity of convergence	ϕ	deg
	slip vector residual	θ	deg
	maximum cumulative earthquake moment	M_w'	...

curvature have been tabulated by several authors [*Aoki*, 1974; *DeFazio*, 1974; *Laravie*, 1975; *Ness and Johnson*, 1976]. A disadvantage of considering arc curvature rather than trench curvature is that not all trenches have currently active arcs. The arcs of southwest Japan, Tierra del Fuego, Central Chile, Peru, North Sulawesi, Yap, and Palau are currently inactive. Their radii of curvature are estimated on the basis of Neogene (first five) or mid-Tertiary (last two) volcanism. Subsequent correlation of Tertiary radii of curvature with modern plate parameters clearly requires caution.

The radius of curvature can be precisely determined for arcs if it is less than about 15° to 20°, but it is much less precise for arcs with large radii of curvature. Some determinations are subjective; for example, the Kurile-Kamchatka region may be a single arc with a radius of curvature of 15°, or it may be two arcs with radii of curvature of 60° to 90°. Several of the subduction zones of Table 1 are tentatively considered to be portions of larger continuous arcs with a single radius of curvature: Kurile-Kamchatka, Java-Sumatra, and Kermadec–New Zealand.

No estimate of radius of curvature is made for the Alaskan and Makran subduction zones, because the Neogene volcanism in both regions is discontinuous along strike and somewhat diffuse [*Jacob et al.*, 1977; *Jacob and Quittmeyer*, 1979].

Benioff Zone Geometry

Most subduction zones have well-defined Benioff zones, with earthquake hypocenter distributions that indicate the geometry of the subducting plate. Except at shallow depths, focal mechanisms indicate that the hypocenters originate within the top 30 km of the subducting plate rather than at its boundaries [*Isacks and Molnar*, 1971]. With exceptionally well located hypocenters (e.g., northeast Japan, East Aleutians) it is sometimes possible to detect a double-plane Benioff zone [*Hasegawa et al.*, 1978; *House and Jacob*, 1983], with an upper zone of earthquakes originating just below the upper surface of the slab and a lower zone originating about 30 km below the upper surface of the slab. More often the hypocenters appear to come from throughout the upper 30 km of the slab, making estimation of the location of the top somewhat subjective. Figure 2 shows the cross-sectional geometry of the subducting slab for most of the subduction zones of Table 1. The location of the top surface of the slab is based on the original author's interpretation for most subduction zones. For some subduction zones the location was interpreted by this author from published cross-sectional plots of hypocenters. Three subduction zones have Benioff zones too short to be determined: Yap, Palau, and Tierra del Fuego.

Most cross sections utilize hypocenters located with a worldwide network rather than local networks. Although local networks are capable of locating earthquakes of smaller magnitude than those detected by a worldwide network, they may yield biased estimates of slab dip. For example, the Benioff zones of Nicaragua and Costa Rica have been determined both with local and global networks; the result is a steeper deep dip with the local networks [*Burbach et al.*, 1984]. The deep dip of the New Zealand Benioff zone was originally thought to be 67°, based on a local network [*Ansell and Smith*, 1975]. However, by using velocities that were about 11% faster for raypaths within the slab than outside the slab, *Adams and Ware* [1977] found that station residuals were reduced and that relocated hypocenters indicated a corrected deep dip of only 50°.

Cross sections of many Benioff zones were determined by *Isacks and Barazangi* [1977]. Other Benioff zones come from a variety of sources: Aegean [*Richter and Strobach*, 1978], Alaska [*Lahr*, 1975], Andaman [*Mukhopadhyay*, 1984], Cen-

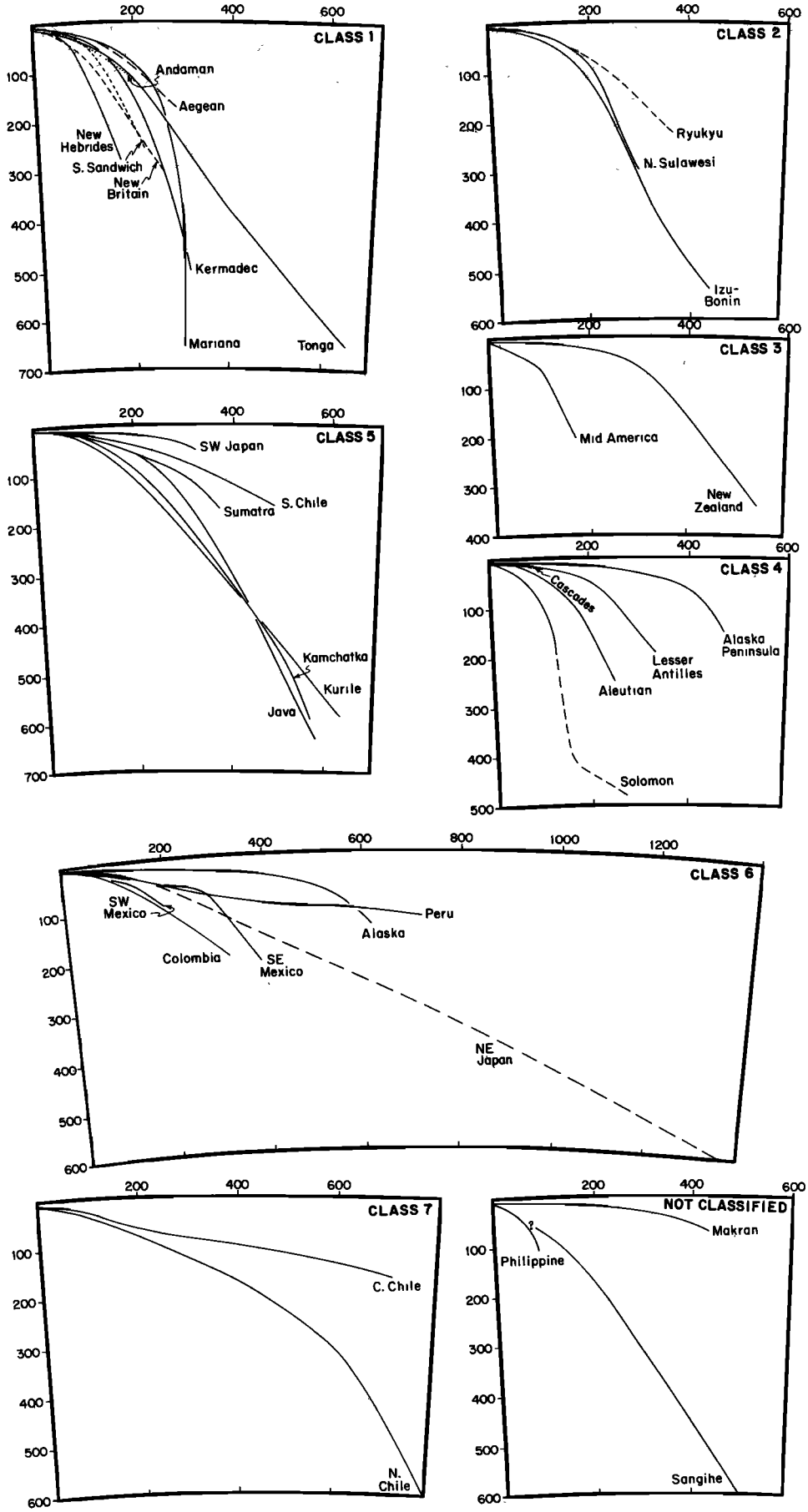

Fig. 2. Cross-sectional profiles of the tops of seismically defined subducted slabs. Each profile starts (left) at the trench and ends (right) at the tip of the Benioff zone. Slab position is interpolated across seismic gaps. Slab segments that are interpreted as disconnected from the main slab are not shown. Profiles are grouped according to strain classification of Table 3.

tral Aleutians [*Engdahl*, 1977], Colombia [*Pennington*, 1981], East Alaska Peninsula [*Lahr*, 1975], Ecuador [*Bevis and Isacks*, 1984], Java (K. R. Newcomb and W. R. McCann, unpublished manuscript, 1986), Lesser Antilles [*McCann and Sykes*, 1984], Makran [*Jacob and Quittmeyer*, 1979], Middle America [*Burbach et al.*, 1984], New Britain [*Pascal*, 1979], New Zealand [*Adams and Ware*, 1977; *Katz*, 1982], northeast Japan [*Ichikawa*, 1966; *Hasegawa et al.*, 1978; *Yoshii*, 1979], Philippines [*Cardwell et al.*, 1980], Ryukyu [*Utsu*, 1974; *Katsumata and Sykes*, 1969], Sangihe [*Cardwell et al.*, 1980], Solomon [*Pascal*, 1979], South Sandwich [*Brett*, 1977], South Mexico [*Burbach et al.*, 1984], southwest Japan [*Kanamori*, 1972], and Sumatra (K. R. Newcomb and W. R. McCann, unpublished manuscript, 1986).

Problems arise in the determination of Benioff zones for the Cascades, Ecuador, Philippines, and Sangihe. The Cascades Benioff zone, beneath Washington and Oregon, is poorly defined by seismicity [*Smith and Knapp*, 1980]; the combination of seismicity and gravity modeling permits its location to be estimated down to only 20-km depth [*Jachens and Griscom*, 1983]. The Ecuador Benioff zone has poor shallow seismic control and a deep Benioff zone with an anomalous strike approximately perpendicular to the trench [*Pennington*, 1981; *Bevis and Isacks*, 1984]. The southern Philippines Benioff zone was once thought to extend to great depth. However, more detailed work shows that the deep seismicity is actually related to underthrusting of the nearby Molucca Sea beneath the Sangihe Trench and that the Philippine Trench is a very young trench with only a shallow Benioff zone [*Cardwell et al.*, 1980].

Benioff zone geometry is parameterized in Table 1 according to both length and dip. Dip is not constant within a slab; characteristically, dip increases gradually from the trench to about 80- to 150-km depth and remains almost constant below this depth. The "inflection point," or greatest change in dip, usually occurs between 60 and 100 km. Table 1 includes (whenever possible) the dip from the trench to 60-km depth ("shallow dip," or DipS), dip from the trench to 100-km depth ("intermediate dip," or DipI), and the deep dip (DipD, usually of part or all of the interval from 100 to 400 km). The dip to 60-km depth was selected because the basalt/eclogite transition occurs at about 60 km [*Ahrens and Schubert*, 1975], substantially increasing the density of the slab and presumably also affecting the dip inflection point near this depth. The dip to 100-km depth was selected because arc volcanism generally occurs above the portion of the slab at about 100- to 125-km depth; thus this dip may be estimable in ancient arc-trench systems. Thickness of the overriding plate, though generally unknown, is probably about 80–100 km for most subduction zones; thus DipI is also an approximate measure of the average dip of the contact zone between underriding and overriding plates. Estimates of DipI are usually much more accurate than estimates of DipS, because it is often difficult to distinguish intraplate from interplate earthquakes near 60-km depth. Because of this uncertainty and the very high correlation between DipS and DipI, DipS is omitted from most subsequent statistical analyses. Both the 60-km and 100-km measured dips are based simply on the horizontal distances from the trench to points above the 60-km and 100-km portions of the slab; thus they do not represent dips at these depths but approximate average dips from the trench to these depths. For simplicity, depth at the trench is assumed to be zero in Figure 2 and calculations of shallow and intermediate dip; in actuality it is usually 5–10 km and varies substantially along the trench axis [e.g., *Grellet and Dubois*, 1982; *Hilde and Uyeda*, 1983]. It should be noted that DipS, DipI, and DipD do not correspond to the epicenter depths normally referred to as shallow, intermediate, and deep.

For brevity in this paper, the term "slab" is used instead of "seismically active portion of the underthrust plate." This usage does not imply that the underthrust plate ends at the seismically determined "slab tip." For example, seismic activity beneath the Marianas extends to 700-km depth, but a detectable velocity anomaly to at least 1000-km depth indicates the presence of much deeper subducted plate [*Creager and Jordan*, 1985].

Also shown in Table 1 are the maximum horizontal extent of the slab, the maximum depth of slab earthquakes, and the length of the slab (measured along its upper surface). Maximum slab depth and horizontal extent are included only for completeness; they are not subsequently considered in this paper. Caution must be exercised in comparing any of these three parameters between different subduction zones, as the deepest hypocentral depths detected for a Benioff zone depend somewhat on the duration of the available data and on whether a worldwide or a local network was utilized. For example, the maximum depth of hypocenters from the South Sandwich Arc was extended from 170 km [*Barker*, 1972] to 250 km [*Brett*, 1977] by a single earthquake; slab length and horizontal extent were similarly affected. Another extreme example is northeast Japan, whose 1480-km slab length is the longest of any current slab; this length is reduced by 560 km if the Benioff zone of *Yoshii* [1979] is used, omitting two very deep epicenters of *Ichikawa* [1966]. *Farrar and Lowe* [1978] defined the tip of the slab not on the basis of the single deepest earthquake but on the basis of a percentage of total earthquakes. This criterion partially ameliorates the problems above; it is not followed herein because one cannot accurately determine which shallow earthquakes are within the lower plate.

Estimates of slab length, depth, and horizontal extent may also be biased by seismic gaps, generally in the depth range of about 300 to 500 km. In some cases (e.g., Java, North Chile, and Solomon) a deeper seismic zone appears geometrically to be a continuation of the shallower Benioff zone. For these subduction zones it is assumed that the gap is caused by a change in downdip stress [*Isacks and Molnar*, 1971] rather than a break in the slab. In contrast, deep epicenters beneath the Peru, New Hebrides, and New Zealand subducted slabs and some of the deep epicenters beneath the New Britain, Solomon, and Tonga slabs are not geometrically continuous with the shallower slabs and are not included in estimates of Benioff zone parameters. Deep seismicity beneath the Tonga subduction zone has been attributed to collision of the modern slab with part of an older slab [*Hanus and Vanek*, 1978]. It is possible that the anomalous deep seismicity of the Tonga, New Britain, New Hebrides, and Solomon Benioff zones is a relict of the late Miocene arc polarity reversals that have occurred in these regions.

Compression/Extension

Of the variables listed in Table 1, perhaps the most difficult to quantify is the strain regime of the overriding plate. The stress (or strain) at any point in a subduction zone is optimally described as a stress (or strain) tensor. Because of data limitations, determination of the full stress or strain tensor is gen-

erally not possible. Instead, a more limited description of strain is used here, focussing on the azimuth of the maximum horizontal component of strain. Thus a "compressional environment" is usually manifested by thrusting or reverse faulting with maximum compression approximately perpendicular to the trench. However, the less common environment in which normal faults strike perpendicular to the trench is also considered compressional, because the maximum horizontal compression is perpendicular to the trench. Similarly, a strike-slip focal mechanism is considered compressional if the maximum horizontal compression is perpendicular to the trench. "Extensional environments" are those with maximum horizontal extension approximately perpendicular to the trench, usually manifested by normal faults striking parallel to the trench or by back-arc spreading.

A variety of stress and strain indicators is used to characterize the strain regime of the overriding plate, including focal mechanisms, Quaternary faults and folds, volcanic vent alignments, overcoring, and presence of back-arc spreading. These indicators and their limitations have been described by *Richardson et al.* [1979] and by *Zoback and Zoback* [1980]. This approach has two principal limitations. First, motion on a preexisting fault is not a reliable indicator of exact stress direction. This limitation is probably not critical, as the focus here is on component of strain perpendicular to the trench rather than precise stress direction, and data from many faults are usually used for a single subduction zone. Second, data types vary from "instantaneous" (e.g., focal mechanisms and overcoring) to Quaternary and sometimes slightly older in age (e.g., faults, folds, and volcanic vent alignments). We must therefore assume that the state of stress has not changed substantially over the past 2 m.y.

Subduction zones can be ranked to some extent in terms of their positions along a continuum from strongly extensional to strongly compressional [*Uyeda and Kanamori*, 1979]; however, no quantitative estimation of either their stress states or strain regimes is possible. Therefore the strain regimes of the overriding plates in modern subduction zones are considered semiquantitatively by grouping them into seven strain classes (Table 3). Class 1 subduction zones are the most extensional, with active back-arc spreading. Class 2 zones are those with very slow, incipient, or waning back-arc spreading. Class 3 zones are mildly extensional, with normal faulting but no substantial crustal thinning. Class 4 zones include two different environments that are difficult to rank relatively on an extension/compression continuum: "neutral" zones, with little evidence of either compression or extension, and zones with a mildly compressional arc and forearc and mildly extensional back-arc. Class 5 zones are mildly compressional, with gentle folding or with somewhat more reversed than normal faulting. Class 6 zones exhibit consistent folding and/or reverse faulting. Class 7 zones are the most compressional, with substantial folding, faulting, and foreland thrusting.

These seven strain classes are merely arbitrary points along the extension/compression continuum. Although relative ranking of the strain classes is straightforward, it is not possible to infer that the different classes constitute equally spaced points along either stress or strain continua. For instance, the data may justify the separation of only five strain classes, with classes 2 and 3 combined and classes 6 and 7 combined.

Because of the assumptions made and the widely varying quality and quantity of strain indicators for individual subduction zones, some zones have a classification uncertainty of one class. For example, folds, reverse faults, and thrusts are often difficult to date precisely; a class 7 subduction zone may have all three of these active but may be classified as class 6, because no known Quaternary sediments are offset by the thrust(s).

TABLE 3. Strain Classification

Class	Description	Subduction Zones
1	active back-arc spreading	South Sandwich New Britain Marianas New Hebrides Tonga Kermadec Andaman Aegean
2	very slow back-arc spreading	Ryukyu Izu-Bonin North Sulawesi
3	mildly tensional	Middle America New Zealand (Tierra del Fuego?)
4a	neutral	Lesser Antilles Solomon Cascades (Palau?) (Yap?)
4b	gradient: mildly tensional to mildly compressional	Aleutians Alaska Peninsula
5	mildly compressional	SW Japan Java Sumatra South Chile (Kurile?) (Kamchatka?)
6	moderately compressional	Colombia Ecuador Peru Alaska NE Japan SE Mexico (SW Mexico?)
7	very strongly compressional	North Chile Central Chile

Subduction zones with slow, incipient, or waning back-arc spreading (class 2) are tentatively considered to be lower in tensional stress than subduction zones with active, well-developed back-arc spreading (class 1), yet this assumption may not always be correct. All known examples of back-arc spreading are short-lived, as shown by the compilations of *Weissel* [1981] and of *Taylor and Karner* [1983]. It is not known whether the early stage of a back-arc spreading episode is lower tensional stress than the active-spreading stage; we know only that it is lower extensional strain. The same uncertainty applies to distinguishing class 2 subduction zones from class 3 zones, those with a tensional back-arc environment but no significant extension.

Throughout the discussions of compressional and extensional environments in this paper, the focus is on the back-arc, arc, and (to a lesser extent) forearc portions of the overriding plate. The variations in strain regime of the underriding plate, accretionary prism, and plate interior are ignored. The interiors of most plates are in a state of horizontal compression

[*Sykes and Sbar*, 1973; *Richardson et al.*, 1979]; this environment is generally not difficult to distinguish from zones of strain associated with modern subduction. Strain in the accretionary prism may be substantially different from strain in the forearc. For example, normal faulting is common in the inner trench slope of Alaska Peninsula [*Fisher*, 1979], Peru-Chile [*Thornburg and Kulm*, 1981; *Shepherd and Moberly*, 1981], and northeast Japan [*von Huene et al.*, 1982], though compression dominates part or all of the more landward portions of these overriding plates. Recent exciting work on the dynamics of accretionary prisms suggests that much of their variability (including erosion or active accretion, and thrusting or normal faulting) may be explicable ultimately in terms of a "bulldozer" model in which one of the most important variables is pore pressure [*Davis et al.*, 1983]. Analysis of states of stress in the subducting plate, the accretionary prism, and the plate interior is important but beyond the scope of this paper.

In the remainder of this section, evidence is compiled for the classification of modern subduction zones into the seven strain classes, from class 1 (active back-arc spreading) to class 7 (active thrusting). Two subduction zones are not classified because of insufficient evidence for their strain regime: Palau and Yap. Four subduction zones are tentatively classified but are not used in subsequent statistical analyses, because of limited data concerning their strain regime: Kamchatka, Kuriles, southwest Mexico, and Tierra del Fuego. The Philippine and Sangihe subduction zones are excluded because arc-arc collision may dominate the stress pattern [*Silver and Moore*, 1978]. Similarly, the Makran subduction zone is excluded because continent-continent collision in the flanking Zagros and Hindu Kush regions may mask the normal stress pattern.

Subduction zones with a highly extensional environment in the overriding plate (class 1) exhibit back-arc spreading, the formation of oceanic crust in a marginal basin behind the arc [*Karig*, 1971; *Packham and Falvey*, 1971]. Initial rifting may occur on either side of the arc or may split the arc [*Taylor and Karner*, 1983]; subsequent arc volcanism is always between the trench and the growing marginal basin. *Taylor and Karner* [1983] have listed all known Neogene back-arc basins and compared their characteristics to "normal" oceanic spreading. Older back-arc basins are often difficult to distinguish from trapped portions of "normal" oceanic crust [*Weissel*, 1981; *Taylor and Karner*, 1983]. Recognition of ancient back-arc spreading is even more difficult if the basin was collapsed by subsequent compression [e.g., *Dalziel*, 1981].

Active back-arc spreading is currently occurring behind the New Britain, South Sandwich, New Hebrides, Tonga, Kermadec, Mariana, and Andaman subduction zones. Bismarck Sea spreading, behind the New Britain Trench, has been active for the last 3.5 m.y. at a total opening rate of 13.2 cm/yr [*Taylor*, 1979], the fastest modern back-arc spreading. The most recent episode of back-arc spreading in the East Scotia Sea, behind the South Sandwich Trench, began about 8 m.y. ago with a full rate of 5 cm/yr, accelerating to the current 7 cm/yr rate about 4 m.y. ago [*Barker*, 1972; *Barker and Hill*, 1981]. Back-arc spreading in the Mariana Trough began about 6 to 7 m.y. ago, with a full rate of 4.3 cm/yr [*Hussong and Uyeda*, 1982; *Bibee et al.*, 1980]. Back-arc spreading in the Andaman Sea has averaged 3.7 cm/yr for the last 13 m.y.; prior spreading is poorly known because of very subdued magnetic anomalies [*Curray et al.*, 1982; *Lawver and Curray*, 1981]. A few focal mechanisms from behind the Andaman-Nicobar Ridge are interpreted by *Mukhopadhyay* [1984] as indicating forearc thrusting; however, only one of these indicates pure thrusting, and assignment to the upper plate is generally uncertain. In spite of possible minor thrusting, presence of back-arc spreading causes the Andaman subduction zone to be included in the highly extensional class 1.

Back-arc spreading behind the New Hebrides and Tonga trenches is apparently complicated by proximity to a 90° bend in the Australia/Pacific plate boundary; both involve three-plate back-arc systems. Spreading on the Fiji Plateau, behind the New Hebrides Trench, began about 10 m.y. ago [*Malahoff et al.*, 1982], rotating the New Hebrides Arc clockwise from its former position behind the Vitiaz Trench. Back-arc spreading rates are best known for the southern ridge of the three-plate system, where a 7.0-cm/yr full rate for the last 8 m.y. is observed [*Malahoff et al.*, 1982]. The present 500- to 700-km separation of the spreading axis from the New Britain Trench is much wider than any other current back-arc spreading region; concurrent incipient spreading is also apparently occurring just behind the arc, in the Coriolis Trough [*Dubois et al.*, 1978; *Carney and Macfarlane*, 1982]. Spreading in the Lau Basin, behind the Tonga Trench, began about 6 m.y. ago; the full rate for the last 2 m.y. is 7.6 cm/yr [*Weissel*, 1980*b*]. Magnetic anomalies have not been identified in the portion of the Lau Basin corresponding to the reference location of Table 1. Because this portion of the Lau Basin is only two-thirds the width of the region interpreted by *Weissel* [1980*b*], a full rate of only 5 cm/yr is assumed for back-arc spreading here. Just south of the Lau Basin, back-arc spreading in the Havre Trough began about 2 m.y. ago, with a full rate of 5.4 cm/yr [*Malahoff et al.*, 1982].

For every active back-arc basin except the Andaman, the spreading direction is approximately perpendicular to the trench. Indeed, the oblique spreading and major transform faults of the Andaman Sea are often interpreted [*Curray et al.*, 1982; *Weissel*, 1981; *Taylor and Karner*, 1983] as evidence that it may not be appropriate to consider the origin of this marginal basin as typical back-arc spreading.

Active thinning of continental crust is occurring in a diffuse zone behind the Hellenic Trench in the Aegean Sea. Focal mechanisms [*McKenzie*, 1978], overcoring [*Paquin et al.*, 1984], and Quaternary faults [*Mercier*, 1981] indicate a dominantly north-south extensional strain in the back-arc region, with both extension and compression in the more heterogeneous forearc. This extension is not simple back-arc spreading; high heat flow and crustal thickness variations indicate that extension occurs both in the forearc and behind the Aegean Arc in a laterally heterogeneous pattern [*McKenzie*, 1978; *Le Pichon and Angelier*, 1981]. At present it is not possible to unambiguously attribute this extension to subduction dynamics, as the back-arc region is complicated by collision of a Turkish plate with the Eurasian plate [*McKenzie*, 1978]. Subduction-related extension of about 4 cm/yr [*Le Pichon and Angelier*, 1981] is tentatively assumed herein.

Three subduction zones exhibit incipient or very slow back-arc spreading (class 2): Ryukyu, Izu-Bonin, and North Sulawesi. The Okinawa Trough, behind the Ryukyu Trench, has a single normal fault focal mechanism [*Fitch*, 1972], shallow focus earthquakes, high heat flow, thinned continental crust, and a thick sediment fill with growth-faulted grabens indicative of currently slow extension [*Herman et al.*, 1979; *Lee et al.*, 1980; *Letouzey and Kimura*, 1985]. Spreading here may have been more rapid in the Pliocene, based on apparent patterns in the lower portion of the sediment fill [*Herman et*

al., 1979]. Extension may have begun about 6–9 m.y. ago [*Letouzey and Kimura*, 1985].

Incipient or very slow back-arc spreading is evident in the Bonin Arc, where fresh, glassy tholeiites have been dredged from 40-km-wide grabens [*Taylor et al.*, 1984]. Total extension appears to decrease northward from near the actively spreading Mariana Trough to near the north end of the arc at the Nankai Trough [*Karig and Moore*, 1975]. The northern end of the Bonin Arc has been broken by north-south compression approximately parallel to the arc [*Karig and Moore*, 1975; *Bandy and Hilde*, 1983]. This compression, tentatively dated as Miocene [*Bandy and Hilde*, 1983], is probably unrelated to the modern stress pattern, though strike-slip and reverse-faulting focal mechanisms are common [*Ichikawa*, 1980].

Slow or waning spreading may be occurring in the Gorontalo Basin and Gulf of Tomini, behind the North Sulawesi Trench. *Hamilton* [1979] infers a Neogene opening of this region, following late Miocene or Pliocene arc polarity reversal [*Hamilton*, 1979; *Silver et al.*, 1983*a*]. Four shallow focal mechanisms from within the Gorontalo Basin indicate normal faulting [*Cardwell et al.*, 1980], suggesting that the region may still be extensional.

The Middle America and North New Zealand subduction zones represent class 3, with a tensional environment but no significant extension. It is plausible to assume that the Middle America and possibly New Zealand subduction zones have had a relatively constant subduction environment long enough to proceed to the spreading stage, unless they are truly lower in tensional stress than the slow-spreading arcs. However, this assumption is not testable. Indeed, the Tonga–Kermadec–New Zealand trench system may be experiencing a southward propagation of back-arc spreading, beginning about 5 or 6 m.y. ago in the Lau Basin [*Weissel*, 1980*b*], about 2 m.y. ago in the Havre Trough [*Malahoff et al.*, 1982], and less than 2 m.y. ago in the Taupo Zone of New Zealand [*Ballance*, 1976]. The Taupo Zone of volcanism and minor extension is laterally continuous with the Kermadec Arc rather than the actively spreading Lau Basin; consequently, *Ballance* [1976] concluded that the Taupo Zone is not a zone of incipient back-arc spreading. However, back-arc spreading does not always begin behind the arc [*Taylor and Karner*, 1983]. Active back-arc spreading in the Taupo Zone was inferred by *Stern* [1985], on the basis of tensional tectonics, geodetic evidence of slow historic extension, anomalously thin crust, and very high heat flow. The future evolution of the Taupo zone is uncertain, but the current environment is apparently one of tension but minor extension. Tension is not confined to the Taupo Zone; the East Coast fold belt of North New Zealand is also currently extensional [*Katz*, 1982]. However, this zone should probably be considered as accretionary prism and therefore may not be relevant to the strain regime of the overriding plate. The North New Zealand extensional environment changes rapidly to strike-slip and oblique compression farther south [*Carter and Norris*, 1976], beyond the region considered here.

The Middle America (Nicaragua) subduction zone is similar to North New Zealand, with arc volcanism occurring within an actively subsiding region, the Nicaragua depression [*McBirney and Williams*, 1965]. North striking tensional fractures associated with Recent volcanoes suggest mild east-west extensional strain in the vicinity of the arc [*McBirney and Williams*, 1965; *Dewey and Algermissen*, 1974; *Nakamura*, 1977]. Young strike-slip faults and thrusting have been observed in seismic lines near the east Nicaragua shelf, but the most recent deformation is clearly extensional [*Bowland*, 1984]. This extensional graben formation may be part of a transtensional plate boundary [*Christofferson*, 1983] rather than a part of the subduction-related extensional environment of Nicaragua. South of Nicaragua, collision of Panama with South America creates a complex pattern of deformation of the Caribbean plate [*Pennington*, 1981]. Whether this collision affects the Nicaraguan stress pattern is not known. *Burbach et al.* [1984] present 10 published and new focal mechanisms from Nicaragua; of these, nine indicate shallow thrusting near the contact between the two plates or compression in the downgoing slab. The only mechanisms that are clearly within the overriding plate are one strike-slip mechanism of *Burbach et al.* [1984] and the strike-slip mechanism of the 1972 Managua earthquake [*Dewey and Algermissen*, 1974].

Class 4 subduction zones include two types: those with little evidence of either compression or extension and those that exhibit back-arc extensional strain but arc and forearc compression. Examples of the former are the Cascades, Lesser Antilles, and Solomons; examples of the latter are Central Aleutians and Alaska Peninsula. Recognition of strain gradients across subduction zones led *Nakamura and Uyeda* [1980] to conclude that the continuum in subduction strain regime hypothesized by *Uyeda and Kanamori* [1979] is overly simplistic. While recognizing that this is true and that the two types of class 4 subduction zones may be fundamentally different, both are nevertheless tentatively considered to represent an intermediate point on a continuum from totally extensional to totally compressional overriding plates.

The strain regime of the Aleutians is better documented in the eastern Aleutians than in the Central Aleutian zone chosen as a reference location. Focal mechanisms and volcanic vent alignments in the eastern Aleutians and Alaska Peninsula indicate horizontal compression roughly perpendicular to the trench in the forearc and arc, possibly changing to extension behind the arc [*Nakamura et al.*, 1980]. The paucity of data from the back-arc regions of the Aleutians and Alaska Peninsula make the inferred transition from compression to extension highly tentative for these regions [*Nakamura et al.*, 1980]. In general, reverse faults are dominant in the forearc of the Alaska Peninsula, with normal faults dominant in the back-arc [*Nakamura et al.*, 1980]. However, the transition from compression to extension is probably at least 250 km behind the arc of the Alaska Peninsula, as thrusting and reverse faulting accompany strike-slip motion on the Holitna and Togiak-Tikchik faults, both thought to be still active [*Lathram et al.*, 1974]. Pliocene to Recent folding occurs in the forearc, attenuating to minor folding in the arc and only tilting beyond the Holitna and Togiak-Tikchik faults [*Lathram et al.*, 1974]. In the Aleutian Arc the most recent folding appears to be early Miocene to late Pliocene, with Quaternary faulting and uplift but no folding [*Lathram*, 1974].

The Cascades, Lesser Antilles, and Solomons represent the "neutral" group of class 4 strain environments. The Pacific Northwest (including the Cascades Arc) has north-south compression approximately parallel to the trench, resulting in strike-slip and thrust focal mechanisms [*Zoback and Zoback*, 1980] and active north-south trending normal faults [*Hammond*, 1979]. This environment, in which the least principal strain is perpendicular to the trench, includes both the forearc (Olympic Peninsula) and the back-arc (Columbia Plateau).

Classification of the Cascades as "neutral" is therefore clearly an oversimplification. The Cascades may be more appropriately considered as mildly extensional [*Cross and Pilger*, 1982], or the subduction-related strain pattern may be dominated by the more pervasive strike-slip environment of the westernmost United States and Canada.

The Lesser Antilles experienced forearc folding until the Pliocene but apparently no Quaternary deformation [*Tomblin*, 1974], except in the accretionary prism. Faulting in the Solomons is dominated by late Pliocene to Quaternary strike-slip roughly parallel to the arc, with Pliocene-Pleistocene normal faulting common and reverse faulting occasional near the arc [*Coleman and Hackman*, 1974]. Back-arc folding of Miocene to Recent age is observed only on the islands of Santa Ysabel and Malaita [*Coleman and Hackman*, 1974], east of the segment studied and behind a portion of the Solomon Trench currently experiencing ridge-crest subduction [*Weissel et al.*, 1982].

Southwest Japan, Sumatra, and possibly Java, South Chile, and Tierra del Fuego represent the class 5 subduction zones, which are considered to be mildly compressional. *Ichikawa* [1980], synthesizing the results of over 1500 focal mechanism solutions from the Japanese region, found generally low seismicity in Southwest Japan, with a slight dominance of normal faulting over reverse faulting in the forearc and with reverse faulting dominant farther from the trench, in the Japan Sea. Late Quaternary thrusting with a right-lateral component has occurred on the Median Tectonic Line, and some mid-Pleistocene thrusting occurs on faults north (landward) of the Median Tectonic Line [*Matsumoto and Kimura*, 1974]. Synthesizing the results of active faults, focal mechanisms, and late Quaternary dikes, *Nakamura and Uyeda* [1980] find that the direction of principal horizontal strain is roughly parallel to the direction of plate convergence, except near the Ryukyu Arc where a gradual change to the class 2 extensional environment of the Ryukyus occurs. Analysis of older faults and dikes suggests that southwest Japan was also compressional from 11 to 2 m.y. ago, though with a somewhat different azimuth of maximum compression. Southwest Japan had a compressional forearc and extensional back-arc (class 4) from about 21 to 11 m.y. ago [*Nakamura and Uyeda*, 1980].

The back-arc region of eastern Sumatra exhibits moderate but pervasive Pliocene-Pleistocene folding and some Quaternary thrusting, both with compression approximately parallel to the plate convergence direction [*Katili*, 1974]. Similarly, compression along the northwest coast is indicated by two focal mechanisms [*Fitch*, 1972]. Except for these two back-arc regions, little or no evidence of compression or tension is found in Sumatra [*Katili*, 1974].

The Java segment, adjacent to Sumatra, also appears to be mildly compressional. A single focal mechanism, from beneath the arc near the eastern end of Java, indicates intraplate thrusting [*Fitch*, 1972]. Deformation is active in the foreland basin of North Java and the nearby offshore area, with mild open folds in north central Java and the South Madura Basin in the Quaternary, and Miocene to Quaternary northward directed folds and thrusts in the West Java Basin [*Hamilton*, 1979]. However, much of this deformation may be attributable to magmatism rather than subduction-related compression, as the folds arc around large volcanic edifices [*Hamilton*, 1979]. *Chotin et al.* [1985] conclude that south central Java is experiencing north-south to northeast-southwest compression, mostly accommodated on many strike-slip faults, though *Hamilton* [1979] found no evidence of major strike-slip faults on Landsat images. Back-arc thrusting east of Java is probably caused by continental collision of Australia with the Banda subduction zone and is not relevant to the strain regime of Java [*Silver et al.*, 1983*b*].

The adjacent segments of South Chile and Tierra del Fuego are considered mildly compressional (class 5), though seismicity and other relevant data are sparse for Tierra del Fuego. The boundary between these two segments is chosen as the intersection of the Chile Rise with the Chile Trench. The forearc in South Chile appears to be mildly extensional, with both uplift and subsidence. The only focal mechanism available from South Chile is from the arc and indicates compression [*Jordan et al.*, 1983]. Andean volcanoes in a portion of the South Chile segment (37.5°–41.5°S) exhibit flank crater distributions suggesting a maximum horizontal compression direction of N65°E $\pm$ 10° [*Nakamura*, 1977], relatively close to the present convergence direction of N79°E. Active gentle folding is observed in the foreland of South Chile between 33° and 34.5°S, while farther south extensive Pliocene-Pleistocene foreland volcanism occurs with only minor faulting and folding [*Jordan et al.*, 1983]. Foreland volcanism continues south through the Tierra del Fuego segment. Episodes of extensive plateau basalt volcanism away from the main arc, such as the Pliocene-Pleistocene episode in South Chile and Tierra del Fuego, are interpreted by *Malumián and Ramos* [1984] as indicative of an extensional regime, consistent with the generalization of *Christiansen and Lipman* [1972] and of *Lipman et al.* [1972] concerning stress environments of basaltic and andesitic magmas. Indeed, fissures in the Pleistocene Palei-Aike volcanic field have east-west and northwest-southeast orientations [*Skewes and Stern*, 1979], suggesting extension approximately perpendicular to the trench. The strain regime of Tierra del Fuego is considered to be too poorly known for inclusion in subsequent statistical analyses, but the available data suggest the possibility of a gradual southward decrease in compression through both South Chile and Tierra del Fuego.

Class 6 subduction zones, characterized by active folding and reverse faulting with no significant extension, include northeast Japan, Alaska, the three adjacent segments Colombia, Ecuador, and Peru, and possibly southeast Mexico, the Kuriles and Kamchatka. Thrusting, if present, appears to be confined to preexisting fault zones.

The strain regime of northeast Japan is well known: the maximum compression direction is approximately parallel to convergence direction throughout northeast Japan, based on vent distributions of numerous polygenetic volcanoes [*Nakamura and Uyeda*, 1980] and on several hundred focal mechanisms [*Ichikawa*, 1980; *Maki*, 1983]. Most epicenters within the overriding plate occur in the forearc, between the coast and the trench, with reversed focal mechanisms about twice as common as normal [*Ichikawa*, 1980]. Rare inland focal mechanisms are almost all reversed [*Ichikawa*, 1980]. Quaternary folding is observed [*Matsuda and Kitamura*, 1974], and a leveling net demonstrates that both folding and reverse faulting are occurring in the inner zone of northeast Japan, near the Japan Sea [*Mizoue et al.*, 1982]. The current strain regime of the Japan Sea is poorly known; a single focal mechanism indicates compression [*Hager*, 1983]. A tensional environment for both Japan and the nearby Kuriles has been inferred by some authors [e.g., *Molnar and Atwater*, 1978; *England and Wortel*, 1980], based on Cenozoic back-arc spreading in the Japan Sea and Kurile Basin. However, neither basin is cur-

rently active, and Neogene change from extension to compression in northeast Japan is now well documented [*Nakamura and Uyeda*, 1980].

The strain regimes of the nearby Kurile and Kamchatka segments are largely unknown. These subduction zones are tentatively considered to be similar to northeast Japan, based on dominantly reversed focal mechanisms in the forearc of the South Kuriles [*Ichikawa*, 1980] and late Pliocene folding roughly parallel to the Kamchatka Arc, adjacent to Kamchatka in the Sea of Okhotsk [*Gnibidenko and Khvedchuk*, 1982]. *Udias and Stauder* [1964] report 34 focal mechanisms from the Kurile-Kamchatka region; all may be interplate thrusts, but depth control is poor. *Stauder and Mualchin* [1976] determined 120 focal mechanisms from this region. Of these, one reversed faulting mechanism from the back-arc region of the South Kuriles is certainly within the upper plate; two other reversed focal mechanisms from the forearc region may be within the upper plate. Because of the limited strain data for the Kuriles and Kamchatka, the strain classes for these regions are not used in subsequent statistical analyses.

Alaska is similar to the class 4 regions of Alaska Peninsula and Central Aleutians in one respect: all three regions show a strain gradient, with decreasing compression away from the trench [*Nakamura et al.*, 1980]. However, unlike the latter two, the maximum compressional axis remains horizontal and roughly parallel to convergence direction for a much greater distance from the trench, about 500 km. The few volcanic alignments and fault offsets farther inland suggest that the maximum compressional axis changes to vertical but that the maximum horizontal compressional axis does not undergo substantial change [*Nakamura et al.*, 1980]. The many strike-slip faults in Alaska, with ages of initiation ranging from Jurassic to Pleistocene, show Quaternary dextral slip, commonly with either reverse or thrusting components [*Lathram et al.*, 1974]. Quaternary folding appears to be largely confined to the arc and forearc regions [*Lathram et al.*, 1974].

The class 6 segments Colombia, Ecuador, and Peru are adjacent. In all three regions, intracontinental seismicity is concentrated along the easternmost (foreland) flank of the Andean Cordillera, generally with strike-slip or high-angle thrust focal mechanisms [*Stauder*, 1975; *Pennington*, 1981; *Suárez et al.*, 1983]. Much of the east-west compression appears to be accommodated through a combination of underthrusting of the Brazilian shield beneath the eastern margin of the Andes [*Dalmayrac and Molnar*, 1981; *Suárez et al.*, 1983] and strike-slip motion of the Ecuadorian and Colombian forearc as a relatively rigid block [*Pennington*, 1981]. In Ecuador and Colombia the main Andean orogeny appears to have peaked in the late Miocene or Pliocene, with major thrusting and moderate folding in the eastern Andes [*Campbell*, 1974*a*, *b*]. Similarly, moderate Neogene folding and northeast verging reverse faulting have been mapped in the eastern Andes of Peru [*Jordan et al.*, 1983]. In the Altiplano (or high plateau) of Peru, seismicity is low and normal faulting is occurring on planes approximately parallel to the trench. This extension is probably a local effect of body forces associated with the higher elevation of the uplifting Altiplano compared with flanking regions; the overall strain regime of the Peruvian segment is clearly compressional [*Dalmayrac and Molnar*, 1981; *Suárez et al.*, 1983] but probably less compressional than Central Chile [*Jordan et al.*, 1983].

Southeast Mexico is tentatively included in class 6, based on limited data. Compression in the back-arc region was inferred by *Cross and Pilger* [1982], based on subtle northeast-southwest regional alignments of volcanoes, but relevant data were not shown. Thrusting and east-west compression are clearly present on seismic lines offshore eastern Mexico, involving beds as young as Pleistocene and possibly Recent [*Buffler et al.*, 1979]. This thrusting could result either from deep crustal stress or massive gravity sliding [*Buffler et al.*, 1979]. Some thrusts can be followed updip into normal faults; thus gravity sliding appears to be the more likely origin of at least some of this thrusting [*Tharp*, 1985]. A possible gradient in stress exists between the southeast Mexico and southwest Mexico subduction zones: the westernmost portion of the Mexican Arc occupies grabens that are probably currently extensional. This extension may be caused by an incipient ridge jump rather than subduction-related extension [*Luhr et al.*, 1985], but the latter may be a necessary prerequisite for the former [*Vink et al.*, 1984]. Although the southwest portion of the Mexican subduction zone is tentatively considered as more tensional than the class 6 southeast portion, it is not known well enough for use in subsequent statistical analyses. Of 13 focal mechanisms for southern Mexico, none appears to be within the overriding plate [*Burbach et al.*, 1984].

The adjacent Central Chile and North Chile subduction zones appear to be the most compressional (class 7) of all modern subduction zones. The discussion that follows is based primarily on the detailed analysis of *Jordan et al.* [1983]. In both regions, modern deformation is concentrated in the foreland. In North Chile, 30 to 80 km of shortening since the end of the Miocene has been accommodated on east verging folds and west dipping, thin-skinned thrusts. Continuing major compression in North Chile is indicated by focal mechanisms [*Chinn*, 1982] and Holocene folds and thrusts [*Lohmann*, 1970]. Foreland compression in Central Chile is different in style, with uplift of crystalline basement on reverse faults in the Pliocene-Pleistocene, as well as late Pliocene to Quaternary imbricate thrusting. Upper plate seismicity in Central Chile occupies a broader zone, with larger magnitudes, than in North Chile. The forearc region of Central Chile exhibits Quaternary stability, while uplift and subsidence in the North Chilean forearc suggest some extension.

Mercier [1981] has emphasized alternation of compressional and extensional periods in the Andes of North Chile, suggesting that active normal faulting extends from the Western Cordillera to the Eastern Cordillera, with only the sub-Andean zone (foreland) currently experiencing compression. Pleistocene to Recent normal faults in the Altiplano, striking east-west, have also been noted by other authors [e.g., *James*, 1971; *Sebrier et al.*, 1982] and detected through focal mechanisms [*Grange et al.*, 1984]. These observations led *England and Wortel* [1980] to classify North Chile as extensional. As in the normal faulting of the Peruvian Altiplano, body forces associated with uplift may be responsible [*Jordan et al.*, 1983]. Unlike the Peruvian Altiplano, the maximum horizontal compression axis in the North Chilean Altiplano is approximately perpendicular to the trench [*Grange et al.*, 1984]. The low seismicity of the Altiplano contrasts markedly with the high seismicity of the actively deforming foreland. In both North Chile and Central Chile, compression appears to have been even greater in the Miocene and Pliocene [*James*, 1971; *Rutland*, 1974; *Mercier*, 1981].

Because compression is accommodated in a generally different style in Peru and Central Chile than in North Chile and South Chile [*Jordan et al.*, 1983], relative strain rankings for

these four regions are tentative. For example, it is not known whether the amount of uplift in North Chile is indicative of more or less compression than the more diffuse faulting of Central Chile. Although the differences in style are often interpreted as differences in stress, they probably are more closely related to differences in crustal composition and paleogeography [*Jordan et al.*, 1983; *Allmendinger et al.*, 1983].

Convergence Rates

Present convergence directions at subduction zones are indicated by slip vectors of shallow interplate thrust earthquakes. Convergence rates cannot be directly measured. Accurate convergence rates between the major plates can be determined from world wide motion models [*Chase*, 1978*a*; *Minster and Jordan*, 1978], based on inversion of Pliocene-Pleistocene spreading rates, transform fault azimuths, and focal mechanisms. Table 1 includes convergence rates from both inversions. Confidence limits for convergence rates are not included in Table 1, because they can be readily estimated from these authors' 95% confidence limits for angular rotation rates about relevant poles of rotation. Because the pole of rotation is also subject to some uncertainty, such confidence limits slightly underestimate the total uncertainty in convergence rate.

With two exceptions, convergence rates listed in Table 1 are for the component of convergence perpendicular to the trench. For the Alaska and Alaska Peninsula subduction zones, the very wide accretionary prism makes the present trench axis of limited physical significance; downdip azimuth of the Benioff zone is used instead. Rates are given for both the relative motion between the underthrusting plate and the major overriding plate (V_c) and relative motion between the underriding plate and the forearc (V_{cba}). Unless specifically stated otherwise, subsequent references to convergence rate refer to V_c, not V_{cba}.

The arc and forearc may have substantial motion relative to the major overriding plate, manifested as strike-slip faults [*Fitch*, 1972] or back-arc spreading. Slip vectors used in worldwide motion models reflect motion between forearc and underthrusting plate. Consequently, both *Chase* [1978*a*] and *Minster and Jordan* [1978] largely avoided using slip vectors from regions with back-arc spreading. However, most slip vectors used by *Minster and Jordan* [1978] from the India/Pacific plate boundary were from the Kermadec Trench, with current back-arc spreading in the Havre Trough of 5.4 cm/yr full rate [*Malahoff et al.*, 1982]. Similarly, estimates of Philippine/Pacific relative motion by *Seno* [1977] and *Chase* [1978*a*] use slip vectors from the Mariana Trench, though back-arc spreading of 4.3 cm/yr full rate occurs in the Mariana Trough [*Hussong and Uyeda*, 1982]. Resulting errors in India/Pacific and Philippine/Pacific relative motions may be small, because in both regions the back-arc spreading direction is approximately parallel to the convergence direction of the major plates.

Convergence rates for many of the trenches in Southeast Asia are poorly known for two reasons: (1) uncertainty in rate of Philippine plate rotation relative to Eurasia and Pacific plates and (2) largely unknown motion of the Southeast Asia plate. Because the Philippine plate is bounded on all sides by trenches, its convergence rates are uncertain by about a factor of 2 [e.g., *Chase*, 1978*a*]. *Minster and Jordan* [1978] did not model Philippine plate motion; the rates shown in the Minster and Jordan (M) column of Table 1 for Philippine plate boundaries combine their Pacific/Eurasia relative motions with the Pacific/Philippine motion determination of *Karig* [1975]. As discussed in the subsequent section on strike-slip faulting, the existence of a Southeast Asia plate suggests that actual convergence rates may be about 1–2 cm/yr larger than those given in Table 1 for the Philippine, Sangihe, Ryukyu, and southwest Japan arcs, and the perpendicular component of convergence may be substantially smaller than is given for the Andaman and Sumatran arcs.

The least known convergence rates among Southeast Asian subduction zones are those for the Philippine, Sangihe, and North Sulawesi trenches. Subduction of the small Molucca plate on both the east and west sides is causing arc-arc collision in southern Mindinao and incipient collision in the Molucca Sea [*Hamilton*, 1979; *Cardwell et al.*, 1980]. The relative motion between the Southeast Asia and Philippine plates just south of the southern Philippines is therefore partitioned between the waning East Sangihe and Halmahera trenches and the recently formed Philippine Trench [*Hamilton*, 1979; *Cardwell et al.*, 1980]. The North Sulawesi Trench is the leading edge of a small plate that appears to be driven northward by collision of the Sula platform. Fault offsets and volumetric analysis of the accretionary prism suggest a possible convergence rate of 5 cm/yr at the western end of the trench, but this rate is highly dependent on the assumed duration of subduction [*Silver et al.*, 1983*a*].

Convergence rates for the Yap and Palau subduction zones reflect relative motions between the Caroline and Philippine plates [*Weissel and Anderson*, 1978]. The Caroline/Philippine relative motion pole is near the southern end of the Palau Trench, at the transition from a subducting to a spreading plate boundary [*Weissel and Anderson*, 1978]. Rotation rate uncertainties, compounded by proximity of the Yap and Palau trenches to the Caroline/Philippine pole, lead to very large uncertainties in Yap and Palau convergence rates.

The global motion models of both *Chase* [1978*a*] and *Minster and Jordan* [1978] assume that India and Australia are part of a single plate. However, significant relative motion between the two can be resolved [*Minster and Jordan*, 1978; *Stein and Gordon*, 1984], indicating compression of about 1.4 cm/yr in the vicinity of the Ninetyeast Ridge. Model A of *Minster and Jordan* [1978], which describes this relative motion, is used as an approximate adjustment to both global models. The effect of this correction is to decrease convergence rates by 0–1.5 cm/yr for the following subduction zones: Andaman, Sumatra, Java, New Britain, Solomon, New Hebrides, Tonga, Kermadec, and New Zealand.

Convergence rates for both the New Britain and Solomon subduction zones combine Australia/Pacific relative motions [*Chase*, 1978*a*; *Minster and Jordan*, 1978] with Australia/Solomon relative motions determined from magnetic anomaly correlations in the Woodlark Basin [*Weissel et al.*, 1982]. However, the overriding plate for the New Britain Trench is not known with certainty. If the nearly aseismic West Melanesian Trench is currently inactive, the overriding plate is probably the Caroline plate. If the West Melanesian Trench is currently a plate boundary, then the overriding plate is either the Pacific plate or possibly a North Bismarck plate [*Hamilton*, 1979]. Assuming Caroline/Solomon relative motion for the New Britain subduction zone, instead of Pacific/Solomon relative motion, reduces the total convergence rate of Table 1 by 2.4 cm/yr but changes the convergence rate perpendicular to the trench and component of absolute motion perpendicular to the trench by less than 0.3 cm/yr.

Assuming North Bismarck/Solomon relative motion has a similar effect.

Complexities in the spreading pattern behind the New Hebrides Trench preclude determination of accurate convergence rates, both with and without back-arc spreading. Australia/Pacific relative motion is assumed for V_c; this choice appears to be reliable only for the northern half of the New Hebrides Trench. The overriding plate for the southern half of the trench may be a small subplate, separated from the Australian plate by a small amount of strike-slip motion on the Hunter fracture zone. Back-arc spreading of 7 cm/yr full rate is well documented [*Malahoff et al.*, 1982] between this hypothesized microplate and the New Hebrides forearc. Strike-slip motion of about 2 cm/yr on the Hunter fracture zone can reconcile the rates for the northern and southern portions of the New Hebridean forearc, implying very little back-arc spreading between the Pacific plate and northwest New Hebrides. The rates shown in Table 1 are substantially less than the 12 cm/yr inferred by *Dubois et al.* [1977] on the basis of uplift rates on the outer rise of the New Hebrides Trench. In view of the uncertainties, convergence rates for New Hebrides are not used in subsequent statistical analyses.

Convergence rates for the South Sandwich Arc assume the existence of a Scotia plate [*Forsyth*, 1975; *Barker and Hill*, 1981] between South America and Antarctica. The transform faults bounding the Scotia plate on the north and south must together accommodate the 1.8 cm/yr relative motion between South America and Antarctica. Since both exhibit weak seismic activity [*Forsyth*, 1975], equal offset rates are tentatively assumed.

Convergence rates for the Cascades combine Pacific/North America relative motion [*Chase*, 1978*a*; *Minster and Jordan*, 1978] with Pacific/Juan de Fuca relative motion [*Engebretson*, 1982; *Wilson et al.*, 1984].

Motion of the Caribbean plate is based on the analysis of *Sykes et al.* [1982]; their results suggest about 2 cm/yr more eastward component of motion than previous analyses [e.g., *Minster and Jordan*, 1978].

Seafloor spreading in the Bismarck Sea [*Taylor*, 1979] and crustal thinning behind the Aegean Arc [*McKenzie*, 1978] are tentatively considered as back-arc spreading and not included in convergence rates. However, as previously mentioned, Aegean crustal thinning may reflect collision-driven motion of an Aegean plate rather than subduction-driven extension [*McKenzie*, 1978].

Absolute Motions

The search for an "absolute," or deep mantle, reference frame has led to numerous absolute motion models based on different assumptions: (1) fixed hot spots [*Morgan*, 1972; *Minster et al.*, 1974; *Minster and Jordan*, 1978; *Chase*, 1978*a*; *Morgan*, 1980], (2) no net motion of the lithosphere as a whole [*Lliboutry*, 1974; *Minster et al.*, 1974; *Solomon and Sleep*, 1974; *Minster and Jordan*, 1978], (3) no motion of the African plate [*Burke and Wilson*, 1972], (4) no motion of the Caribbean plate [*Jordan*, 1975], and (5) minimum horizontal motion of plate boundaries [*Kaula*, 1975].

Table 1 lists the component of absolute motion perpendicular to the trench for the overriding plate at each subduction zone, based on the worldwide motion models of *Chase* [1978*a*] and of *Minster and Jordan* [1978] and the fixed-hot-spot hypothesis. As with convergence rates, the overriding plate is defined as the major plate behind the arc, not the forearc region. The sign convention is that positive absolute motions are toward the underthrusting plate. As with convergence rates, minimum uncertainties can be readily calculated from 95% confidence limits in rate of rotation given by *Chase* [1978*a*] and *Minster and Jordan* [1978].

The absolute motion model of *Minster and Jordan* [1978] is based on their RM2 world relative motion model, azimuths of nine hot-spot traces, and volcanic propagation rates of five Pacific hot-spot traces. Eight of the nine hot-spot azimuths are from the Pacific Ocean. The similar analysis of *Chase* [1978*a*] is based on his P071 world relative motion model and 18 worldwide azimuths of hot-spot traces from *Minster et al.* [1974]. Neither the hot-spot rates nor azimuths are truly instantaneous; those of *Minster and Jordan* [1978] represent an average of up to 10 m.y., and several of those of *Minster et al.* [1974] are substantially older. Absolute motion of the Pacific plate appears to have changed significantly about 5 m.y. ago, but reference frames based on hot spots [*Cox and Engebretson*, 1984] and torque balance [*Davis and Solomon*, 1981] do not agree on the direction of this change. This change is not fully reflected in the uncertainties assigned to absolute motions by *Chase* [1978*a*] and *Minster and Jordan* [1978], and the two absolute motion models must therefore be considered tentative.

Slight motion between hot spots is likely. Relative motion of about 1 cm/yr was suggested by early studies [*Morgan*, 1972; *Molnar and Atwater*, 1973; *Burke et al.*, 1973; *Molnar and Francheteau*, 1975], but more recent studies suggest substantially less motion [*Morgan*, 1980; *Duncan*, 1981]. Much larger relative motions among Pacific hot spots have been inferred by *Chase and Sprowl* [1984]. However, the likelihood of a change in Pacific/hot-spot motion at 5 m.y. B.P. and the tendency of hot-spot volcanism to be affected by zones of crustal weakness cast doubt on this conclusion. Slow relative motion of hot spots is also implied by mantle/lithosphere mass balance models [e.g., *Hager and O'Connell*, 1978], unless the mantle source of hot spots is deeper than mantle flow. The hot-spot azimuth misfits for both the *Chase* [1978*a*] and *Minster and Jordan* [1978] models are generally less than 10°, suggesting that the hot-spot reference frame is viable, in spite of its uncertainties and slow relative motions among hot spots.

Minster and Jordan [1978] have compared their absolute motion model with models based on different assumptions. Models based on no net rotation of the lithosphere or on a fixed African plate are broadly similar to the hot-spot model; however, they appear to be significantly different at the 95% confidence level. A model based on the assumption of a fixed Caribbean plate is not significantly different from the hot-spot model. This conclusion would probably not be changed by using the revised Caribbean/North America relative motions of *Sykes et al.* [1982], which would have the effect of increasing predicted volcanic propagation rates by about 2 cm/yr, to values more in agreement with those observed.

As with convergence rates, the largest uncertainties in absolute motion are associated with the Southeast Asian and Philippine plates.

Modification of the *Chase* [1978*a*] and *Minster and Jordan* [1978] absolute motion models was required for some subduction zones, resulting from the relative motion revisions discussed in the preceding section. Tonga, Kermadec, and New Zealand were considered part of an Australian plate rather than a combined India-Australia plate. Caribbean plate motion was modified as suggested by *Sykes et al.* [1982]. Exis-

tence of a Scotia plate was assumed. Because *Minster and Jordan* [1978] did not determine Philippine plate motion, absolute motion of the Philippine plate combines their Pacific absolute motion with the Pacific/Philippine relative motion of *Karig* [1975].

Slab Age

Two measures of the age of the downgoing slab are tabulated in Table 1: the average age of crust now entering the trench and the average age of the tip of the slab. The latter is not the present age of the slab tip, but the age at the time that the current slab tip first entered the subduction zone, based on the relationship

$$A_t = A_s + L_s \times (dA/dL - 1/V_{cba})$$

where A_t is effective age of the slab tip, A_s is the age of crust now entering the subduction zone, L_s is the downdip length of the slab, dA/dL is the age gradient of the slab perpendicular to the trench (m.y./km, positive for age increasing downdip), and V_{cba} is the perpendicular component of convergence rate (km/m.y.), including back-arc spreading. As discussed subsequently, this effective age is relevant to models of the thermal history of the slab [*Farrar and Lowe*, 1978; *Sykes et al.*, 1982], in which the oceanic crust is assumed to cool until it begins subducting, and thereafter to heat.

Calculated time since subduction of the slab tip (T_{st}) and effective age of the slab tip are compiled in Table 1. Separate estimates of A_t are not shown for *Chase* [1978*a*] and *Minster and Jordan* [1978] rates, as other sources of variance generally dominate the uncertainties shown for A_t. Convergence rates used to calculate T_{st} and A_t differ from those given in Table 1 for Tonga, Kermadec, Marianas, and South Sandwich. In these four regions the present back-arc spreading rate has not persisted since subduction of the slab tip. Therefore a time-varying convergence rate was used to determine T_{st}. The effect of this correction is to reduce A_t by 1.0–3.5%, compared with assuming present V_{cba} since the slab tip was subducted. The history of crustal extension in the Aegean is not known with confidence; *Le Pichon and Angelier* [1981] suggest that crustal extension began at about the same time as subduction. Because of uncertainty in both timing and rate of early extension in the Aegean, the estimate of T_{st} may be a minimum value.

Determination of A_t is often much more uncertain than determination of A_s, primarily because of uncertainty in age gradient. Age gradients used in Table 1 are based usually on age gradients near the trench, but changes in spreading rates and ridge jumps within the subducted lithosphere are often unknown. Three extreme examples of this problem are the Central Aleutians, Sumatra-Andaman, and Peru–North Chile. The Kula/Pacific ridge may have ceased in the late Paleocene [*Byrne*, 1979], implying increasing slab age downdip in the Central Aleutians, or about 43 m.y. ago [*Engebretson*, 1982], implying decreasing age downdip. In the Sumatra and Andaman segments, ages increase northward, but because of oblique convergence and closely spaced fracture zones, age probably decreases discontinuously downdip. In the Peru and North Chile segments, extrapolation of age gradients from unsubducted to subducted crust can be substantially in error because of changes in spreading rate. For these two segments only, A_t is based on a reconstruction of the subducted portion of the Nazca plate [*Cande*, 1983]. Ideally, all estimates of A_t should be based on such reconstructions.

Almost all estimates of A_s and A_t are based on the world-wide magnetic anomaly compilation (S. C. Cande, unpublished manuscript, 1986) used by *Larson et al.* [1985]. Other sources were used for Colombia [*Pennington*, 1981], Ecuador [*Pennington*, 1981], Mexico [*Klitgord and Mammerickx*, 1982], Middle America [*von Huene et al.*, 1980], North Sulawesi [*Weissel*, 1980*a*], Palau [*Weissel and Anderson*, 1978], South Sandwich (J. L. LaBrecque, personal communication, 1985), and Yap [*Weissel and Anderson*, 1978]. Slab ages used for the Makran, Ryukyus, New Britain, and Solomon zones require some explanation.

The estimate of slab age for the Makran is based on extensive field work in the nearby Samail ophiolite of Oman. No magnetic anomalies are identified in the remnant of Tethyan oceanic crust in the Gulf of Oman, probably because of crustal formation during the Cretaceous Quiet Zone. The Samail ophiolite includes a paleo–spreading ridge [*Pallister*, 1981] formed 95 m.y. ago, based on uranium-lead dating [*Tilton et al.*, 1981]. Because of probable high spreading rates [*Tilton et al.*, 1981], the Makran slab age most likely can be estimated relatively accurately, in spite of the tectonic complexities summarized by *Coleman* [1981].

The Ryukyus segment used is southwest of the probably Cretaceous Daito Ridge. The northwest subbasin of the West Philippine Basin probably originated as part of the main basin but acquired a NNE trending fabric during later deformation [*Mrozowski et al.*, 1982]. If so, its age may be similar to that at Deep Sea Drilling Project (DSDP) sites 294 and 295 to the east, where $^{40}Ar/^{39}Ar$ dating yields an age of 48.8 ± 2 m.y. [*Ozima et al.*, 1977]. An alternative interpretation, not followed here, is that anomaly 9 and possibly 8 can be identified near the Ryukyus as part of an anomaly pattern decreasing in age to the north [*Shih*, 1980]. If the latter is correct, the age of the slab is much younger than assumed in Table 1.

No magnetic anomalies have been identified in the Solomon Sea, the basin being consumed at the New Britain and Solomon trenches. *Davies et al.* [1984] estimate an age of 40 to 60 m.y. for this basin based on heat flow, depth, paleomagnetism of New Britain, flexure, and slab length. Age gradients are unknown, both within the basin and within the slabs.

No age estimates are included in Table 1 for crust subducting at the Aegean, Sangihe, and Philippine zones. The portion of Tethys now subducting in the Aegean is undated but may be Cretaceous or Jurassic (W. B. F. Ryan, personal communication, 1985). Only a thin, undated sliver of the Molucca plate remains seaward of the Sangihe Trench [*Silver and Moore*, 1978]. The southern subbasin of the West Philippine Basin, adjacent to the Philippine Trench, does not appear to be a continuation of the spreading pattern in the rest of the West Philippine Basin [*Mrozowski et al.*, 1982].

Arc Age

Initiation of subduction is usually followed in less than 5 m.y. by initiation of arc volcanism [*Gill*, 1981]. Therefore the oldest arc-related rocks in a subduction zone provide an estimate of duration of subduction.

Arc ages in Table 1 indicate for each arc the oldest arc-related rocks that are associated with the current trench. In some cases (e.g., Sumatra and Java), older granites have been dated but appear to be associated with an arc-trench system having a substantially different trend than the present one. In other cases (e.g., New Britain, Solomons, New Hebrides, and Philippines) an older arc has a trend similar to the present one, but a reversal of subduction polarity has occurred. If an

apparent pause in subduction has occurred, the older age is still used. When such pauses are prolonged, they can perhaps affect current tectonic style and probably should be used to correct somehow the arc age. However, often the apparent pauses are an artifact of incomplete exposures and dating; thus no attempt to correct for pauses is made herein. Error limits shown for ages in Table 1 represent age uncertainties in dating of the oldest dated arc-related rocks. These error limits do not indicate uncertainties in the age of the arc, as in most cases the possibility remains that the earliest arc-related rocks are not exposed or dated.

Dickinson [1973] has compiled estimates of arc ages for most of the subduction zones of Table 1. In general, ages given herein are similar to his in spite of access to newer age data. However, field work and dating in the last decade suggest that the ages of several arcs require substantial revision (e.g., Sumatra, Java, Philippines, and New Britain).

The Tonga–Kermadec–New Zealand convergent margin is approximately middle Tertiary in age. The oldest K-Ar age from andesitic volcanism in New Zealand is 18 m.y., but the presence of underlying volcaniclastic sediments suggests that subduction here began about 18–24 m.y. B.P. [*Ballance*, 1976]. For the Kermadec zone the Colville Ridge yields middle Oligocene ages at both DSDP site 205 and in the Lau Islands [*Hochstein et al.*, 1974]. Subduction in Tonga is well represented for late Oligocene–early Miocene to present [*Hochstein et al.*, 1974]. Rare middle Eocene ophiolitic rocks may indicate an earlier inception of subduction, but their provenance is uncertain [*Ewart and Bryan*, 1972].

The present subduction patterns in the New Hebrides, New Britain, and Solomon zones began with arc polarity reversal. In the New Hebrides, arc polarity reversal occurred in the middle Miocene; a new arc formed in the late Miocene, coeval with rifting in the North Fiji Basin [*Carney and Macfarlane*, 1982]. In New Britain, Eocene andesites and volcaniclastics and late Oligocene–Miocene plutons show increasing K_2O/SiO_2 to the southeast, indicating a subduction polarity opposite to the present [*Page and Ryburn*, 1977]. Modern arc polarity began in the upper Miocene [*Page and Ryburn*, 1977], substantially younger than the Eocene age used by *Dickinson* [1973]. Solomon polarity reversal is less reliably timed but may be similar: upper Eocene and Oligocene basaltic and andesitic rocks preceded polarity reversal and were followed by deposition of widespread lower-middle Miocene shallow water limestones [*Karig and Mammerickx*, 1972].

The present arcs of Izu-Bonin, Marianas, Yap, and Palau all appear to have initiated as part of the Palau-Kyushu Arc about 45 ± 3 m.y. ago. DSDP site 296, near the Palau-Kyushu Ridge, bottomed in tuffs yielding an $^{40}Ar/^{39}Ar$ age of about 48 m.y. [*Ozima et al.*, 1977], and DSDP site 290 in the West Philippine Basin penetrated a middle Eocene conglomerate in an apron derived from the Palau-Kyushu Ridge [*Karig et al.*, 1975]. Upper Eocene fossils have been identified on Palau [*Hamilton*, 1979], near the southern end of the Palau-Kyushu Ridge. Back-arc spreading in the Parece Vela Basin [*Mrozowski and Hayes*, 1979], Shikoku Basin [*Kobayashi and Isezaki*, 1976; *Watts et al.*, 1977], and Mariana Trough [*Bibee et al.*, 1980] have subsequently split the ancestral Palau-Kyushu Arc and led to the isolation of the present Izu-Bonin, Marianas, and probably Yap arcs. A late Eocene arc complex has been dredged on the landward slope of the Mariana Trench [*Bloomer*, 1983], consistent with outcrops of Eocene volcanogenics on Guam and Saipan. Eocene volcanic and volcanogenic rocks also outcrop on the Bonin Islands [*Karig*, 1971].

Suggestions of both younger and older ages for the trenches from Izu-Bonin to Palau also exist, however. The oldest dated rocks from Yap are breccias with middle(?) Miocene shallow water Foraminifera [*Cole et al.*, 1960]. DSDP site 448 on the Palau-Kyushu Ridge bottomed in middle Oligocene volcanics [*Kroenke and Scott*, 1978]. In neither case is an older arc age excluded. Dredges on the inner wall of the Mariana Trench recovered (in addition to the late Eocene arc complex) isolated assemblages of alkalic basalts, chert, and Late Cretaceous sediments interpreted as accreted seamount fragments [*Bloomer*, 1983]. Reworked Late Cretaceous foraminifera have also been identified at DSDP site 290 [*Karig et al.*, 1975], located on the Palau-Kyushu apron on oceanic crust thought to be Eocene in age [*Watts et al.*, 1977; *Shih*, 1980]. This age implies that at least part of the Palau-Kyushu Ridge existed in the Late Cretaceous, though possibly not as an arc. *Uyeda and Ben-Avraham* [1972] suggested that the Palau-Kyushu Ridge was a fracture zone until a major change in Pacific plate motion 43 m.y. ago [*Clague and Jarrard*, 1973; *Dalrymple et al.*, 1980] caused initiation of subduction along this ridge. Although details of this model have been revised owing to newer data on the location of the Philippine/Eurasia/Pacific triple junction and age of the Philippine Basin, the estimated timing of subduction initiation has not changed [*Ben-Avraham and Uyeda*, 1983]. This 43 m.y. estimated age corresponds well with the majority of age estimates for the Palau-Kyushu Arc system. However, the curvature of the Palau-Kyushu Ridge and the azimuth of anomalies in the West Philippine Basin are difficult to reconcile with this model [*Mrozowski et al.*, 1982]. These uncertainties in the early history of the West Philippine Basin and Palau-Kyushu Ridge do not weaken the firm age of 45 ± 3 m.y. for inception of subduction.

Inception of the modern subduction pattern in Andaman-Sumatra-Java is controversial. In Sumatra, scattered Cretaceous and Paleogene K-Ar ages are found for granitic rocks, but the orientation of these belts is not reliably known. *Katili* [1973] interpreted the Cretaceous arc as parallel to the modern one, while *Hamilton* [1979] suggested that the belt may be strongly oblique to the modern trench and truncated at the trench. Similarly, *Hamilton* [1979] interpreted Late Cretaceous and Paleogene melanges and igneous rocks in Java as forming an arc trending from western Java through Borneo. In both Java and Sumatra, late Oligocene calc-alkaline rocks are the oldest arc-related rocks that are clearly part of the present subduction geometry [*Hamilton*, 1979]. The interpretation of Hamilton is tentatively followed here, though a much older age may be appropriate. The poorly dated Andaman region is at least as old as the late Oligocene start of continental thinning, and probably Cretaceous [*Curray et al.*, 1982].

Middle Miocene K-Ar ages in North Sulawesi probably predate polarity change [*Hamilton*, 1979]. The current polarity may have been established as recently as 5 m.y. B.P., based on amount of accretion and slab length [*Silver et al.*, 1983*a*]. Progressive polarity reversal along this arc has not yet reached the Sangihe Arc; Sangihe may therefore be middle Miocene, but it has not yet been directly dated [*Hamilton*, 1979]. Just north of Sangihe, Miocene and older andesitic rocks are found in Mindinao [*Martin*, 1976]. These rocks are not associated with the very recent breakthrough of the Philippine Trench but with an older arc of uncertain polarity that

preceded arc-arc collision and development of the Philippine Trench [*Hamilton*, 1979].

Andesitic volcanogenics in the Ryukyus indicate that this subduction zone is at least as old as the beginning of the Miocene [*Matsumoto and Kimura*, 1974]. *Karig* [1973] suggested that the Ryukyu Arc may have been active throughout the Tertiary; a 55 ± 5 m.y. K-Ar age [*Nozawa*, 1968] is consistent with this interpretation.

Southwest Japan, adjacent to Ryukyu, has probably the most uncertain duration of modern subduction of any subduction zone. Granitic rocks as old as 420–430 m.y. form a belt striking obliquely to the present trench [*Maruyama et al.*, 1984]. Intermittent arc volcanism from that time to the present is detected, punctuated by more pronounced volcanism in Cretaceous and early Tertiary but also including weak to moderate volcanism through most of the Neogene [*Matsumoto and Kimura*, 1974]. Plutons 170–180 m.y. in age may represent the oldest belt parallel to present tectonic trends [*Dickinson*, 1973]. *Choi* [1984] considered evidence of possible microplate accretion and rifting in Japan and concluded that large landmasses rifted away from both northeast and southwest Japan during the Permian. A post-Permian age therefore seems appropriate for modern subduction geometry, but the 175 m.y. age assigned in Table 1 is extremely tentative. Duration of the present pattern is apparently better known for northeast Japan, with 110–120 m.y. plutons the oldest that are related to the modern trend [*Kawano and Ueda*, 1967].

Middle Late Cretaceous through Cenozoic volcanism is well documented for the nearby Kuriles [*Markhinin*, 1968]. Older K-Ar ages of about 150 m.y. and 219 ± 5 m.y. are also found for dredged granites of this continental region [*Gnibidenko and Khvedchuk*, 1982], but their subduction geometry is unknown. A middle Late Cretaceous age is tentatively used here, while recognizing that the 150 m.y. ages are more consistent with the Late Jurassic [*Avdeiko*, 1971] beginning of arc volcanism in adjacent Kamchatka.

The Aleutian Arc is at least as old as Eocene, based on dating of volcaniclastic rocks [*Scholl et al.*, 1975], and younger than the *M* sequence oceanic crust trapped behind the arc. An age of about 56 m.y. (D. Scholl, personal communication to D. C. Engebretson, 1982) is tentatively assumed. Initial plutonism in nearby Alaska and Alaska Peninsula is well dated as 150–175 m.y., with subsequent extensive volcanism from Late Cretaceous to middle Tertiary [*Reed and Lanphere*, 1969]. However, estimation of duration of the modern subduction pattern is complicated by contradictory evidence of possible polarity reversal, middle Cretaceous suturing [*Csejtey et al.*, 1982], and possibly even later terrane emplacement [e.g., *Stone et al.*, 1982]. A substantially younger age than the 160 ± 10 m.y. assumed here may be appropriate.

Arc volcanism began in the Cascades in the Middle Jurassic [*Coney*, 1972; *Dickinson*, 1972] and in Mexico in the Turonian [*Coney*, 1972]. In both regions, subsequent disruption of subduction patterns by terrane motions is possible. In Middle America the oldest arc-related rocks are middle Cretaceous, with Late Cretaceous volcanics common [*Dengo and Bohnenberger*, 1969].

The oldest arc-related rocks from the Lesser Antilles are spillites and keratophyres at least 142 ± 10 m.y. old, found only on the island of Desirade [*Tomblin*, 1974]. The relation of these rocks to former subduction patterns is unknown. More likely, arc volcanism began in about the middle Eocene, as Eocene and younger calc-alkaline volcanics are found throughout the arc [*Tomblin*, 1974]. Late Cretaceous to Eocene arc magmatism is common in the nearby Greater Antilles [*Malfait and Dinkelman*, 1972; *Mattson*, 1976], but no subsequent arc magmatism is observed there [*Mattson*, 1979]. Thus the age data from both arcs are most consistent with a hypothesized Eocene change from subduction beneath the Greater Antilles and a transform boundary in the Lesser Antilles to subduction beneath the Lesser Antilles [*Sykes et al.*, 1982].

Most of the Pacific margin of South America has been a site of subduction since at least the early Paleozoic [e.g., *Allmendinger et al.*, 1983], but the present magmatic trends date only from the Triassic [*James*, 1971; *Campbell*, 1974*a*, *b*]. In Tierra del Fuego, the southernmost part of South America, arc volcanism began in the Jurassic [*Skewes and Stern*, 1979], probably in the uppermost Jurassic [*Malumián and Ramos*, 1984].

In the South Sandwich region, the present subduction geometry has persisted for at least 7–8 m.y., the duration of the current back-arc spreading pattern [*Barker and Griffiths*, 1972]. Back-arc spreading from 21 m.y. to about 8 m.y. was associated with more northerly subduction than the present pattern but probably included some subduction along the modern trench [*Barker and Hill*, 1981]. In contrast, 21–30 m.y. spreading in the West Scotia Sea was approximately parallel to the present direction of back-arc spreading but cannot be unambiguously attributed to back-arc spreading [*Barker and Hill*, 1981].

In the Aegean, initiation of the modern trench and back-arc extension probably began only shortly before intrusion of granodiorites dated as 10–12 m.y. [*Le Pichon and Angelier*, 1981].

The duration of subduction and arc volcanism for the Makran subduction zone may vary substantially along strike. The overriding Eurasian plate here is composed of two continental blocks, the Lut and Afghan, which collided and sutured at about the end of the Paleogene [*Arthurton et al.*, 1979]. The present Benioff zone may be segmented into two segments [*Jacob and Quittmeyer*, 1979], with the boundary occurring near the Lut/Afghan suture. Only the western (Lut) segment is considered in Table 1, because sparse seismicity in the eastern zone precludes identification of a Benioff zone. Prior to collision, widespread Senonian (Late Cretaceous) arc volcanism occurred around the southern boundary of the Afghan block [*Auden*, 1974; *Arthurton et al.*, 1979], roughly parallel to the modern trench. Scattered sills, dikes, and stocks, some of late Paleogene age, also occur in this region. Northward subduction beneath the Lut block probably began in the Eocene, based on the ages of calc-alkaline volcanics in this region [*Jung et al.*, 1976]. Extensive forearc flysch sedimentation of Eocene through Miocene age [*Auden*, 1974], accompanied and followed by rapid development of a very wide accretionary prism [*White*, 1979], occurs south of both blocks. The modest volcanism of the modern arc probably began in about the late Pliocene or early Quaternary [*Arthurton et al.*, 1979]. Thus subduction beneath the Lut block appears to have begun in the Eocene, much later than the Senonian inception of subduction beneath the Afghan block.

Durations of subduction should always be greater than time since subduction of the slab tip (T_{st}). Comparison of these two columns in Table 1 shows only one exception: North Sulawesi has an estimated arc age of 7 ± 4 m.y. and T_{st} of 15.3 m.y. When the large uncertainty assigned to convergence rate is considered (3 ± 2 cm/yr), the resulting range of T_{st} is 9.2–46

m.y. Thus this comparison may indicate that convergence rate is faster than assumed. However, neither value has been modified in Table 1, because one cannot confidently identify which variable is erroneous.

Trench Depth

Two measures of trench depth are included in Table 1: the maximum trench depth within the segment and relative depth, the difference between maximum trench depth and abyssal plain depth. Most values are from the compilation of *Hilde and Uyeda* [1983], who cite the original sources. Maximum trench depth for Java and abyssal plain depth for Palau are from *Grellet and Dubois* [1982]. For the following subduction zones not analyzed by either of the above, depths are from the GEBCO maps [*IHO/IOC/CHS*, 1984]: Sumatra, Kurile, Kamchatka, Central Aleutians, Lesser Antilles, and Colombia. Some abyssal plain depths are also from the GEBCO maps: Java, southwest Mexico, southeast Mexico, Peru, North Chile, Central Chile, and South Chile. Maximum trench depths for southwest Mexico and southeast Mexico are from the *Times Atlas* [*Times*, 1975]. Most of the depths based on GEBCO maps are considered less reliable than other depths, because of the 100- to 500-m contour interval employed. All abyssal plain depths are determined from regions seaward of the outer rise, thereby avoiding any subduction effects on depth.

Trench depths can be affected by three variables that are not specifically treated in this study: thickness of sedimentary trench fill, thickness of sediments on the oceanic crust before entering the trench, and presence of aseismic ridges. Thickness of trench fill is usually difficult to estimate for trenches lacking migrated multichannel seismic data. This effect, as well as the effect of subducting aseismic ridges, is reduced by considering maximum trench depth rather than average trench depth. Pelagic sediment thickness on the abyssal plain is generally similar to that on the portion of plate at the trench; thus this effect can be largely avoided by focusing on relative trench depth rather than maximum trench depth. Sediment effects are further reduced by excluding depth estimates from Table 1 for subduction zones with very thick trench fill or very thick sediments in the nearby abyssal plain.

Trench depth estimates in Table 1 differ from all other parameters in Table 1 in an important respect: they do not necessarily come from near the reference position at which other parameters are determined. This difference is a consequence of the focus on maximum trench depth within a segment. The most extreme example of this is the Marianas, with a maximum depth of 11 km, the deepest of all trenches. This maximum depth occurs in the southernmost Marianas, which is characterized by highly oblique convergence and a poorly defined Benioff zone. Maximum trench depth in the vicinity of the Marianas reference location is 1.3 km shallower, and this depth is used in Table 1. Another notable example is the South Sandwich subduction zone, which has a major change in trench depth across a fracture zone separating crust of very different ages. In subsequent analyses of trench depth, an age of 65 m.y. is assumed for the subducting slab in this region, rather than the 49 m.y. average for the entire subduction zone. Although 65 m.y. is a more appropriate age than 49 m.y. for the slab at the maximum trench depth, both ages are highly uncertain. For all other subduction zones, differences between trench depth location and reference location probably have a relatively minor effect.

STRIKE-SLIP FAULTING

Characteristics

Most considerations of convergence rate in this paper focus on the component of convergence perpendicular to the trench rather than total convergence rate, as the former is probably more relevant to such subduction zone parameters as overall stress state. Indeed, because of the control of downdip slab pull on motion of the subducting plate, most convergence directions are within 25° of perpendicular to the trench (Figure 3). Nevertheless, oblique convergence has an important impact on the overriding plate, through its control of strike-slip faulting.

Strike-slip faults often develop parallel to the trench and 100 to 300 km inland from it, usually near or within the arc. These faults accommodate part of the trench-parallel component of oblique convergence. Reliable estimation of current rates of strike-slip motion from field relations is seldom possible, so the proportions of trench-parallel component accommodated by strike-slip motion and oblique convergence are not known.

These strike-slip faults separating the forearc from the remainder of the overriding plate are probably transform faults, with the forearc acting as a narrow or sliver plate [*Fitch*, 1972; *Dickinson*, 1972; *Karig and Mammerickx*, 1972]. The variety of relative movements possible for such sliver plates, potentially including transform faulting and/or back-arc spreading, is considered in detail by *Dewey* [1980]. In the discussions that follow, the term "strike-slip fault" is used rather than "transform fault," because near-arc strike-slip faults may form a more diffuse zone than typical oceanic transform faults and because the subsurface nature of the plate boundary is not known.

In most modern subduction zones only a narrow zone of anastomozing or en echelon faults is present, usually occurring along the arc. The most notable and longest recognized of these "simple" strike-slip faults are the Semangko (or Sumatran) Fault of Sumatra, the Philippine Fault, the Median Tectonic Line of southwest Japan, the Atacama Fault of Chile, and the Alpine Fault of New Zealand. Similar strike-slip faults are the Dolores-Guayaquil of Colombia and Ecuador and the Liquina-Ofqui of South Chile. Of these, the clearest association between fault location and the location of the modern arc is found in the Semangko, Dolores-Guayaquil, and Liquine-Ofqui faults. In many subduction zones, strike-slip faulting is not confined to the modern arc. The Atacama Fault of North Chile and Central Chile is located seaward of the present arc, along an older magmatic belt (Figure 4). Strike-slip faulting in Alaska has involved several widely spaced major faults, with an overall seaward migration of activity: the Jurassic or Early Cretaceous initiation of motion on the Tintina Fault, Late Cretaceous or Paleocene initiation of the Denali Fault, and Pleistocene initiation of the Fairweather Fault [*Lathram et al.*, 1974]. Although current motion here is predominantly on the Fairweather Fault, all three show some Holocene motion [*Lathram et al.*, 1974]. Strike-slip faulting in Colombia and Ecuador is somewhat analogous to that in Alaska, occurring not only along the modern arc but also farther inland, along older magmatic belts [*Pennington*, 1981]. In contrast, in both Sumatra and Andaman subduction zones, major dextral faults occur both within the arc and forearc [*Karig et al.*, 1980; *Mukhopadhyay*, 1984]. In the South Kuriles and northeast Japan, diffuse strike-slip faulting occurs be-

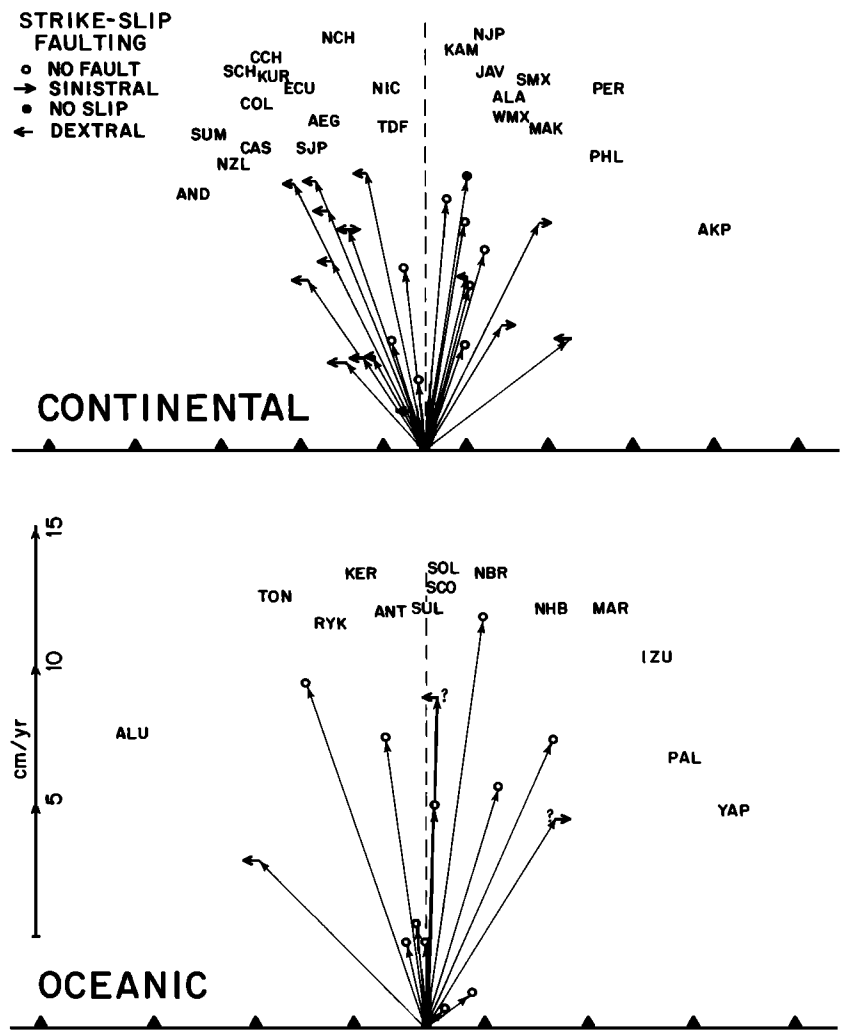

Fig. 3. Convergence rate and azimuth with respect to the trench for each modern subduction zone of Table 1. Symbols at the head of each convergence vector indicate geological evidence of Pleistocene strike-slip faulting and associated offset direction. Note that nearly all offset directions are consistent with the directions of oblique convergence.

tween the coast and the trench [*Ichikawa*, 1980]. In southwest Japan, no active arc is found; the Median Tectonic Line lies mostly along an older arc. Modern strike-slip faulting is not only along the Median Tectonic Line but also along numerous faults, with various azimuths, north of the Median Tectonic Line [*Matsumoto and Kimura*, 1974].

Once a strike-slip fault has been established due to oblique convergence, subsequent stress is accommodated along this zone of weakness, though not necessarily as pure strike-slip motion. For example, the northern portion of the Alpine Fault of New Zealand is undergoing a transition from pure dextral slip prior to 10 m.y. B.P. to transpression since 10 m.y. B.P.; uplift and mountain building now dominate strike-slip motion along the fault [*Carter and Norris*, 1976]. This change is apparently a response to southward migration of the India/Pacific pole of relative motion [*Norris and Carter*, 1982] and accompanying change to less oblique convergence. The Tintina, Denali, and Fairweather faults of Alaska currently include both dextral slip and reverse faulting [*Lathram et al.*, 1974]. Similarly, both reverse and strike-slip components characterize faulting along the Median Tectonic Line of southwest Japan [*Matsumoto and Kimura*, 1974] and the faults of Peru [*Philip and Megard*, 1977]. In contrast, nearly perpendicular convergence in northeast Japan causes current activity on the North Japan Line to be almost pure dip-slip [*Okayama*, 1961], though this fault may have begun as strike-slip [*Kaizuka*, 1975] and focal mechanisms indicate a diffuse zone of current strike-slip motion in the forearc [*Ichikawa*, 1980]. The Coriolis Trough of the New Hebrides may be another example; *Dubois et al.* [1978] suggest a strike-slip origin, but the trough is now entirely extensional. Substantial dip-slip also accompanies modern strike-slip motion on the Semangko Fault of Sumatra [*Katili*, 1974; *Page et al.*, 1979], the Liquina-Ofqui Fault of South Chile [*Hervé et al.*, 1979], and the Atacama Fault of North Chile and Central Chile [*St. Amand and Allen*, 1960].

Transpression sometimes forms en echelon ridges, usually just behind the strike-slip fault but sometimes within the forearc [*Kaizuka*, 1975]. The sense of en echelon arrangement in these ridges depends on the direction of oblique convergence. En echelon ridges, such as those of Sumatra and the Kuriles, are analogous to the smaller-scale drag folds that often accompany strike-slip faults. More rarely, strike-slip motion is accommodated through a complex pattern of fault-bounded

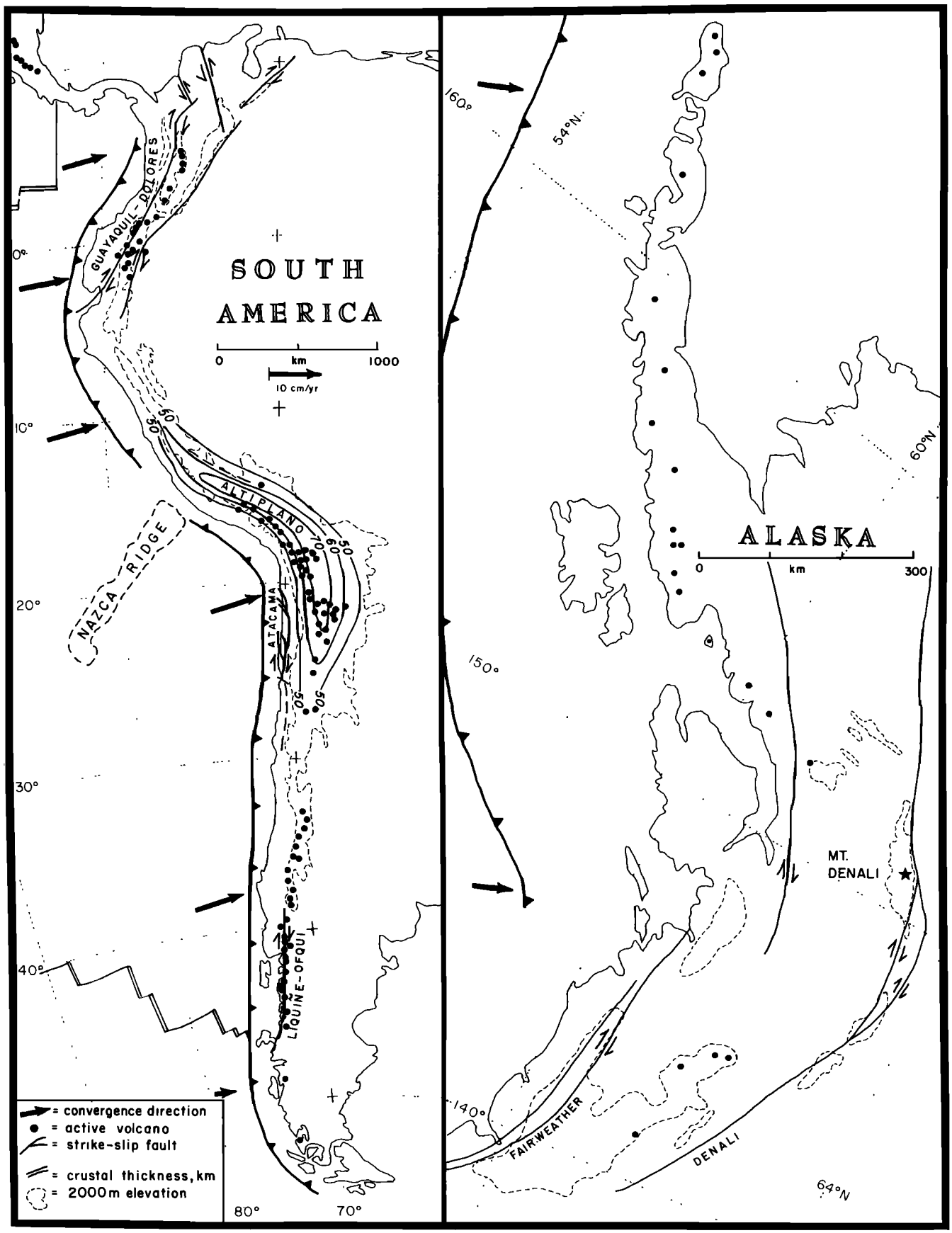

Fig. 4. Modern plate tectonic setting and locations of active strike-slip faults in western South America and southern Alaska.

blocks which may experience differential rotation and uplift, such as in New Zealand [*Norris and Carter*, 1982]. Local forearc block rotation may be more common than is geologically recognized; paleomagnetic evidence of such rotations is not unusual [e.g., *Jarrard and Sasajima*, 1980; *Stone et al.*, 1982; *Beck*, 1980].

Leading and Trailing Edges of Forearc Slivers

The relative motion of forearc slivers has important implications for the tectonics of regions at the leading and trailing edges of slivers: compression is often predicted at the leading edge, and tension is predicted at the trailing edge of each sliver. The Sumatra sliver plate, bounded by the Semangko Fault and Sunda Trench, is perhaps the best example of a forearc plate, with a trailing edge in the Sunda Strait. The fault apparently does not extend all the way to the trench as a simple strike-slip fault; instead a diffuse zone of crustal extension in the southern Sunda Strait accommodates the motion [*Huchon and Le Pichon*, 1984]. Similarly, the Liquine-Ofqui Fault of South Chile has a trailing edge which curves away from the arc and into the Golfo de Penas-Taitao Basin, where extension is probable [*Forsythe and Nelson*, 1985]. Alternatively, the location of this trailing edge adjacent to the South America/Nazca/Antarctica triple junction makes it possible that the fault morphology and offset are a spreading-center indenter effect [*Forsythe and Nelson*, 1985]. The Dolores-Guayaquil Fault of Colombia and Ecuador appears to be similar to the Semangko and Liquine-Ofqui faults in that its trailing edge swings offshore and is lost in a gulf, the Gulf of Guayaquil [*Campbell*, 1974*b*]. It is not known whether the fault continues to the trench or causes crustal thinning in the Gulf of Guayaquil.

The leading edges of most forearc slivers are characterized by compression, but the structural style depends on curvature of the edge of the overriding plate. For example, the strongly convex (as seen from the upper plate) western end of the Sunda Trench causes Sumatran strike-slip motion to be accommodated westward as back-arc spreading in the Andaman Basin (Figure 7). In contrast, both Alaska and Peru-Chile have concave plate boundaries and therefore compression.

Present motion of the Nazca plate causes sinistral strike-slip in Peru and dextral slip in Chile, implying compression between colliding slivers in the bight of northernmost Chile and southeastern Peru (Figure 4). Northwest-southeast shortening in the Western Cordillera of South Peru is indicated by focal mechanisms [*Grange et al.*, 1984]; collision may be the cause of this otherwise inexplicable compression direction. *Cande* [1983] has shown that the present convergence direction has remained relatively constant since about 26 m.y. B.P.; earlier Tertiary convergence was consistently to the northeast. Thus compression in the Peru-Chile bight is expected throughout the Tertiary, with a change from Early Tertiary dominance of motion on the Chilean faults to late Tertiary dominance of the Peruvian faults. One may speculate that the substantially greater crustal thickness in the bight [*James*, 1971] and much greater present relief and width of the Altiplano compared with other portions of the Andes are consequences of the continuous strike-slip-driven collision (Figure 4). If so, the wide zone of crustal thickening is not a simple collision of "sliver plates"; it is the cumulative effect of transpression on many faults. This speculation is dependent on the assumption that present Altiplano relief and crustal thickness are affected more by shortening than by extrusive and intrusive activity; *Isacks* [1985] shows that this assumption is probably valid.

The bight of Alaska may be analogous to that of Peru-Chile (Figure 4). At present, oblique convergence in Alaska suggests collision of a dextrally slipping eastern and slightly sinistrally slipping western portion of the sliver plate(s) of south central Alaska. During the early Tertiary and all of the Cretaceous, the convergence direction was closer to due north, implying major strike-slip motion on both segments and consequent compression in this bight. The substantial convexity of this region is more appropriately seen in the faults than in the present trench, because of the very wide accretionary prism. It may not be coincidental that the tallest mountain in North America, Mount Denali (formerly McKinley), is at the apex of this bight and adjacent to the major Tertiary strike-slip fault of Alaska, the Denali Fault (Figure 4). The Cenozoic history of strike-slip motion on the faults of Alaska is enigmatic, with major dextral slip east of Mount Denali [*Forbes et al.*, 1974] but little evidence of substantial offset near Mount Denali [*Reed and Lanphere*, 1974; *Csejtey et al.*, 1982]. Perhaps some of the motion of the sliver plates has been accommodated as crustal thickening, due to the change in sense of oblique convergence near the bight. An additional probable source of the apparently conflicting evidence is the assumption of constant strike-slip rates since the time of formation of the offset rocks; Tertiary changes in convergence obliquity imply substantial changes in strike-slip rates and even sense of offset in the vicinity of Mount Denali.

Compression at the head of a sliver has also been suggested as a cause of mountain building in Japan [*Kaizuka*, 1975]. The change in azimuth from oblique convergence in the Kuriles to perpendicular convergence in northeast Japan occurs in the vicinity of the Hidaka Mountains of Hokkaido, one of the areas of strongest Neogene folding in Japan [*Matsuda et al.*, 1966]. Shallow focal mechanisms from this region indicate reverse faulting with maximum compressional axes approximately parallel to the trench; similar focal mechanisms are found in the underlying slab, possibly indicating tearing of the slab [*Stauder and Mualchin*, 1976]. However, the structural style in this region may be complicated by proximity to the poorly located Pacific/North America/Eurasia triple junction. Farther south, sinistral slip of the Izu-Bonin sliver may be responsible for the strong Neogene folding in the adjacent portion of Japan [*Kaizuka*, 1975]. Again, however, proximity to a triple junction (Pacific/Philippine/Eurasia) may complicate the structural style. Furthermore, the presence of active strike-slip faulting parallel to the Izu-Bonin Arc has not been clearly demonstrated.

Continental Versus Oceanic Strike-Slip Faulting

A remarkable correlation exists between the presence of strike-slip faults and the type of crust in the overriding plate. Two thirds of the modern subduction zones with continental crust as the overriding plate have active strike-slip motion near the arc, while only one fifth of oceanic overriding plates have similar faulting (Table 4). In part, this observation could be an artifact of the less complete outcrops within oceanic overriding plates, but the scarcity of strike-slip focal mechanisms and tendency of strike-slip faults to lie within the arc largely obviate this qualification. Because continental arcs are generally older than oceanic arcs, the paucity of strike-slip faults in oceanic overriding plates could be due to the shorter

TABLE 4. Arc-Parallel Strike-Slip Faulting

Type Crust	Subduction Zone	Major Fault	Offset*	Reference
Continental	New Zealand	Alpine	D	*Wellman* [1964], *Carter and Norris* [1976], *Norris and Carter* [1982]
	Aegean		...	*Mercier* [1981]
	Makran		...	*Kazmi* [1979], *Quittmeyer et al.* [1979]
	Andaman		D	*Mukhopadhyay* [1984]
	Sumatra	Semangko (Barisan)	D	*Fitch* [1972], *Katili* [1974], *Huchon and Le Pichon* [1984]
	Ryukyu		...	
	SW Japan	Median Tectonic Line	D	*Okada* [1971], *Matsumoto and Kimura* [1974], *Ichikawa* [1980]
	NE Japan	North Japan Line, etc.	D	*Okayama* [1961], *Matsuda and Kitamura* [1974]
	Kurile		D	*Kaizuka* [1975], *Ichikawa* [1980]
	Kamchatka		...	
	Alaska Peninsula	Farewell, Holitna, Togiak-Tikchik	D	*Lathram et al.* [1974]
	Alaska	Fairweather, etc	D	*Lathram et al.* [1974]
	Cascades	St. Helens	D	*Weaver and Smith* [1981]
	SW Mexico		...	
	SE Mexico		...	
	Middle America		...	
	Colombia	Dolores	D	*Campbell* [1974*a*], *Pennington* [1981]
	Ecuador	Guayaquil	D	*Campbell* [1974*b*], *Pennington* [1981]
		Cotopaxi-Banõs	S	
	Peru		S	*Stauder* [1975], *Philip and Megard* [1977], *Suárez et al.* [1983]
	North Chile	Atacama	D	*St. Amand and Allen* [1960], *Arabasz* [1971]
	Central Chile	Atacama	D	*St. Amand and Allen* [1960], *Arabasz* [1971]
	South Chile	Liquiñe-Ofqui	D	*Hervé et al.* [1979]
	Tierra del Fuego		...	
Transitional	Java		S	*Tjia* [1968], *Katili* [1970], *Chotin et al.* [1985]
	Philippines	Philippine	S	*Allen* [1962], *Fitch* [1972], *Hamilton* [1979]
Oceanic	Kermadec		...	
	Tonga		...	
	New Hebrides	?Coriolis (inactive)	...	*Dubois et al.* [1978]
	Solomon		D?	*Coleman and Hackman* [1974]
	New Britain		...	
	Palau		...	
	Yap		...	
	Marianas		...	
	Izu-Bonin	?Nishi-Schichito Bonin Ridge (inactive)	S? S?	*Kaizuka* [1975], *Karig and Moore* [1975], *Ichikawa* [1980]
	North Sulawesi		...	
	Sangihe		...	
	Central Aleutians		D	*Cormier* [1975]
	Lesser Antilles		...	
	South Sandwich		...	

*D, dextral; S, sinistral; three dots, none.

opportunity for oblique convergence to occur and initiate strike-slip motion. However, in neither continental nor oceanic overriding plates is there a correlation between subduction duration and occurrence of strike-slip faults.

Of the 23 subduction zones with continental overriding plates of Table 4, arc-parallel strike-slip faults appear to be absent only in the Aegean, Makran, Mexico, Kamchatka, Middle America, Ryukyu, and Tierra del Fuego. Discrete strike-slip faults are apparently unnecessary in the Aegean, because of diffuse and variable crustal thinning. Scattered strike-slip faults in the far northern Aegean [*Mercier*, 1981] are probably related to collision of the Turkish and Eurasian plates [*McKenzie*, 1978]. The Makran forearc is heavily faulted, but these faults are mainly thrust faults; all major strike-slip faults are approximately perpendicular to the trench, associated with the Eurasia/India plate boundary [*Kazmi*, 1979; *Quittmeyer et al.*, 1979]. Strike-slip faults are common in southern Mexico only east of the Isthmus of Tehuantapec. The Salina Cruz fault, a major sinistral strike-slip fault which may be currently active, trends approximately perpendicular to the Mexican trench and separates the zone of numerous Paleogene sinistral faults from the subduction segments considered here [*Viniegra*, 1971]. Strike-slip focal mechanisms are reported from the Cascades region [*Zoback and Zoback*, 1980], but slip planes may differ substantially from the arc trend [*Crosson and Lin*, 1975], and only one significant strike-slip fault parallel to the arc is reported [*Weaver and Smith*, 1981]. In Middle America, three dominant structural trends are probably currently active, with northwest-southeast, north-south, and northeast-southwest azimuths, but strike-slip

focal mechanisms such as that of the Managua earthquake indicate slip planes perpendicular to the trench [*Ward et al.*, 1974].

Java and the Philippines might more appropriately be considered transitional crust than continental. True continental crust in Java is confined to the northwest portion, though crustal thicknesses typical of continental crust are present throughout Java [*Hamilton*, 1979]. Nearly perpendicular convergence in Java is not accommodated by any significant trench-parallel strike-slip faults [*Hamilton*, 1979], though a short sinistral fault has been inferred in continental westernmost Java [*Tjia*, 1968; *Katili*, 1970] and many minor strike-slip faults with a wide variety of azimuths have been mapped throughout Java [*Chotin et al.*, 1985]. A long history of arc magmatism and collision in the Philippines has resulted in near-continental crustal thicknesses, and current oblique convergence in the Philippines makes the Philippine Fault one of the most obvious of modern strike-slip faults [*Fitch*, 1972]. However, this fault may be more complex in origin than simple oblique convergence, as it extends from behind the eastward dipping Manila Trench of the northern Philippines to behind the westward dipping Philippine Trench of the southern Philippines.

The Andaman subduction zone is included in subduction zones with continental overriding plates, though the present distribution of continental crust within the arc and forearc is discontinuous [*Curray et al.*, 1982]. Strike-slip faulting within the Andaman region is mostly associated with transform faults that offset the back-arc spreading segments, but focal mechanisms [*Mukhopadhyay*, 1984] and seismic profiling [*Curray et al.*, 1982] indicate the presence of other strike-slip faults within and parallel to the forearc.

In contrast to the ubiquity of strike-slip faulting within continental overriding plates, only 2 or 3 of the 14 oceanic overriding plates possess known arc-parallel strike-slip faults. The best example of the latter is the Western Aleutians, omitted from Tables 1 and 4 because "convergence" is almost pure strike-slip. Nevertheless, an underthrust slab is present, and focal mechanisms indicate the presence of a major dextral fault along the north ("landward") margin of the Aleutian Ridge, extending from the Near Islands to Kamchatka [*Cormier*, 1975]. Whether this faulting extends as far east as the Central Aleutian transect of Table 1 is not yet known. In the Izu-Bonin region, Oligocene sinistral displacement of the Bonin Ridge has been hypothesized [*Karig and Moore*, 1975]. A diffuse zone of sinistral motion near the eastern ("landward") margin of the northern Bonin Ridge, the Nishi-Shichito zone, may be currently active [*Kaizuka*, 1975]. Strike-slip focal mechanisms are common from the Izu-Bonin region [*Ichikawa*, 1980], but slip planes are generally not parallel to the arc. Thus the existence of modern arc-parallel strike-slip faulting in Izu-Bonin is uncertain. In the Solomons, late Pliocene and Quaternary strike-slip fractures are common, along trends approximately parallel to the arc. These possibly dextral faults are also found within the arc, although normal faulting predominates [*Coleman and Hackman*, 1974].

Mechanism

The mechanism of strike-slip decoupling of the forearc from the remainder of the overriding plate was first explored by *Fitch* [1972], based on consideration of the Semangko, Philippine, Median Tectonic Line, and Alpine faults. Oblique convergence without strike-slip motion distributes frictional shear over a long path at the boundary between overthrusting and underthrusting plates. In contrast, a vertical surface can concentrate shear more effectively and minimize the total effective length of plate boundary accommodating the shear. By this rationale, a strike-slip fault would develop whenever convergence is oblique by more than about 45° [*Fitch*, 1972]. Strike-slip faulting is currently active even in some subduction zones with near-perpendicular convergence (e.g., Chile), though it is more common when subduction is oblique (Figure 3). Fitch's 45° estimate assumes equal friction per unit area for the thrust boundary between plates and the strike-slip fault. Instead, the strike-slip fault must be much weaker, as evidenced by absence of major earthquakes and occurrence of strike-slip in subduction zones with low obliquity of convergence. Figure 3 and Table 4 yield information on the conditions required for present activity on a preexisting strike-slip fault; they cannot place useful empirical limits on the amount of convergence obliquity required for initiation of strike-slip motion.

Beck [1980] revised the criterion of *Fitch* [1972] for initiation of strike-slip faulting, by assuming oblique shear rather than horizontal shear and allowing the resistance to slip per unit area on the strike-slip fault (r_t) to differ from that on the contact between major plates (r_s). *Beck* [1980] concluded that strike-slip faulting is expected whenever

$$\frac{\tan \phi}{\sin D_s} > \frac{r_t}{r_s}$$

where ϕ is the obliquity of convergence and D_s is the dip along the interface between subducting and overriding plates. Using modern values of ϕ and D_s, this inequality allows one to estimate an average ratio of r_t to r_s required for active strike-slip faulting. Eighty-six percent of the modern subduction zones with active strike-slip faulting have a ratio $\tan \phi / \sin D_s$ of greater than 0.8; in contrast, 80% of modern subduction zones lacking active strike-slip faulting have a ratio of less than 0.8. Before attaching physical significance to this cutoff ratio of about 0.8, however, two important assumptions made by *Beck* [1980] must be verified. First, the inequality is based on the assumption that partitioning of the arc-parallel component of oblique convergence into strike-slip is either complete or completely absent. Second, presence or absence of strike-slip faulting is assumed to be independent of the compressional or extensional regime of the overriding plate. As we will see subsequently, neither assumption appears to be valid.

The sense of strike-slip motion is nearly always consistent with the direction of oblique convergence (Figure 3). Only Solomon, Alaska, and Alaska Peninsula are apparent exceptions. All three regions appear to have dextral slip though sinistral motion is predicted. Solomon motion is possibly dextral but not known with confidence [*Coleman and Hackman*, 1974]. Furthermore, the convergence obliquity is smaller than combined uncertainties in Pacific/Australia and Australia/Solomon relative motions. The discrepancy for Alaska and Alaska Peninsula is more important, though it is much less than implied by Figure 3 when azimuth perpendicular to the currently active faults is considered rather than azimuth perpendicular to the present arcs (Figure 4). One possible explanation is that the major dextral motion known and expected farther east along the Denali Fault may be more important for overall motion of the "sliver plate" than local slightly sinistral forces. More study of Pleistocene fault motions in Alaska is required to resolve the possible inconsistencies in this region.

The much more common occurrence of strike-slip faulting in continental lithosphere than in oceanic lithosphere is a consequence of the greater strength of oceanic lithosphere. *Vink et al.* [1984] have considered the analogous case of preferential rifting of continental lithosphere. Little difference is found in the strengths of continental and oceanic upper crust. Because olivine has a greater tensile strength than quartz, the compositional difference between continental and oceanic lithosphere below 13 km results in much weaker continental lithosphere. When lithospheric tensile strength is integrated over depth, the total strength of continental lithosphere is found to be about a factor of 3 less than oceanic lithosphere [*Vink et al.*, 1984]. Thus not only rifting [*Vink et al.*, 1984] but also major strike-slip faulting should be much more common within continental lithosphere.

For either type of lithosphere, both increased thermal gradient and greater crustal thickness substantially decrease lithospheric strength [*Vink et al.*, 1984]. The magmatic arc, characterized by higher thermal gradients, decreased lithospheric thickness due to heating, and increased crustal thickness due to plutonism, is thus by far the weakest portion of the overriding plate and most likely to accommodate either strike-slip faulting or rifting [*Beck*, 1980]. For example, crustal temperatures in Japan at 20-km depth are about 700°–800° near the arc, but only 100°–150° in the forearc [*Uyeda and Horai*, 1964], suggesting at least a factor of 10 difference in overall strength (Figure 4 of *Vink et al.* [1984]).

In addition to strength of the overriding plate and oblique convergence, a third factor is probably an important control on strike-slip faulting: coupling between the subducting and overriding paltes. Of 14 subduction zones with low coupling (strain classes 1–3), only two or three have arc-parallel strike-slip faults: Andaman, New Zealand, and possibly Izu-Bonin. Andaman and New Zealand both have very oblique convergence. It may not even be appropriate to include the Alpine Fault of New Zealand with the other occurrences of strike-slip faulting, as it forms part of the boundary between two major plates, Australia and Pacific. As previously discussed, the presence of arc-parallel strike-slip faulting in Izu-Bonin is uncertain. Of 15 subduction zones with high coupling (strain classes 5–7), only three or four lack strike-slip faults: southeast and southwest Mexico, Kamchatka, and possibly Java. Convergence in southeast and southwest Mexico and Kamchatka is nearly perpendicular to the trench, and presence of arc-parallel strike-slip faulting in Java is uncertain.

Coupling is expected to affect strike-slip faulting, because the shear traction along a potential strike-slip fault is a function of the transverse component of the plate boundary coupling force, not simply of the convergence vector. This shear traction equals the local stress difference induced by the plate boundary (which is larger for better coupling) multiplied by the sine of twice the angle between the principal compression axis and the potential strike-slip fault (which is larger for more oblique convergence). If the product of these coupling and obliquity effects exceeds the strength of the possible fault zone, then active strike-slip faulting is expected.

Although the expected correlation between coupling and strike-slip faulting is strongly confirmed by the data, an alternative explanation of this correlation is also likely. When back-arc spreading occurs, arc-parallel strike-slip faulting is usually not required to accommodate a portion of oblique convergence. Instead, partitioning of oblique convergence can occur through a back-arc spreading direction that is not perpendicular to the trench [*Dewey*, 1980], as in the Andaman and Ryukyu subduction zones. Even back-arc spreading perpendicular to the trench reduces the probability of strike-slip faulting parallel to the trench, because the additional component of convergence reduces the convergence obliquity. An extreme example is New Britain, where back-arc spreading reduces obliquity from 57°–67° to less than 8°.

It is possible that the good correlation of lithospheric type with presence or absence of strike-slip faulting is an indirect rather than causal relationship. The excellent correlation of strain regime with strike-slip may lead to an indirect correlation of lithospheric type with strike-slip, because continental overriding plates tend to be more compressional than oceanic ones. As discussed in subsequent sections on dip and strain regime models, the greater ages of continental than oceanic subduction zones are responsible for shallower intermediate dips and therefore higher strain classes in continental subduction zones.

Effect of Strike-Slip Faulting on Slip Vectors

Worldwide motion models [*Minster et al.*, 1974; *Chase*, 1978*a*; *Minster and Jordan*, 1978] utilize slip vectors of shallow thrusting earthquakes as constraints on subduction direction. However, if a forearc sliver plate is present, the slip vectors indicate motion of the underthrusting plate with respect to the forearc sliver, not with respect to the major overriding plate. A detailed vector analysis of the important distinction between azimuths of these and other convergence vectors is given by *Dewey* [1980]. If convergence is not strongly oblique and the strike-slip rate is low, resulting errors will be minor. For example, a strike-slip rate which is 10% of the overall convergence rate causes a 5.2° change in slip vector for oblique convergence of 30°. For strike-slip rates that are a larger percentage of the overall convergence rate, the effect can be substantial. For example, the present strike-slip rate on the Median Tectonic Line of southwest Japan is only 0.5 cm/yr [*Okada*, 1971], but because convergence is very slow (Table 1), an 8° to 19° error in inferred convergence direction between Eurasia and the Philippine plate probably results.

For most other subduction zones, geologic evidence of modern strike-slip rates is very inexact. Another approach to the estimation of strike-slip rates is analysis of slip vector residuals, the differences between observed slip vector azimuths and predicted azimuths based on known major-plate motions. This method makes three important assumptions: (1) the slip vector indicates relative motion of the forearc sliver plate with respect to the underriding plate, (2) the relative motion model used [e.g., *Minster and Jordan*, 1978] is not biased by the fact that these same slip vectors were inverted without considering presence of sliver plates, and (3) slip vectors are not biased by the velocity structure of the slab. The second assumption is probably reasonable for North America/Pacific, North America/Cocos, and South America/Nazca rotation poles, which are constrained by global closure requirements as well as many slip vectors that are near perpendicular. However, uncertainties in Caribbean, Philippine, Southeast Asian, and Australian plate motions must be considered larger than those assigned, because of possible systematic slip vector residuals along the subduction zones. The third assumption is more difficult to evaluate. Velocity in the slab higher than in the upper mantle can cause significant errors in focal mechanism solutions, particularly for those determined from local networks [*Engdahl et al.*, 1977]. Evaluation of

TABLE 5. Slip Vector Residuals

Subduction Zone	Slip Vector Residual*				Obliquity†		Focal Mechanisms Used‡	Focal Mechanism Sources§	Convergence¶ Rate, cm/yr	Predicted Strike-Slip Rate, cm/yr	
	N	$\bar{X}$	σ	95% Confidence Limits	$\bar{X}$	σ				$\bar{X}$	95% Confidence Limits
South Kurile (42.5°–44.7°N)	24	6.6	9.0	3.8	28.2	0.6	SM: 42–65	*Stauder and Mualchin* [1976]	9.2	1.1	0.5, 1.8
Central Kurile (44.8°–47.0°N)	21	2.9	6.4	2.9	26.4	0.7	SM: 21–41	*Stauder and Mualchin* [1976]	9.1	0.5	0.0, 1.0
North Kurile and Kamchatka (47.1°–56.0°N)	18	0.7	8.7	4.4	0.8	2.4	SM: 2–15, 17–20	*Stauder and Mualchin* [1976]	8.8	0.1	−0.6, 0.8
Aleutians (168°E–167.6°W)	7	11.0	6.0	5.3	45.9	23.6	MJ: 21–27	*Minster and Jordan* [1978]	8.3	1.9	1.1, 2.7
Alaska Peninsula	4	1.5	2.5	4.0	−15.2	1.7	MJ: 17–20	*Minster and Jordan* [1978]	6.8	0.2	−0.3, 0.7
Mexico	8	1.0	4.5	3.7	19.9	7.2	B: 4, 6, 7, 10, 13, 20, 37, 39, 40, 42, 52, 62	*Molnar and Sykes* [1969], *Dean and Drake* [1978], *Chael and Stewart* [1982], *and Burbach et al.* [1984]	7.2	0.1	−0.4, 0.6
Ecuador and Colombia	5	11.4	14.1	17.5	22.6	17.3	P: 17–19, 23; S: 15; C: 69	*Pennington* [1981], *Suárez et al.* [1983], *Chase* [1978*a*]	7.7	1.6	−0.9, 3.7
Peru	4	−7.7	12.5	19.9	−24.5	7.8	MJ: 107–109; C: 71	*Minster and Jordan* [1978], *Chase* [1978*a*]	8.7	−1.2	−4.0, 2.3
Chile	18	4.1	8.6	4.3	20.9	5.4	MJ: 110–127	*Minster and Jordan* [1978]	9.1	0.7	−0.0, 1.4
Sumatra‖	7	27.9	···	5.8	55.4	···	K: L1, L4, L9, L12, F7, F8, F10	*Kappel* [1980], *Fitch* [1972]	6.8	3.6	3.1, 4.1

*Azimuth of slip vector from focal mechanism minus predicted convergence azimuth from model RM2 of *Minster and Jordan* [1978].
†Azimuth perpendicular to arc minus predicted convergence azimuth from model RM2 of *Minster and Jordan* [1978].
‡Letters refer to source to right in same row.
§References to *Minster and Jordan* [1978] and *Chase* [1978*a*] are not original sources; *Minster and Jordan* [1978] recalculated slip vectors by rotating into horizontal plane; *Chase* [1978*a*] references cite B. L. Isacks (in preparation) as source.
¶From *Minster and Jordan* [1978].
‖Slip vector residuals and obliquity for Sumatra were determined assuming that true convergence direction is that of Java slip vectors (see text).

errors due to slab heterogeneity requires detailed modeling in each region studied. *Engdahl et al.* [1977] found that this effect had a minor impact on slip directions from Kurile-Kamchatka and a possibly significant impact in the Aleutians. Thus slip vector residuals from any one region should be treated with some caution, while consistent patterns among different regions are more trustworthy.

Table 5 and Figure 5 summarize slip vector residuals for those subduction zones with well-constrained plate motions: Kurile-Kamchatka, Aleutian–Alaska Peninsula, Mexico, and South America. Also shown are data for Sumatra, to be discussed in the next section. All 10 segments considered have continental overriding plates, and all except Kamchatka and Mexico have active strike-slip faults near their arcs (Table 4). Most of the slip vectors considered were included in the global inversions of *Minster and Jordan* [1978] and *Chase* [1978*a*], but some newer data are included. The extensive data coverage of *Stauder and Mualchin* [1976] for the Kurile-Kamchatka region allows subdivision of this zone into three latitudinal intervals; *Minster and Jordan* [1978] use only a subset of these results, presumably to avoid extremely heavy weighting of this zone in their inversion. When they are available from *Minster and Jordan* [1978], corrected slip vectors are used, based on the horizontal projection of the slip vector. However, no attempt was made to correct other slip vectors, as the correction is usually only about 1° [*Minster and Jordan*, 1978].

The obliquity of convergence (Table 5) is here taken as the difference between the azimuth perpendicular to the arc and the major plate motion, where the latter is based on model RM2 of *Minster and Jordan* [1978]. In principle, it would be preferable to use the azimuth perpendicular to strike-slip faults rather than the arc. However, fault locations are not always known; where they are known, they usually lie along the arc.

The relation between obliquity of convergence and slip residuals is shown in Figure 5. Clearly, oblique convergence causes systematic slip residuals, as expected from the concept of forearc slivers driven by oblique convergence. However, the 95% confidence limits are often large; many more focal mechanisms would be needed before one could draw conclusions concerning either the threshold amount of oblique convergence required for sliver plate motion or whether or not the partitioning between oblique convergence and strike-slip is affected by parameters other than obliquity (e.g., convergence rate or slab age).

The rate of strike-slip motion (V_{ss}) of the forearc sliver with respect to the major overriding plate is determined from the

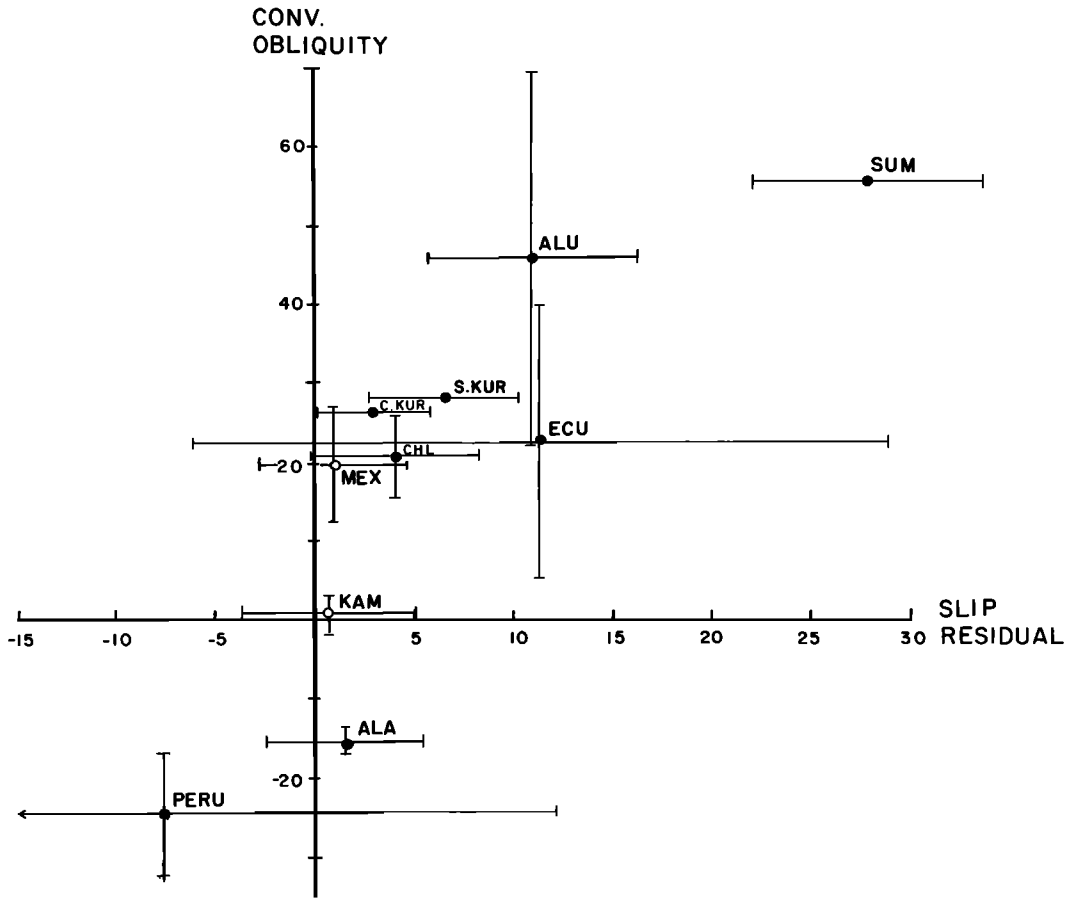

Fig. 5. Slip vector residual versus convergence obliquity for subduction zones with both a reliably determined convergence azimuth and at least four slip vectors of shallow underthrusting earthquakes. The slip residual is the angle between the mean slip vector azimuth and the convergence direction. The convergence obliquity is the angle between convergence direction and the azimuth perpendicular to the arc. Horizontal lines are 95% confidence limits; vertical lines are one standard deviation. Data are from Table 5. Open circles indicate subduction zones with no modern strike-slip faulting; solid circles indicate subduction zones with active strike-slip faulting. Note that most points plot in the upper right or lower left quadrants; this suggests that oblique convergence is causing strike-slip displacement of the forearc, thereby biasing slip vectors.

simple geometrical relation

$$V_{ss} = V \tan \theta/(\sin \phi \tan \theta + \cos \phi)$$

where V is the convergence rate between the major plates, θ is the slip vector residual, and ϕ is the obliquity of convergence. Predicted strike-slip rates are small for the subduction zones of Table 5 (except for Sumatra) and are generally less than 1 or 2 cm/yr (Figure 6). Including the 95% confidence limits for the slip vector residuals, only South Kurile, Central Kurile, and Aleutian strike-slip rates are significantly nonzero at the 95% confidence level. However, of the seven mean strike-slip rates for subduction zones with known active strike-slip faults, all show predicted strike-slip directions (Table 5) consistent with those observed in the field (Table 4). The slowest predicted strike-slip rates are in Kamchatka (0.1 ± 0.7 cm/yr) and Mexico (0.1 ± 0.5 cm/yr), the only two regions of Table 5 with no known modern strike-slip faulting.

Minster et al. [1974] noticed the systematic mismatch of observed to predicted slip directions in the Aleutians, and they hypothesized the presence of a Bering plate to account for this mismatch. Although this discrepancy persists in subsequent analysis with more data, *Minster and Jordan* [1978] withdrew the Bering plate hypothesis, because the extensive newer data from Kurile-Kamchatka [*Stauder and Mualchin*, 1976] show a good match of observed to modelled slip vectors. The Aleutian mismatch and Kurile-Kamchatka match are readily explicable as sliver plate response to oblique convergence. More generally, the effect of sliver plates on slip vectors urges caution in the use of global inversions to test for the existence of uncertain plate boundaries, if slip vectors constitute an important constraint in the test [e.g., *Stein and Gordon*, 1984].

Implications for Southeast Asian Plate Motions

Based on the concept of slip deviations caused by strike-slip faulting, a reevaluation of Southeast Asia/India relative motions at the Sunda Arc is warranted. Although all global motion inversions can predict Eurasia/India relative motions in the Sunda Arc, slip vectors from this region were not used in the inversions, because of possible internal deformation in East Asia and Southeast Asia. Existence of a Southeast Asian plate, probably with a diffuse "plate boundary" within China, is implied by the work of *Molnar and Tapponnier* [1975]; they demonstrate that collision of India with Eurasia is causing

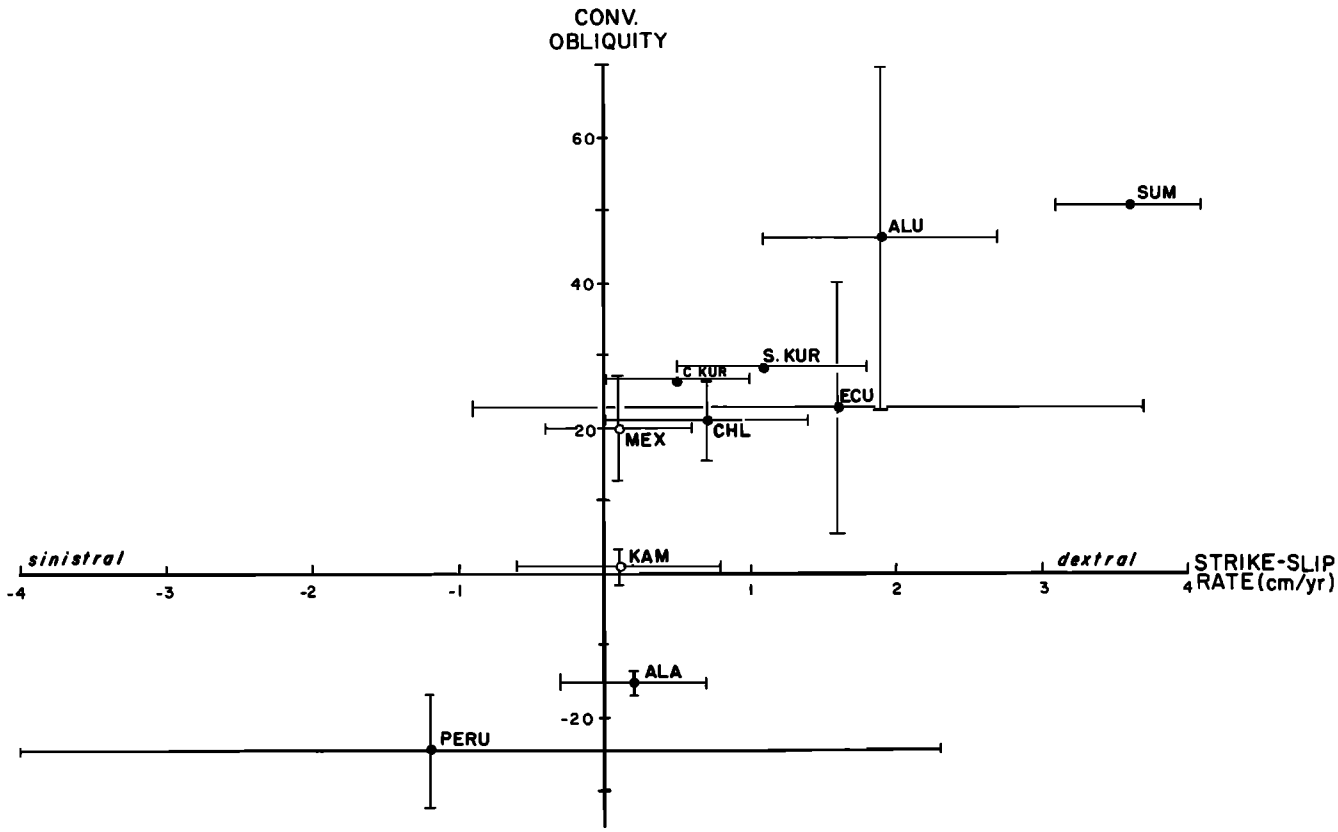

Fig. 6. Modern strike-slip rates estimated from the slip vector residuals of Table 5 and Figure 5. Note that rate of strike-slip motion of forearc sliver plates appears to increase with increasingly oblique convergence. Also note that the two smallest strike-slip rates are for subduction zones with no known active strike-slip faults (open circles). All calculated offset directions (sinistral or dextral) are consistent with geological evidence of modern offset direction (Table 4).

both strike-slip faulting and crustal thinning in China. The plate's existence is confirmed by systematic differences between observed focal mechanisms in the Sunda Trench [*Fitch*, 1972; *Kappel*, 1980] and predicted convergence directions based on Eurasia/India relative motions.

Predicted convergence directions vary only slightly along the Sunda Arc: N18°E at Andaman, N24°E at Sumatra, N23°E at Java, and N19°E at East Banda according to the model of *Minster and Jordan* [1978] or N23°E, N28°E, N27°E, and N24°E, respectively, according to *Chase* [1978*a*]. The "Indian" plate may actually be two plates that have a small component of convergence along their common boundary, the Ninetyeast Ridge [*Minster and Jordan*, 1978; *Stein and Gordon*, 1984]. If so, predicted motion between the Australian plate and Sunda Arc is about 10° closer to north-south, based on model A of *Minster and Jordan* [1978]. The predicted motion at the northeast end of the Banda subduction zone implies strike-slip or extension in this region rather than the observed subduction. An analysis of slab geometry beneath the Banda Arc led *Cardwell and Isacks* [1978] to conclude that the convergence direction is approximately NNW, about 40° ± 20° from that predicted from Eurasia/India relative motions.

Kappel [1980] presents 47 new and published focal mechanisms from the Sunda Arc. Of these, 19 are shallow underthrusting solutions indicative of interplate motion. The mean direction indicated by 5 slip vectors from Java is N1.0°W ± 6.7° (95% confidence limits), and the mean of 7 slip vectors from Sumatra is N26.9°E ± 6.8°. Seven slip vectors with focal depths greater than 50 km were not used in this calculation because of higher dispersion; including them does not significantly change the means. The two directions are significantly different at much more than the 95% confidence level.

The Sumatran slip direction is consistent with predicted Eurasia/India motions while the Java slip direction is highly discordant. Thus one possible interpretation is that Sumatra is part of the Eurasian plate but Java and Banda are not, with east-west extension implied between Java and Sumatra. Although extension is recognized in the southern Sunda Straits between these islands [*Huchon and Le Pichon*, 1984], there is no evidence of the required extension north of the Sunda Straits.

An alternative explanation for the slip vector discrepancies involves the effect of strike-slip faulting on slip vectors. There is no evidence of significant arc-parallel strike-slip faulting in Java, except for a short segment of unknown age in westernmost Java (Table 4). As the slip vectors indicate convergence nearly perpendicular to the trench (obliquity of 13°), it is probably unlikely that they are biased by more than about 4° clockwise (Figure 5) by strike-slip faulting. Thus the true direction of convergence between Southeast Asian and Indian plates at the Sunda subduction zone is probably close to north-south, a conclusion consistent with Javanese slip vectors and subduction geometry of the Banda Arc.

A further constraint that must be satisfied by the inferred north-south convergence between the Southeast Asia and Indian plates is convergence all along the Andaman subduc-

tion zone. The Banda–Sunda–Andaman Trench curves northward not only at its eastern (Banda) end but also at its western (Andaman) end (Figure 7). The maximum Andaman reentrant angle of about 33° between 14° and 15°N would require extension instead of subduction, if not for back-arc spreading in the Andaman Basin and dextral strike-slip faulting within the Andaman forearc. A vector diagram for 14° to 15°N (Figure 7) indicates that the combination of India/Southeast Asia (N1°W, about 6 cm/yr) and Southeast Asia/Andaman [*Lawver and Curray*, 1981] vectors is sufficient to remove the need for extension at the boundary and results in strike-slip motion. Because seismic profiles indicate subduction here [*Hamilton*, 1979], an additional northward component is required, from strike-slip faults within the Andaman forearc. These mapped strike-slip faults [*Curray et al.*, 1982] are currently active, as indicated by focal mechanisms [*Mukhopadhyay*, 1984]. However, neither the rate of subduction at 14° to 15°N nor the rates of motion on the strike-slip faults are known, and too few interplate slip vectors are available to estimate these rates. Furthermore, strike-slip faults appear to extend northward from northwest Sumatra into the North Malay Peninsula, potentially complicating Andaman/Sunda motion comparisons. The offset direction of these faults and whether or not they are currently active is debatable [*Hamilton*, 1979]. Thus although the geometry of the Andaman subduction zone is consistent with north-south convergence between the Australian and Southeast Asian plates, it does not preclude a somewhat different convergence direction.

North-south convergence at the Sunda Arc, when compared with the N18°E to N24°E India/Eurasia motion there, implies a significant east-west component of extension between Eurasia and Southeast Asia (Figure 7). This east-west component is smaller, but apparently still significant, if the India plate actually comprises two plates: West India and Australia (Figure 7). This extra component of eastward motion for Southeast Asia is consistent with, but not required by, the eastward component of China imparted by collision of India with Asia [*Molnar and Tapponnier*, 1975]. Determination of the Southeast Asia/Eurasia pole and rate of rotation is not currently possible; the one published pole, near 28°N, 97°E [*Hamilton*, 1979] compounds the problems of predicted extension in the Banda Trench and of Javanese slip vector mismatch. Indeed, it is not even possible to specify with confidence the northern limit of the Southeast Asia plate. However, the interpreted east-west components of extension in both China and Sunda allow a tentative conclusion that the Southeast Asia/Eurasia rotation pole is far enough away from the Sunda Arc to allow the convergence direction in Java (N1°W $\pm$ 6.7°) to be appropriate also for adjacent Sumatra.

If the Australia/Southeast Asia convergence direction at Sumatra is N1°W, then the Sumatran slip vector orientation of N26.9° $\pm$ 6.8°, when combined with an approximate convergence rate of 6.8 cm/yr [*Minster and Jordan*, 1978], indicates a strike-slip rate in Sumatra of 3.6 $\pm$ 0.5 cm/yr. Of course, the Southeast Asia plate may also have a north-south component with respect to Eurasia; for example, if it is about 0.7 cm/yr, or 10% of the 6.8 cm/yr assumed, then the estimate of strike-slip rate would also be in error by 10%. Such errors are comparable to the 96% confidence limits of 3.1 to 4.1 cm/yr on strike-slip rate, derived from combining the 80% one-tailed confidence limits for Java slip direction (N1°W $\pm$ 2.3°) with those for Sumatran slip direction (N26.9°E $\pm$ 2.5°).

The inferred dextral strike-slip motion of about 3.6 cm/yr of the Sumatran forearc is substantially larger than that calculated for the other arcs of Table 5, consistent with the highly oblique convergence angle of about 55°. The Semangko Fault (also known as the Barisan Fault or Sumatran Fault System) is one of the most geomorphically obvious arc strike-slip faults in the world. Geologic evidence of both total offset and offset rates on the Semangko is contradictory [*Page et al.*, 1979]; the 20- to 25-km offset of Quaternary formations found by *Katili and Hehuwat* [1967] indicates a minimum rate of 1 cm/yr. Strike-slip motion on the Semangko is accommodated to the west by transform faults and back-arc spreading in the Andaman Sea. The 460–480 km of spreading in the Andaman Sea since 13 m.y. B.P. [*Lawver and Curray*, 1981; *Curray et al.*, 1982] requires an average rate of dextral strike-slip faulting somewhere in western Sumatra of 3.7 cm/yr, remarkably (and perhaps coincidentally) similar to the 3.6-cm/yr rate inferred from slip vectors. Not all of the motion by either estimate need be accommodated on the Semangko Fault alone, as other strike-slip faults have been mapped in the west Sumatran forearc (Figure 7, *Karig et al.* [1980]). However, some or all of the Sumatran forearc faults extend westward into strike-slip faults in the Andaman forearc rather than into the Andaman back-arc spreading system [*Karig et al.*, 1980; *Curray et al.*, 1982].

Forearc Slivers and Terrane Motions

Forearc sliver motion often accompanies normal subduction; optimum conditions are oblique convergence, strong interplate coupling, and possibly a continental overriding plate. The importance of forearc sliver motion for terrane displacement stems more from its ubiquity than from its rates; half of modern subduction zones possess forearc slivers, generally with strike-slip rates of less than 2 cm/yr. Prolonged periods of slightly oblique subduction are likely to result in substantial terrane migration (e.g., 1000–2000 km in 100 m.y. at 1–2 cm/yr). Several of the terranes of western North America, which have moved northward at rates of a few centimeters per year, may therefore have been transported as forearc slivers rather than on oceanic plates [*Beck*, 1980].

Two factors will limit comparisons of observed to predicted forearc sliver motions for the Tertiary and Cretaceous: (1) uncertainties in convergence rates and azimuths and (2) uncertainties in the partitioning of oblique convergence into strike-slip. The slip vector residuals of Table 5 suggest that partitioning of the arc-parallel component of convergence into strike-slip varies from about 15% for 20° obliquity to about 60% for 60° obliquity. However, confidence limits for these estimates are quite large, and the partitioning is likely to depend on friction at both the subducting and strike-slip interfaces of the forearc sliver.

STATISTICAL ANALYSIS

Methods and Limitations

The interrelations of subduction parameters are a subject of continuing controversy. We seek geologically meaningful quantitative relationships between the dependent and independent variables of Table 1. Dependent variables include the strain regime and strike-slip faulting in the overriding plate, arc-trench gap, trench depth, Benioff zone length, and both shallow and deep dip of the subducting slab. Independent variables that have been proposed as affecting these dependent variables include convergence rate and angle, absolute motion

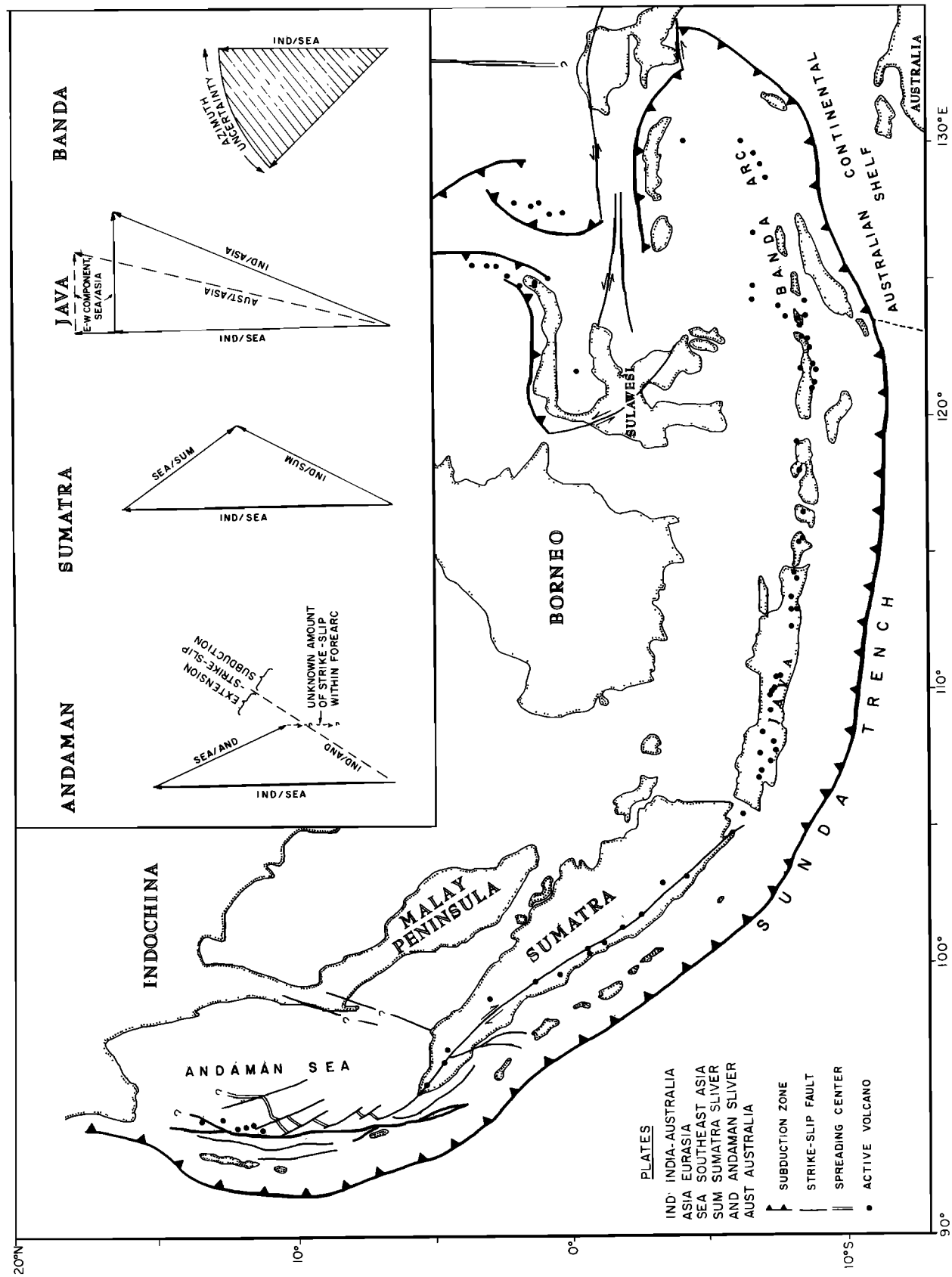

Fig. 7. Map of the Sunda-Banda subduction zone, showing locations of major strike-slip faults. Vector diagrams constraining motion of the Southeast Asia plate and Sumatra sliver plate are described in the text. Note that the length of convergence vectors in the Banda region is arbitrary, as only the azimuth of convergence is constrained by slab geometry in this region.

of overriding and underriding plates, slab age, and duration of subduction. At least three other independent variables may be important but are too poorly known to quantitatively include: mantle flow patterns, width of the accretionary prism, and width of the interface between overriding and underriding plates.

Most theoretical analyses have yielded only qualitative and often contradictory relationships, partly because key parameters such as shear stress between plates are poorly known. An alternative approach is used herein: empirical quantitative relationships are statistically derived, through application of multivariate analysis to modern subduction zones. This approach is not meant to substitute for theoretical analyses, but to complement and perhaps focus them.

Stepwise multiple regression analysis is utilized to isolate the primary independent variables affecting each dependent variable. Unlike conventional multiple linear regression, stepwise multiple regression can successfully cope with independent variables that are themselves partly correlated. Stepwise multiple regression first fits a linear regression between the dependent variable and the most highly correlated independent variable. Residuals to this relation are then correlated with all other independent variables, and the variable with the highest significant correlation is included in the regression equation. Inclusion of an additional independent variable changes the contributions of any independent variables already in the equation. Thus it is possible for an independent variable to enter the equation, gradually lose significance as other independent variables enter the equation and account for some of the same variance that it had accounted for, and eventually be dropped from the equation because it is no longer significant. Examples of this phenomenon will be discussed in the models section; this behavior generally results from correlation between independent variables.

The criterion for addition or subtraction of independent variables is an F test of their significance. In subsequent analyses an F of about 5 is generally used, corresponding to significance at about the 95–99% confidence level for the 30–39 observations in most regressions. The values of F are also given for the overall regression and as a guide to the relative significance of individual independent variables. Significance levels of a given value of F and number of degrees of freedom are available from any statistics book; for the number of nominal degrees of freedom used here, F's of about 2.9, 4.2, 7.6, and 13.3 are significant at the 90%, 95%, 99% and 99.9% confidence levels. Assignment of confidence levels to these regressions is probably misleadingly optimistic, because the individual observations (i.e., subduction zones) used are not strictly independent. Adjacent subduction zones often have very similar values for some or even most variables; thus the true number of degrees of freedom is impossible to estimate but is certainly less than implied by the number of observations used. As an extreme example, suppose that our entire data set consisted of 10 adjacent "segments" from the Marianas and 10 adjacent "segments" from Peru. Correlation between almost any two variables would then be significant at greater than the 95% confidence level based on 19 (i.e., 20–1) degrees of freedom, but in fact the true number of degrees of freedom would be closer to 1 (2–1). In contrast, the subduction zones of Table 1 were selected on the basis of substantial large-scale segmentation marking notable changes in at least some parameters. Nevertheless, substantial similarities remain in some parameters among adjacent subduction zones. For example, the seven subduction zones of South America all have nearly the same absolute motion of the overriding plate, and almost all are among the oldest subduction zones in Table 1. The nonindependence of observations (i.e., subduction zones) is therefore not only a reason for avoiding assignment of confidence levels to regressions, but also (and more importantly) a fundamental limitation of this analysis. Consequently, although the statistical analysis is capable of determining the most likely relationships among variables for modern subduction zones, none of these equations should be confidently used for other areas or times until their predictive value is confirmed on independent data for which both dependent and independent variables are known.

Because of the importance of including completely independent subduction zones with very different values for individual variables, an attempt was made to include in Table 1 as many different "normal" subduction zones as possible. Consequently, not all variables are known for every subduction zone used. An alternative approach is used by most authors, in which only subduction zones with no missing data are used. The stepwise multiple regression algorithm used herein for the isolation of significant independent variables [*Enslein et al.*, 1977] can utilize observations with missing data. However, resulting final correlation coefficients were often found to be optimistic when compared with an analysis of the same independent variables omitting all observations with any missing data. Therefore missing data were allowed in the determination of the significant independent variables, but the final regression equation is based on only those observations containing values for both the dependent variable and all of the selected independent variables.

Another factor that can lead to misinterpretation of significance levels for regressions is the large number of hypotheses tested by multiple regression. For example, if four dependent variables are each tested against five independent variables, then one correlation significant at the 95% confidence level is expected by chance, even if no true physical correlation exists among any of the variables. This problem is largely ameliorated by raising the required confidence level to 99%. However, given that not all observations are independent (as previously discussed), an even higher confidence level may be appropriate. Alternatively, most readers may prefer to make a subjective decision on the reliability of a correlation, based on examination of a plot of dependent versus independent variables.

The regression technique used here assumes that values for each independent variable are perfectly known and that all error is associated with the dependent variable. This assumption is clearly invalid for the data considered here, as all variables in Table 1 have associated errors. Violation of this assumption leads to a calculated slope of the regression line which is lower than the slope of the true relationship between dependent and independent variables. This phenomenon is most noticeable for "noisy" data, in which less than 50% of the variance in the dependent variable is accounted for by the independent variable(s) (e.g., Figure 12). For regression equations with much higher correlations, such as most of those shown subsequently, this effect is subtle. The multiple regression technique used here is adequate for isolation of the relevant independent variables and approximate quantification of their effects. However, other more sophisticated statistical techniques are superior when both independent and dependent variables have associated known uncertainties, when these uncertainties vary between observations, and when the relationship between variables is nonlinear. Nonlinear relationships (e.g., Figure 19) can significantly degrade corre-

lation coefficients based on linear regression. Although careful examination of regression residuals can reveal nonlinear relationships, they can easily be missed.

Because regression is a least squares procedure, both the regression coefficients and correlation coefficients are sensitive to extreme or anomalous points. Such points could be present in Table 1, either because of a misinterpretation by the original author of the value for a single variable for some subduction zone or because the entire subduction zone is anomalous (e.g., due to an unrecognized plate boundary or subduction of an unsuspected fragment of continental crust). In practice, the large number of subduction zones used here makes the contribution of a single anomalous point generally minor. Nevertheless, regression residuals were carefully monitored and, as specifically noted subsequently, residuals differing from the regression line by more than about 3 or 4 standard deviations were used as a criterion for excluding a subduction zone from a regression.

All variables were standardized prior to statistical analysis. Standardization involves subtraction of the variable mean from each data point, followed by division by the standard deviation. Standardization serves two purposes: (1) computer roundoff error is avoided, because the wide variations in magnitudes between variables are removed, and (2) the relative importance of regression coefficients for different variables is more evident. Resulting standardized regression equations are then converted back to the units of original variables.

Correlation pathways can sometimes be used to infer cause and effect relationships, with considerable caution. As we will see in the models section, the dependent variable in one equation may be the independent variable in another equation. For example, if A affects B and B affects C, then correlations A/B, B/C, and A/C may all be significant, with probably the poorest correlation between the three being the indirect path A/C. When stepwise regression is applied to the prediction of C from A and B, B will be added first to the regression equation. Because all of the correlation of A with C arises from A's effect on B, there should be little or no residual correlation of A with C after regression of B on C. In another example, suppose E and F are two independent variables that significantly predict H. One might conclude that variations in E and F cause variations in H. Yet it is possible that unconsidered variable D causes variations in both F and unconsidered variable G, with similar regression coefficients for D/F and D/G due to somewhat similar but distinctive physical processes. Then the true cause and effect relations might be that E and G cause variations in H, without eliminating the usefulness of F in the regression equation. Similarly, if variables I and J significantly predict L, the direct cause and effect relation might be that I and J cause K which causes L. In the case of subduction zone parameters, a combination of stepwise multiple regression and geologic insight may isolate the most likely cause and effect pathways among available variables. However, caution is required and the possibility remains that other important variables were not included because they could not be accurately quantified.

Implicit in statistical analysis of subduction parameters is the assumption that all subduction zones are now in an equilibrium state with respect to the variables considered. This assumption implies that two conditions are met: (1) no significant changes have occurred in any variable over the period of time represented by the variable with the longest response time, and (2) no variable is primarily affected by the rate of change of another variable. The second condition is probably usually valid; however, this generalization may not be true for slab dip. For example, the hypothesis that strain regime is dependent on changes in slab dip [*Furlong et al.*, 1982; *Hager*, 1983] is not readily testable through these analyses.

The variable that may have the longest response time is deep dip, but little is known of its temporal variations. The variable with the longest known response time is slab length, usually representing about 10 m.y. of convergence. Most other variables appear to have changed very little in the last 5 m.y. Changes in absolute motion about 5 m.y. ago [*Cox and Engebretson*, 1984] and in many spreading rates 5–10 m.y. ago undoubtedly are a source of some variance when compared with slab length. Many current episodes of back-arc spreading began about 5–10 m.y. ago. As previously discussed in the section on slab age, a correction for limited duration of back-arc spreading was required for four subduction zones when calculating time since subduction of the slab tip. A similar correction to convergence rates for these subduction zones is applied to statistical analysis of slab length. With the possible exception of deep dip, the different measurement times and response times of different variables do not appear to be an obstacle to their reliable comparison.

Correlation Between Independent Variables

Correlation between independent variables is probably the largest single reason for the profusion of models predicting dependent variables such as strain regime of the overriding plate and slab dip. In theory, stepwise regression can successfully cope with this problem, isolating the key independent variables. In practice, the degree of success expected for stepwise regression depends on how strongly correlated the independent variables are. For example, distinguishing between the independent variables convergence rate (V_c) and convergence rate including back-arc spreading (V_{cba}) is difficult, because their correlation coefficient is 0.72; distinguishing between slab age at the trench (A_s) and age of the slab tip (A_t) is nearly impossible, because the correlation coefficient is 0.93.

Because of correlation between independent variables, the single independent variable showing the highest correlation coefficient with the dependent variable does not necessarily remain in the final regression relationship. For example, the independent variable most strongly correlated with strain regime is arc age. This implausible relationship arises from two factors: (1) South America includes some of the oldest arcs as well as the most compressive environments, and (2) arc age affects intermediate dip (DipI). As subsequent significant independent variables are added, arc age gradually drops out of the equation and intermediate dip becomes more important.

It is worthwhile to briefly examine the correlations between independent variables, in order to isolate the correlations with a physical significance from those that are sampling artifacts. Table 6 lists the correlations for both the *Chase* [1978*a*] and *Minster and Jordan* [1978] motion models. The two are generally similar, so here only the former are mentioned.

Some correlations are trivial, arising from the fact that one independent variable is only a slightly modified form of another. The correlation of 0.72 between convergence rate (V_c) and convergence rate including back-arc spreading (V_{cba}) is dominated by the many subduction zones with no back-arc spreading. The very high correlation of 0.96 between shallow dip (DipS) and intermediate dip (DipI) is expected, since shallow dip is measured from the trench to 60-km depth and intermediate dip is measured from the trench to 100-km

TABLE 6. Correlation Between "Independent" Variables

	DipI	DipD	A_S	A_T	A_a	V_c	V_{cba}	V_{oa}	V_{ua}	V_{sa}	DipU
DipI		0.642	−0.039	−0.075	−0.536	−0.352	0.397	−0.316	0.011	0.103	0.734
DipD	0.642		0.139	0.104	−0.648	−0.568	0.124	−0.686	0.172	−0.215	0.608
A_s	−0.039	0.139		0.927	−0.375	0.168	0.350	−0.648	0.822	−0.468	−0.160
A_t	−0.075	0.104	0.927		−0.276	0.144	0.346	−0.509	0.572	−0.339	−0.121
A_a	−0.536	−0.648	−0.375	−0.276		0.454	−0.014	0.742	−0.322	0.424	−0.267
V_c	−0.071	−0.113	0.291	0.249	0.350		0.704	0.490	0.458	0.118	−0.491
V_{cba}	0.262	0.163	0.398	0.423	0.049	0.736		0.072	0.593	0.503	0.200
V_{oa}	−0.160	−0.274	−0.324	−0.444	0.540	0.460	−0.006		−0.550	0.615	−0.054
V_{ua}	0.054	0.144	0.551	0.525	−0.055	0.744	0.800	−0.250		−0.514	−0.415
V_{sa}	0.386	0.168	−0.090	−0.130	0.102	0.204	0.579	0.330	−0.026		0.628
DipU	0.693	0.740	−0.034	0.035	−0.538	−0.300	0.223	−0.046	−0.285	0.709	

Values below the blank diagonal line are from *Chase* [1978*a*]; values above the blank diagonal line are from *Minster and Jordan* [1978].

depth. The correlation of 0.93 between slab age at the trench (A_s) and age of the slab tip (A_t) results from the generally slow lateral changes in crustal age. Convergence rate, the sum of absolute motions of the overriding and underriding plates, correlates better with absolute motion of the underriding plate (0.74) because that rate is generally faster.

Other correlations between independent variables are more geologically important. The correlation of 0.55 (or 0.82 for Minster and Jordan) between slab age at the trench and absolute motion of the underriding plate results from the slab pull force; a much higher correlation is found when the integrated effect of slab age along an entire plate boundary is considered [e.g., *Forsyth and Uyeda*, 1975]. A lower but still significant correlation of 0.29 between convergence rate and slab age results from the previously mentioned effect of absolute motion of the underriding plate on convergence rate. In contrast, convergence rate including back-arc spreading is more highly correlated (0.40) with slab age than is convergence rate alone; as we will subsequently see, this results from the effect of slab age on the presence of back-arc spreading.

A few correlations are conceptually implausible, suggesting a sampling artifact. Absolute motion of the overriding plate correlates with both slab age (−0.32) and arc age (0.54). The correlation with slab age is the opposite sign of what would be expected from the possible effect of trench suction on the overriding plate. Both correlations are dominated by South America and vanish when South American subduction zones are removed from the correlation. The same is true for the correlation of 0.35 between arc age and convergence rate.

Regardless of the source of correlation between independent variables, the presence of these correlations constitutes an important potential limitation to the reliability of empirical equations between subduction parameters. The problem is dealt with more successfully by stepwise multiple regression than by simple multiple regression. Nevertheless, all resulting empirical equations should be considered tentative, pending confirmation of their predictive value for other data.

MODELS OF SLAB LENGTH

Convergence Rate

The deepest earthquakes in most Benioff zones occur within the subducting slab rather than at the contact with the overriding lithosphere. The tip of the slab marks a transition from brittle to ductile deformation of the slab, a thermal response of gradual slab heating [*Isacks et al.*, 1968; *McKenzie*, 1969].

Isacks et al. [1968] noted a correlation between slab length and convergence rate and found that the lengths of Benioff zones were approximately equivalent to the amount of lithosphere subducted during the last 10 m.y. Two possible reasons for this relation were suggested: (1) a hiatus in spreading prior to 10 m.y. B.P. or (2) a 10 m.y. time constant for resorption of the slab. The latter hypothesis was preferred. Nevertheless, the length of the Benioff zone in individual regions has occasionally been used to estimate duration of subduction. The initiation of subduction in southwest Japan has been estimated as 2 m.y. B.P. [*Kanamori*, 1972], 3–5 m.y. B.P. [*Kobayashi and Isezaki*, 1976], and 5 m.y. B.P. [*Seno*, 1977] based on slab length, though more likely it is considerably older. Because of slab heating, the length of the Benioff zone can only indicate a minimum duration of subduction.

More accurate convergence rate data show the time since subduction of the slab tip to be more variable than originally estimated (Table 1). Based on the subduction zones of Table 1, the correlation between slab length and convergence rate is 0.64.

Slab Age

Convergence rate alone is inadequate as an explanation for variations in slab length in Alaska [*Lahr*, 1975] or variations in slab depth along the Sunda Arc [*Vlaar and Wortel*, 1976]. *Vlaar and Wortel* [1976] considered the alternative hypothesis that slab age may control maximum focal depth. They recognized that the most relevant measure of slab age is age of the slab tip at the time that it entered the trench (A_t), because maximum focal depth depends on the gradual heating of the slab. The correlation between this effective slab age and maximum focal depth was interpreted by *Vlaar and Wortel* [1976] as evidence that the maximum penetration depth of the slab is controlled by the effect of lithospheric age on gravitational instability. Subsequent studies recognize the slab tip as a thermal transition within the slab, with no implications for total depth of slab penetration.

Farrar and Lowe [1978] separated the influence of convergence rate from slab age by demonstrating a correlation between slab age and slab length along the Peru-Chile subduction zone, a region with relatively constant convergence rate.

Product of Convergence Rate and Slab Age

Both convergence rate and slab age affect slab length. The quantitative relationship between these parameters was implicit in a plot by *Deffeyes* [1972], who empirically showed that many subduction zones have an approximately linear relationship between slab age and time since subduction of the slab tip. This relation was demonstrated theoretically by *Molnar et al.* [1979]. The brittle/ductile transition within the

TABLE 7. Slab Length Regressions

Regression Equation*	Comment†	Velocity Source‡	F Ratios: Regression	F Ratios: First Variable	F Ratios: Second Variable	R^2	R
$L_S = 297.4 + 0.0747 \times V_c \times A_t$	1	M	127.6	···	···	0.831	0.911
$L_S = 302.9 + 0.0671 \times V_c \times A_t$§	1	C	156.6	···	···	0.858	0.926
$L_S = 324.8 + 0.0634 \times V_c \times A_s$	1	M	71.0	···	···	0.732	0.856
$L_S = 364.6 + 0.0440 \times V_{cba} \times A_t$	1	M	34.3	···	···	0.569	0.754
$L_S = 368.8 + 0.0412 \times V_{cba} \times A_s$	1	M	34.4	···	···	0.570	0.755
$L_S = 399.9 + 0.0747 \times V_c \times A_t - 4.31 \times$ DipI	1	M	73.8	143.4	4.2	0.855	0.925
$L_S = 396.6 + 0.0669 \times V_c \times A_t - 3.91 \times$ DipI	1	C	89.8	174.6	4.1	0.878	0.937
$L_S = 470.9 + 0.0649 \times V_c \times A_s - 6.39 \times$ DipI	1	C	45.7	88.6	6.2	0.785	0.886
$L_S = 219.3 + 0.0938 \times V_c \times A_t$	2	M	145.9	···	···	0.816	0.903
$L_S = 229.9 + 0.0841 \times V_c \times A_t$	2	C	127.8	···	···	0.795	0.892
$L_S = 458.7 + 0.0829 \times V_c \times A_t - 9.02 \times$ DipI	2	C	103.4	184.1	17.0	0.866	0.931
$L_S = 558.8 + 0.0710 \times V_c \times A_s - 10.95 \times$ DipI	2	C	163.1	292.1	37.7	0.911	0.954

*For units consistency within these equations, velocities are in km/m.y. (i.e., mm/yr); all other velocities in this manuscript are in cm/yr.
†Comment 1: delete both subduction zones with missing data and northeast Japan. Comment 2: all possible data used in correlations; equivalent to deleting missing data when only one term in regression.
‡C, *Chase* [1978*a*]. M, *Minster and Jordan* [1978]. Both revised as indicated in text.
§Preferred model.

slab is controlled by gradual conductive warming of the slab. Therefore the length of the Benioff zone should be proportional to (1) the time since subduction of the slab tip, which is controlled by convergence rate, and (2) the time required to heat the slab to the brittle/ductile transition, which is proportional to the square of lithospheric thickness and therefore also proportional to slab age.

The exact theoretical relationship [*Molnar et al.*, 1979] is

$$L_S = k \times V_c \times A_t$$

where L_S is the length of seismically active slab, k is a constant, V_c is the convergence rate, and A_t is the age of the tip of the slab at the time it entered the trench. *Molnar et al.* [1979] measured slab length and convergence rate along the direction of convergence; these parameters may also be measured perpendicular to the trench, as done herein, without affecting the constant k.

Using slab age at the trench rather than effective age of the slab tip, *Molnar et al.* [1979] estimated a value for k of 0.1, based on the following subduction zones: Aleutian, Kurile, Japan, Tonga-Kermadec, New Zealand, South America, Central America, and Lesser Antilles. In terms of the 39 subduction zone segments of Table 1, 14 were included in the analysis of *Molnar et al.* [1979]; two thirds of the 30 points used came from four subduction zone segments. Other subduction zones were not used in the analysis because of uncertainties in relative plate velocities. *Sugi and Uyeda* [1984] showed that seven subduction zones with young slabs were generally consistent with the relationship of *Molnar et al.* [1979].

For most of the subduction zones considered by *Molnar et al.* [1979] and *Sugi and Uyeda* [1984], slab age increases downdip, so that only minor errors are introduced by use of slab age at the trench rather than effective age of the slab tip. *Sykes et al.* [1982] replotted the data of *Molnar et al.* [1979], using age of the slab tip for the Aleutians (the one region with possibly decreasing slab age downdip) in order to estimate Caribbean plate motion based on slab length in the Lesser Antilles. Their adjusted Aleutian points improve the fit to the overall relation of slab length versus the product of convergence rate and slab age; the estimate of the constant k is unchanged.

Stepwise multiple regression using the subduction zones of Table 1 confirms that $V_c \times A_t$ is the best predictor of slab length. While the correlation coefficients of slab length with V_c, A_s, and A_t are 0.64, 0.72, and 0.69, respectively, the correlations with $V_c \times A_s$ and $V_c \times A_t$ are 0.90 and 0.89, respectively. Regression equations based on $V_c \times A_t$, $V_c \times A_s$, $V_{cba} \times A_t$, and $V_{cba} \times A_s$ are given in Table 7. As we will subsequently see, V_c appears to be preferable to V_{cba}. Use of A_t is theoretically preferable to A_s. However, it should be remembered that knowledge of convergence rate is required for the determination of A_t. Thus convergence rate is implicitly present in both variables of the product $V_c \times A_t$, complicating use of equation 1 of Table 7 for estimating convergence rates in modern subduction zones. Nevertheless, this equation is the preferred model.

The equations given in Table 7 are based on only those subduction zones for which L_s, V_c, and A_t are all known (i.e., no missing data), omitting northeast Japan. As is evident from Figure 8, northeast Japan has an anomalously long L_s. However, if two very deep epicenters of *Ichikawa* [1966] are omitted, L_s is reduced from 1480 km to 920 km, a length much more consistent with other subduction zones. This observation does not imply that the two epicenters are not part of a continuous slab, but rather that they should not be allowed to unduly weight the entire regression line.

Regression residuals such as those evident in Figure 8 probably result from a number of factors, particularly the limited and varying durations of seismic activity included in different subduction zones, downdip gaps in seismic activity caused by a transition from downdip tension to downdip compression, uncertainties in both V_c and A_t, and temporal changes in V_c. Some possibly systematic patterns among regression residuals will be discussed in later parts of this section.

This analysis differs from that of *Molnar et al.* [1979] in several important respects. First, a much larger number of subduction zones was used, thereby reducing the weighting of Kurile, Tonga, Kermadec, and New Zealand subduction zones from two thirds of the total data to 14% of the total data. This change involved inclusion of some subduction zones with less accurate convergence rates. However, it also reduced sensitivity of the results to the 20% uncertainty in slab age in the

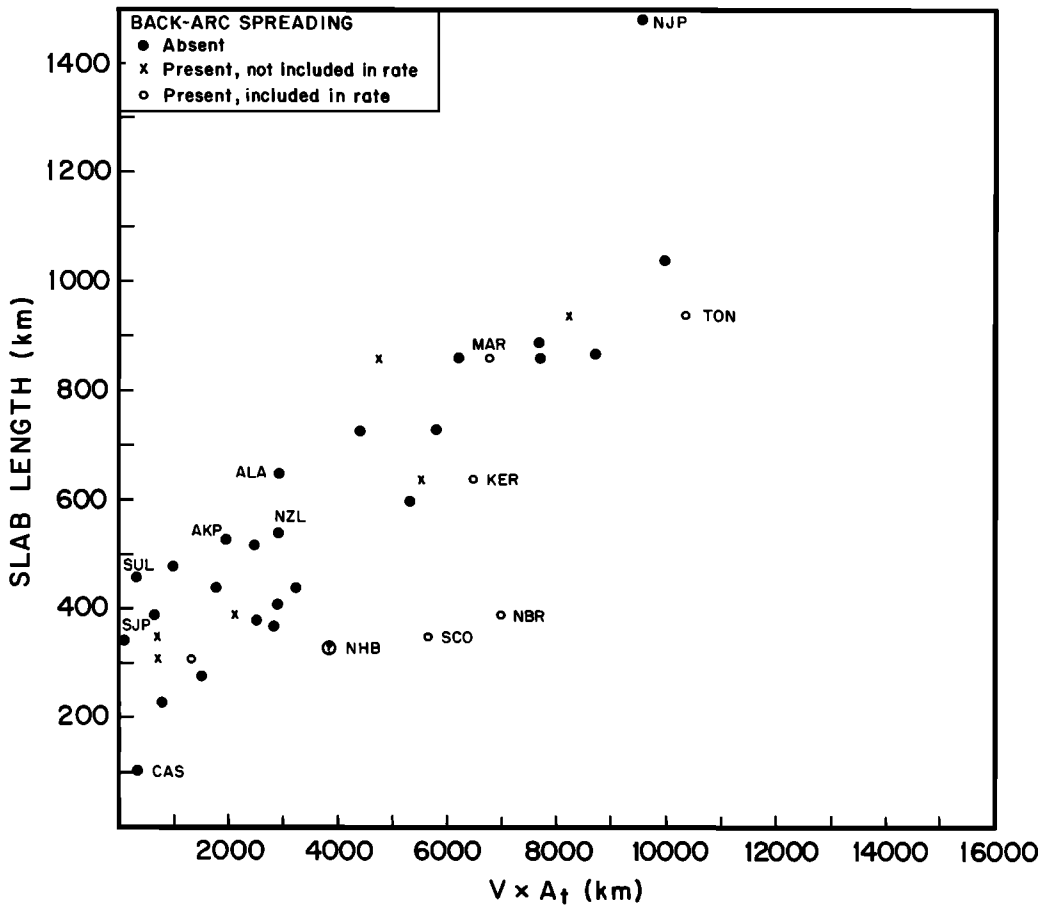

Fig. 8. Cross plot of Benioff zone length versus the product of convergence rate and age of the slab tip, for modern subduction zones. Note the better fit of subduction zones with back-arc spreading to the overall trend when back-arc spreading rate is excluded from $V \times A_t$. Note also the nonzero intercept of the overall trend, which suggests that a constant rate of slab heating is not established until the slab has passed the upper portion of the overriding plate.

four subduction zones. Second, more recent and probably more accurate estimates of convergence rates and slab ages were used, changing most convergence rates and slab ages by about 20%. Third, separate analyses of convergence rates with and without back-arc spreading were undertaken; for example, the convergence rates of 6 and 9 cm/yr used by *Molnar et al.* [1979] for Kermadec and Tonga are revised to 5 and 7.5 cm/yr without back-arc spreading and 6 and 10 cm/yr including back-arc spreading. Fourth, separate analyses were undertaken for A_s and A_t. Fifth, the possibility of a nonzero intercept for the regression line was included. And sixth, correlation of regression residuals with other relevant variables was examined. The utilization in this analysis of convergence rates and slab lengths perpendicular to the trench rather than parallel to the convergence direction does not significantly affect the results.

In theory, convergence rate including back-arc spreading (V_{cba}) is a more relevant parameter than convergence rate excluding back-arc spreading (V_c), because slab length should depend on the time since subduction of the slab tip and therefore on the overall injection rate into the mantle. However, V_c is a consistently better predictor of slab length than V_{cba} (Figure 8), whether A_s or A_t is used, whether rates of *Minster and Jordan* [1978] or *Chase* [1978*a*] are used, and whether individual correlation coefficient or overall regression quality of fit is considered. One possible explanation is that current back-arc spreading rates have not lasted as long as the time since subduction of the slab tip. This appears to be true for the Tonga, Kermadec, Marianas, and South Sandwich subduction zones. However, as previously discussed, calculated ages of the slab tip for these four subduction zones have already been corrected for the slower convergence rates prior to current back-arc spreading. Furthermore, values of V_{cba} used for these four zones also are corrected to slower time-average values.

Figure 8 indicates that use of V_{cba} rather than V_c yields predicted slab lengths that are much longer than observed lengths for South Sandwich and New Britain; a similar but less marked relation is evident for Kermadec and Tonga. Although New Hebrides was not used in the statistical analysis because of uncertainty in V_{cba}, it also appears to have a much longer predicted than observed slab length. This discrepancy appears to be correlated with trench rollback rate. South Sandwich, New Britain, and New Hebrides have by far the largest rollback rates (6.6, 4.6, and 6.9 cm/yr, respectively) of the subduction zones studied. The second highest group of rollback rates is Tonga, Kermadec, and Solomon (3.8, 2.9, and 3.0 cm/yr), which lie at the bottom edge of the overall trend of Figure 8. All other subduction zones have rollback rates of less than 2.5 cm/yr. These cited rollback rates are for the *Chase* [1978*a*] model; the possible pattern is not substantially changed for the *Minster and Jordan* [1978] model.

The physical mechanisms are elusive for both anomalously

TABLE 8. Earthquake Moment

Number	Regression Equation	Comment*	Velocity Source†	F Ratios: Regression	F Ratios: First Variable	F Ratios: Second Variable	R^2	R	Preferred
1	$M_w = 7.95 - 0.0088 \times A_s + 0.134 \times V_c$	1, 2	R	16.2	12.4	12.6	0.643	0.802	
2	$M_w' = 8.02 - 0.0104 \times A_s + 0.143 \times V_c$	2	C	12.9	17.9	14.6	0.577	0.759	
3	$M_w' = 7.85 - 0.0103 \times A_s + 0.172 \times V_c$	2	M	14.2	18.8	16.6	0.600	0.775	
4	$M_w' = 8.01 - 0.0105 \times A_s + 0.159 \times V_c$	3	C	14.5	19.6	17.0	0.605	0.778	yes
5	$M_w' = 7.88 - 0.0096 \times A_s + 0.177 \times V_c$	3	M	15.8	18.0	18.9	0.624	0.790	yes

*Comment 1: A_s from *Ruff and Kanamori* [1980]. Comment 2: total convergence rate. Comment 3: convergence rate perpendicular to trench.
†R, *Ruff and Kanamori* [1980]. C, *Chase* [1978a]. M, *Minster and Jordan* [1978]. Latter two revised as indicated in text.

short slabs associated with back-arc spreading and the possible correlation of anomalously short slabs with rapid trench rollback. One may speculate that rapid trench rollback involves more efficient removal of heat from the portion of mantle adjacent to the slab, associated with increased mantle convective flow. However, this speculation implies that it is a coincidence that predicted slab lengths are consistent with observed lengths when V_c is used instead of V_{cba}.

A major difference between the results of this study and those of *Molnar et al.* [1979] is the nonzero intercept of the regression line (Table 7 and Figure 8). Intercepts of 200–400 km result for statistical analyses using $V_c \times A_t$, $V_{cba} \times A_t$, $V_c \times A_s$, and $V_{cba} \times A_s$. Partly because of this, 100% of the points in Figure 8 lie above the line determined by *Molnar et al.* [1979], $L_s = 0.1 \times V_c \times A_s$. The reality of a nonzero intercept is evident from Figure 8. However, caution must be exercised in interpreting the intercept value, as data dispersion causes regression analysis to yield a slightly larger intercept than one would fit by eye through any data.

The nonzero intercept does not conflict with the theoretical analysis of *Molnar et al.* [1979]. It does suggest that the thermal environment of the slab does not change from cooling to heating exactly at the trench. Instead, the slab continues to cool and "age" for a short time after subduction. The nonzero intercept is probably the sum of three related effects: (1) the time lag between subduction and initiation of heating, (2) the additional time required for heating to counteract this increase in effective slab age, and (3) a slower rate of heating during contact of the slab with the accretionary prism and overriding lithosphere than during contact with the deeper mantle.

Because frictional heating between the slab and accretionary prism is negligible, some cooling of the slab is likely during the early stages of its subduction beneath the accretionary prism. Consequently, subduction zones with very wide accretionary prisms (e.g., Alaska, Alaska Peninsula, North Sulawesi, southwest Japan, and New Zealand) tend to lie near the upper bound of the group of points plotted in Figure 8. This generalization is imperfect: the same is not true for Makran, which has a very wide accretionary prism, and the position of the North Sulawesi point may also be biased by underestimation of convergence rate (as discussed previously in the section on arc age).

The nonzero intercept is not evident in the analysis of *Molnar et al.* [1979] because three regions had short observed and predicted slab lengths: Alaska, Central America, and Lesser Antilles. The latter two regions show lower than average evidence of a nonzero intercept in this analysis (lying near the lower end of the cluster of points in Figure 8) in spite of a 50% increase in observed length of the Lesser Antilles slab resulting from using the length from *McCann and Sykes* [1984] rather than that of *Sykes and Ewing* [1965]. The lengths used here for Alaska and Alaska Peninsula are based on the same sources used by *Molnar et al.* [1979] but are twice as long. This difference apparently arises partly from correction of profiles to an azimuth perpendicular to the trench by *Molnar et al.* [1979] and perpendicular to the strike of Benioff zone contours in this analysis. The latter seems less sensitive to the modifying effects of the very wide accretionary prism on trench azimuth, but caution should be used in either approach, to avoid bias by Alaska to the entire best fit line. The nonzero intercept is evident but not commented on in the slab length plot of *Sugi and Uyeda* [1984], which focusses on subduction of young oceanic crust. It is less evident in their plots of maximum depth versus the product of rate and age, because of shallow dip of the slab beneath southwest Japan and poor depth control for seismicity in Yap and Palau.

The relation of slab length to the product of slab age and convergence rate is both the most firmly based in theory and the strongest empirically constrained relationship of any published relationship between subduction parameters. Therefore the equation of *Molnar et al.* [1979] has sometimes been used to estimate modern convergence rates from known slab lengths and slab ages [e.g., *Molnar et al.*, 1979; *Sykes et al.*, 1982]. The validity of this approach is confirmed by the present analysis. However, this analysis indicates that convergence rates estimated from the equation of *Molnar et al.* [1979] require substantial revision.

Slab lengths for three subduction zones (Yap, Palau, and Tierra del Fuego) have never been determined, presumably because they are too short. Rare shallow seismicity is observed in Palau, Yap [*Katsumata and Sykes*, 1969], and Tierra del Fuego. All three regions have very slow convergence rates and young crust. Based on the empirical equation of Table 7 relating L_s to V_c and A_s (since A_t is not known), predicted slab lengths for these three regions are only about 350 km.

Intermediate Dip and the Product of Slab Age and Convergence Rate

Stepwise regression indicates that length of the slab may be more accurately predicted if intermediate dip (DipI) is included with $V_c \times A_t$ in the regression equation (Table 7). An F test of the significance of this additional variable indicates that DipI is highly significant (>99.9% confidence level) when subduction zones with missing values are included in the analysis and marginally significant (approximately at the 95% confidence level) when subduction zones with missing values are omitted. The significance of the DipI term is also slightly

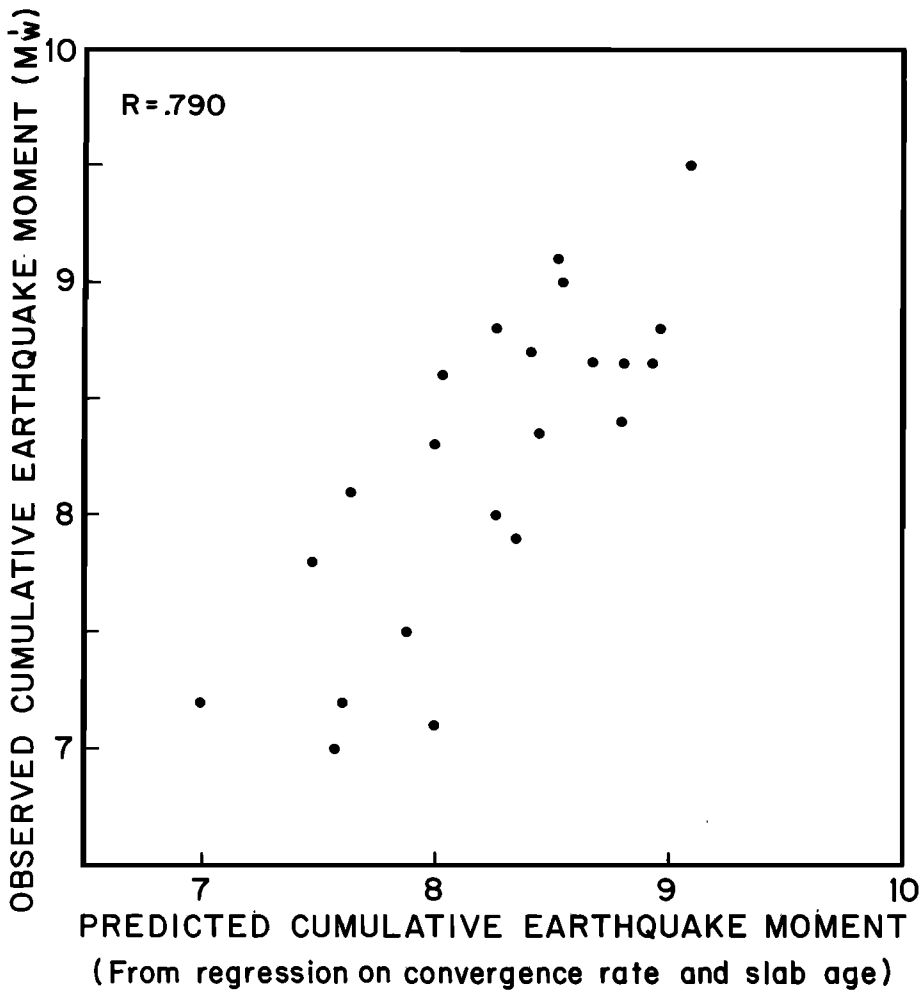

Fig. 9. Cross plot of cumulative earthquake moment (M_w') versus predicted M_w', based on a regression in which convergence rate and slab age are the independent variables (Table 8).

greater when $V_c \times A_t$ or $V_{cba} \times A_t$ is the primary independent variable rather than $V_c \times A_s$ or $V_{cba} \times A_s$. Intermediate dip is more highly significant than either shallow or deep dip.

The significant contribution of DipI may arise from a combination of two sources. First, shallow initial dips are associated with subduction zones with wide accretionary prisms. As previously discussed, slab heating may be slowed during passage beneath accretionary prisms, thus increasing slab length. Second, increasing mantle temperature with greater depth may lead to more rapid heating of steeply dipping slabs than of shallowly dipping slabs [*Toksöz et al.*, 1973; *Molnar et al.*, 1979]. The latter possibility was suggested by *Lahr* [1975] as a contributing factor to the variations in slab length within the Alaska-Aleutian region. Because increasing ambient pressures in deeper, steeper slabs might counteract the temperature effect, a more detailed analysis of temperature and potential temperature of the slab tip is required to evaluate the second possibility. Such an analysis appears warranted but is beyond the scope of this study.

In view of the marginal significance of DipI, currently it may be more appropriate to utilize the regression equation that omits this variable.

Earthquake Magnitude Model

In a statistical analysis similar to this study, *Ruff and Kanamori* [1980] determined the correlation of maximum earthquake magnitude with four possible independent variables: convergence rate, slab age, slab horizontal length, and slab maximum depth. They found that magnitude (M_w) of the largest earthquake within 21 modern subduction zones is significantly correlated with both convergence rate and slab age. Sixty-four percent of the total variance in M_w was accounted for by these two variables (Table 8). Total convergence rates were used [*Minster et al.*, 1974], not including back-arc spreading. Significant correlations were also found between convergence rate and maximum horizontal extent of the slab and between slab age and slab maximum depth. A slightly better fit was achieved ($R^2 = 0.71$) when cumulative moment M_w' was used as the independent variable instead of M_w.

These results are not substantially changed when the revised convergence rates and slab ages of this study are used as independent variables (Figure 9). As shown in Table 8, a slightly better fit was obtained when convergence component perpendicular to the trench is used instead of total convergence rate. The two rates are similar for most subduction zones, and the improvement is not significant. Regression equations using convergence rates perpendicular to the trench are preferred herein, more for consistency with other analyses than for plausibility of physical mechanism. No significant correlation of regression residuals is found with any other of the possible independent variables of Table 1. This suggests that *Ruff and Kanamori* [1980] successfully isolated the key

independent variables. The possibility remains that other unconsidered variables have a significant but secondary influence on M_w'; for example, sediment subduction may decrease M_w' through a lubricating effect.

Ruff and Kanamori [1980] suggest a simple physical model to account for these correlations. Convergence rate affects the rate of horizontal slab migration, while slab age affects the rate of vertical slab migration. The combination of slab age and convergence rate is therefore thought to determine a preferred trajectory for the shallow slab. The difference between this preferred trajectory and the dip of the interface between overriding and underriding plates will directly affect the coupling and therefore maximum earthquake magnitude. Thus increased convergence rate or decreased slab age will increase shear stress between overriding and underriding plates, given that dip and roughness of the interface are constant. No correlation of regression residuals with shallow dip was found in this analysis. This may suggest that the conceptual basis of the empirical relationship needs modification.

STRAIN REGIME MODELS

The primary controls of strain regime in the overriding plate behind trenches are still a subject of active debate, after more than a decade of proliferation of models. Most models are qualitative and conceptual, rather than rigorously quantitative and theoretical. Nearly all have been tested primarily through examination of the correlation between strain regime and one or more subduction parameters in current subduction zones. The approach used here is similar in general but differs in several details.

First, more subduction zones are used than in previous analyses. This is considered to be particularly important in prediction of strain regime, because most proposed causative parameters are correlated with each other. For example, *Uyeda and Kanamori* [1979] have described the characteristics of the two endpoints in the strain continuum, Marianas and Peru-Chile. The highly extensional Marianas has a steeply dipping slab composed of very old lithosphere, absolute motion of the overriding plate away from the trench, and relatively slow convergence rate. In contrast, highly compressional Peru-Chile has a shallowly dipping slab composed of younger lithosphere, absolute motion of the overriding plate toward the trench, and rapid convergence rate. Clearly, determination of which (if any) of these four parameters is controlling strain regime requires examination of subduction zones with very different combinations of these parameters. Because the number of modern subduction zones is limited, the correlation between potential independent variables may preclude reliable isolation of key variables based on modern subduction zones alone.

A second difference between this analysis and previous analyses is the attempt to compile all proposed key variables for the same subduction zones, so that the quality of different correlations can be directly compared. Impressive correlations between back-arc spreading and absolute motion of the overriding plate [*Chase*, 1978*b*], slab age [*Molnar and Atwater*, 1978], and the combination of convergence rate and slab age [*Ruff and Kanamori*, 1980] used different subduction zones and sometimes even different picks for back-arc spreading, making comparison of the models difficult.

A third difference is the emphasis here on consideration of all available data for strain regime of each subduction zone, including apparently contradictory data. It is hoped that sufficient detail is cited to allow the reader to evaluate strain classification of individual subduction zones. The compression/extension continuum was subdivided into seven strain classes. In contrast, several previous models are aimed only at determining the cause of back-arc spreading. A critical assumption is made herein: the entire range of strain regimes in overriding plates results from variations in a few parameters. Thus back-arc spreading and imbricate thrusting are assumed to have the same cause. This assumption is ultimately verifiable only empirically; if it is incorrect, we should be unable to account for a high proportion of the variance in strain regimes through multiple regression.

The final difference is the emphasis on statistical tests of models and on development of regression equations. This approach has already been used by *Ruff and Kanamori* [1980] in a related analysis of factors influencing earthquake magnitude. A complementary approach has been followed by *Cross and Pilger* [1982], who examined the effects of individual variables on strain regime in regions where only one variable changes.

Only models involving the variables of Table 1 are specifically tested. Several models account for back-arc spreading in terms of mantle diapirism or induced asthenospheric flow. In general, these models have difficulty predicting the observed temporal and spatial distribution of back-arc spreading. *Taylor and Karner* [1983] and *Weissel* [1981] review and critique many of these models, and those analyses are not repeated here. Instead it is assumed that more detailed analysis of diapirism and asthenospheric flow models will be warranted only if the variables of Table 1 fail to adequately account for observed regional variations in strain regime.

Convergence Rate

A moderate correlation exists between convergence rate and strain class ($R = 0.52$), with faster convergence corresponding to more compressive environments in the overriding plate (Figure 10). The measure of convergence used here is component of convergence perpendicular to the trench. Components of convergence parallel to the trench have an important impact on strike-slip faulting in the overriding plate (see the section on strike-slip faulting) but may not affect the overall strain regime. However, azimuths of strain indicators are apparently related to convergence direction [e.g., *Nakamura and Uyeda*, 1980; *Cross and Pilger*, 1982]. Back-arc spreading rates are not included in convergence rates, as back-arc spreading is considered to be a manifestation of strain rather than a cause of strain.

The mechanism for an effect of convergence rate on strain regime is the possible influence of convergence rate on shear stress between the overriding and underriding plates. Dip of the boundary between the two plates is generally shallow (10° to 30°); consequently, an increase in convergence rate may increase the component of horizontal compressive force at the boundary. Changes in convergence rate occur every few million years, a time scale comparable to major changes in strain regime.

The correlation between convergence rate and strain regime is too poor for convergence rate to be the only causative factor. Thus most strain models that invoke convergence rate include at least one other primary variable. These models are discussed in subsequent sections.

Jurdy [1979] has compared reconstructions of plate motions within the Pacific Ocean to occurrences of back-arc spreading over the last 80 m.y. A possible correlation of back-

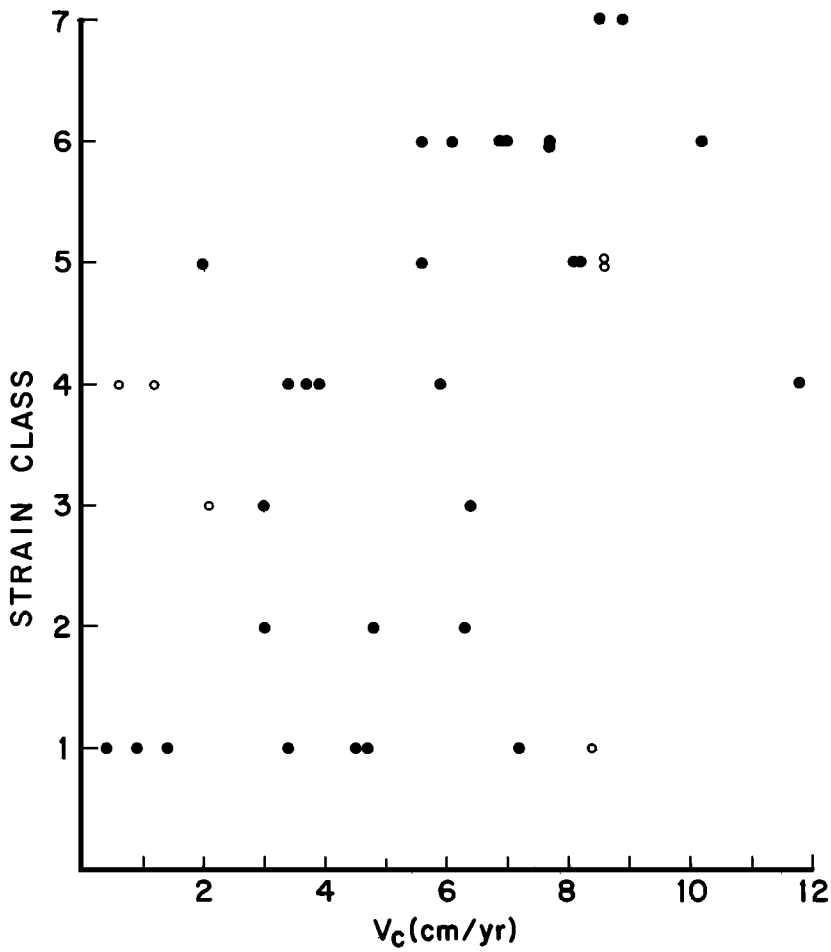

Fig. 10. Cross plot of strain class (Table 2) versus convergence rate for modern subduction zones. Solid circles indicate subduction zones for which both variables are reliably known; open circles indicate that one or both of the variables is only approximately known. Only solid circles are used in the regressions of Table 9. Note that strain class shows only a fair correlation with convergence rate.

arc spreading with high convergence rates was found, opposite to the correlation suggested by Figure 10. However, some of the back-arc basins considered in that analysis may not have been formed by back-arc spreading; both *Weissel* [1981] and *Taylor and Karner* [1983] consider the problematical origins of the South China Sea, West Philippine Basin, and Coral Sea. *Jurdy* [1979] concludes that most back-arc spreading directions are approximately parallel to convergence direction, consistent with observations of most (but not all) modern back-arc spreading.

Slab Age

A weak correlation exists between slab age and strain regime ($R = 0.35$), with increasing slab age corresponding to more extensional environments (Figure 11). *Molnar and Atwater* [1978] classified 26 subduction zones into three strain classes: active back-arc spreading, simple, and Cordilleran tectonics. They found a much stronger correlation between slab age and these strain regimes than is implied by Figure 11. There are apparently two reasons for this discrepancy: additional subduction zones in Figure 11 and differences in estimates of slab age and particularly strain regime. For example, possible Cenozoic spreading in northeast Japan, western Aleutians, Kuriles, and Java is less relevant than the current compressive environments in three of these regions, and the relatively young crust subducting at New Britain is associated with rapid back-arc spreading rather than simple tectonics. In spite of differences in detail, the general correlation of slab age with strain regime of *Molnar and Atwater* [1978] is confirmed by this study.

The mechanism for an influence of slab age on strain regime is probably its effect on coupling between overriding and underriding plates. The density of oceanic lithosphere increases with age due to cooling and contraction, leading to increased gravitational instability and the well-known slab pull force. Estimation of the crustal age of the transition from resisting subduction to slab pull is hampered by uncertainties in key variables [e.g., *Molnar and Atwater*, 1978; *England and Wortel*, 1980], but it is clear that "young" lithosphere resists subduction [*Sacks*, 1983], while subduction of old lithosphere is an important driving mechanism of plate motions. Increased gravitational pull in old slabs probably reduces horizontal compression at the contact between overriding and underriding plates. And even young lithosphere is gravitationally unstable beneath the eclogite transition (about 60 km, but see *Sacks* [1983]).

Active back-arc spreading requires not just reduced horizontal compression but active tension. A possible mechanism

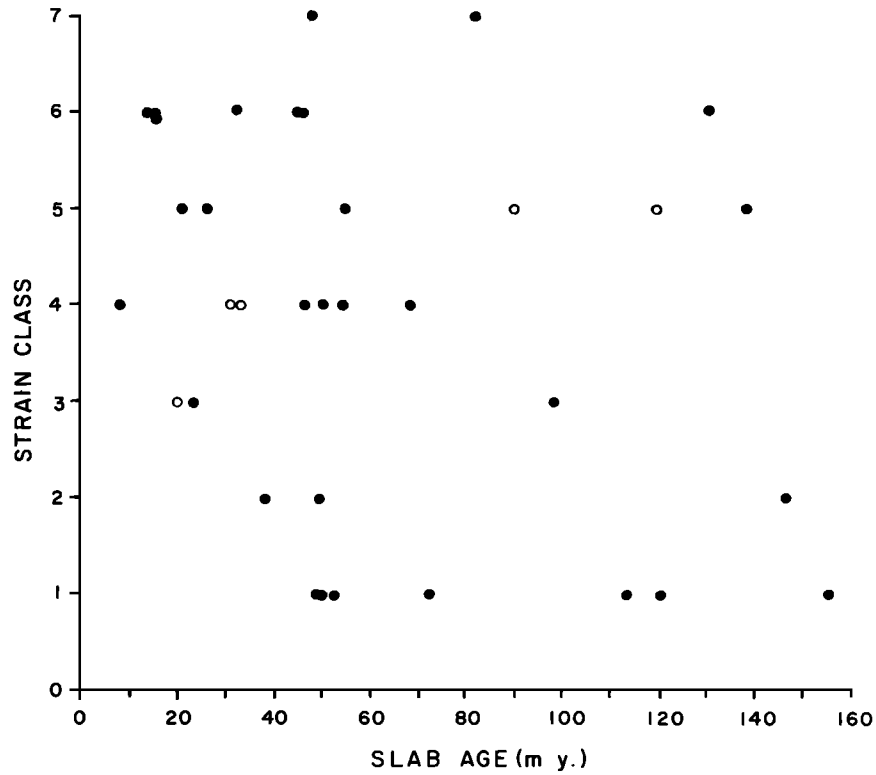

Fig. 11. Cross plot of strain class (Table 2) versus slab age at the trench for modern subduction zones. See Figure 10 for an explanation of symbols. Note that strain class shows only a poor correlation with slab age.

for this is age-dependent slab rollback, a hypothesis suggested by *Molnar and Atwater* [1978] and developed in detail by *Dewey* [1980]. The path followed by any point in a subducting slab is not parallel to slab dip; usually it is steeper than the slab dip, associated with a gradual seaward migration of the hinge line or trench axis. The necessity for rollback was first suggested by *Elsasser* [1971], who noted that the gradual Tertiary and Cretaceous shrinkage of the Pacific Ocean required subduction at an angle steeper than slab dip. This observation does not require active slab rollback driven by the gravitational instability of old lithosphere; alternative driving forces are a trench suction associated with mantle flow toward the trench and down the upper surface of the descending slab, or absolute motion of the overriding plate driven by other forces such as ridge push. Because the age dependence of slab rollback cannot be determined without considering absolute motion of the overriding plate, further analysis of age-dependent rollback will follow the next section, absolute motion.

Absolute Motion

Strain regime is moderately correlated ($R = 0.69$) with absolute motion of the overriding plate. A possible association of compressive mountain building with seaward advancing absolute motion and of back-arc spreading with stationary absolute motion was first suggested by *Wilson and Burke* [1972]. *Hyndman* [1972] independently proposed a rather similar model, except that back-arc spreading was thought to be associated with an overriding plate that is retreating rather than stationary. The global absolute motion model of *Chase* [1978*a*] confirmed the strong correlation between back-arc spreading and retreating absolute motion [*Chase*, 1978*b*]. Figure 12 indicates that absolute motions of subduction zones with compressive and neutral environments (classes 4–7) form a population that is significantly different from subduction zones with extensional environments (classes 1–3). No correlation between absolute motion and strain regime is found within either of these two groups.

The correlation is strong but not perfect. Of the eight subduction zones in Table 1 with the fastest rates of retreating ("landward") absolute motion, only four have active back-arc spreading: Kermadec, Tonga, New Britain, and Marianas. New Zealand and Izu-Bonin have extensional environments but no active back-arc spreading. The strain regime and subduction history of the very short Palau and Yap subduction zones are uncertain, but back-arc spreading is not occurring though absolute motion of the overriding plate is rapidly retreating. Absolute motions for Makran, Alaska Peninsula, and Nicaragua, though apparently retreating, are too close to zero to be considered significant exceptions to the pattern. Of the eight subduction zones with currently active back-arc spreading, only New Hebrides has an apparently advancing overriding plate. However, the advancing Pacific plate is clearly the overriding plate only for the northwestern New Hebrides, where the presence of active back-arc spreading is uncertain. Active back-arc spreading occurs behind the southeastern New Hebrides, where the plate configuration is too complex to even reliably pick the "overriding" plate.

The mechanism for an effect of absolute motion on strain regime is the concept of the downgoing slab as an anchor which resists lateral motion. If the slab cannot readily move landward or seaward because of the difficulty in displacing large amounts of mantle material, then the compressive state of the overriding plate depends entirely on its absolute

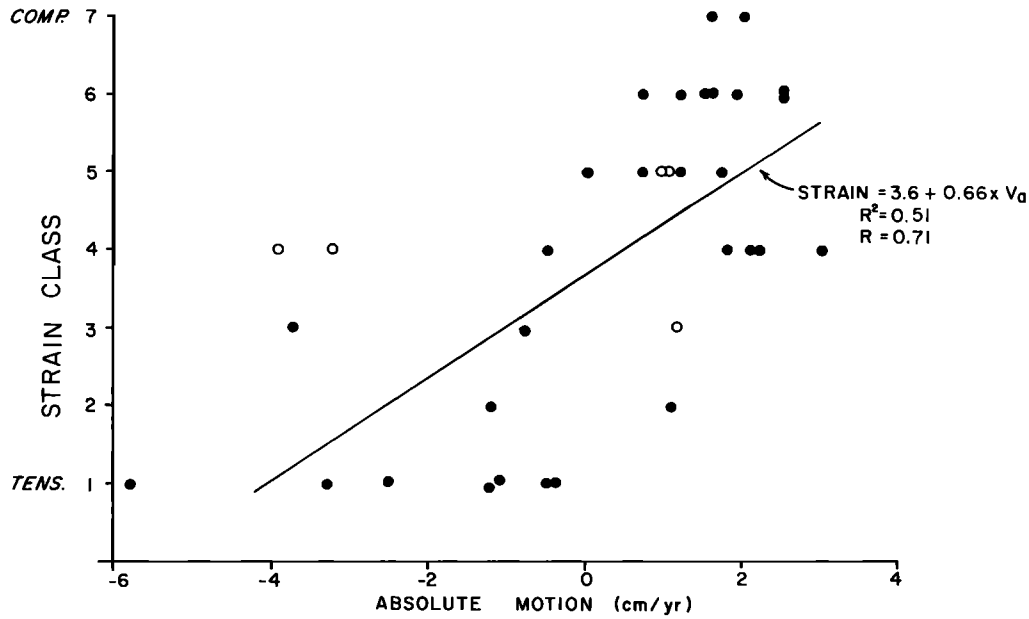

Fig. 12. Cross plot of strain class (Table 2) versus absolute motion of the overriding plate. Positive absolute motion corresponds to trenchward advance of the overriding plate. Note that advancing overriding plates are generally characterized by a compressional or neutral strain regime (classes 4–7), while retreating overriding plates generally have an extensional strain regime (classes 1–3).

motion. Absolute motion away from the trench would require an equal rate of back-arc spreading; absolute motion toward the trench would require an equal rate of lithospheric foreshortening. To the extent that the slab can move laterally through the mantle (through age-dependent rollback, change in dip, or other causes), these predictions could be modified.

The anchoring effect of the slab is clearly relative and not absolute. Actual foreshortening in advancing upper plates is much less than absolute motions, and *Elsasser*'s [1971] observation concerning the shrinking Pacific Ocean indicates that the slab often displaces mantle seaward. *Dewey* [1980] suggests that the slab can only migrate seaward, but the rollback rates of Table 1 indicate that the Izu-Bonin and New Zealand slabs are currently moving landward. The short Yap and Palau slabs, if present, must also be advancing rapidly through the mantle.

One possible mechanism for temporary landward advance of the trench axis with little displacement of mantle is through steepening of slab dip. This steepening can combine landward advance of the upper slab with retreat of the lower slab, only locally displacing mantle instead of forcing a large-scale landward horizontal flow of mantle. Gradual steepening of the New Zealand Benioff zone over the last 15 m.y. has been inferred on the basis of patterns of arc volcanism in New Zealand [*Ballance*, 1976; *Kamp*, 1984].

A more extreme example of rapidly retreating absolute motion without associated back-arc spreading comes not from modern subduction zones but from the Cretaceous of North America. If the absolute motion model of *Morgan* [1980] for North America is even approximately correct, then rapid back-arc spreading totaling about 5000 km must have occurred between 180 m.y. B.P. and 70 m.y. B.P. in southwestern Alaska, as North America moved gradually northwestward. Evidence of basin collapse about 100 m.y. ago exists in the vicinity of Mount Denali [*Csejtey et al.*, 1982], but geologic evidence of back-arc spreading and major basin collapse subsequent to 100 m.y. is lacking.

Major changes in absolute motion occur much less often than the 5–10 m.y. time scale of major changes in strain regime. *Uyeda and McCabe* [1983] suggest that episodic back-arc spreading at the margin of the Philippine plate may result from changes in absolute motion of the Philippine plate, caused by collision of buoyant features along the Philippine Trench. In other regions it is more difficult to envision a mechanism for episodic changes in strain regime associated with little change in absolute motion, unless strain regime is also affected by another variable. For example, the combination of absolute motion and secondary flow induced by subduction may account for episodicity of back-arc spreading [*Jurdy and Stefanick*, 1983]. The problem is exemplified by the Neogene change from back-arc spreading to compression in northeast Japan [*Nakamura and Uyeda*, 1980], which implies a change in absolute motion for all of Eurasia. Such a change has not been detected [*Morgan*, 1980], though uncertainties in Eurasian absolute motions are perhaps large enough to allow it. Rapid lateral changes in strain regime along a plate boundary are also difficult to reconcile with a model in which absolute motion is the only control on strain regime [*Uyeda*, 1984]. For example, the Eurasian plate boundary has a rapid change from class 6 compression in northeast Japan and class 5 compression in southwest Japan to class 2 extension in the Ryukyus. Similarly, Pliocene-Pleistocene variations in extension along the Tonga–Kermadec–New Zealand plate boundary show no apparent relation to lateral changes in absolute motion of the Australian plate.

Absolute motion of the overriding plate cannot account for all modern occurrences of back-arc spreading and compression, nor can it account for variations in strain regime within the broad groupings of compressional or extensional environments. Nevertheless, of the possible independent variables

considered in this analysis, absolute motion of the overriding plate appears to be the best single predictor of strain regime.

Absolute Motion and Slab Age

Molnar and Atwater [1978] first suggested the hypothesis that strain regime may depend on both absolute motion and slab age. The most extensional environments are thought to result from the combination of a retreating overriding plate and old slab, and the most compressional environments result from the combination of an advancing overriding plate and young slab. *Moberly* [1972] had proposed a forerunner of this hypothesis, recognizing that back-arc spreading may result from a combination of slab rollback and a retreating overlying plate. However, his model visualized back-arc spreading as a process partially driven by flow of displaced mantle, rather than a passive response to age-dependent slab rollback and absolute motion.

A more rigorous vector analysis of the model is presented by *Dewey* [1980]. The strain regime of the overriding plate is thought to depend on the relative magnitudes of absolute motion of the overriding plate (V_{oa}) and age-dependent slab rollback (V_r). As in analyses in this paper, only the component of absolute motion perpendicular to the trench is considered relevant. If V_{oa} is advancing (toward the trench axis) and greater than V_r, compression in the overriding plate results. If V_{oa} is less than V_r, then extension in the overriding plate results.

The *Dewey* [1980] model can be used for quantitative prediction of strain regime only if we can estimate V_r, the spontaneous rollback caused by gravitational instability of the underriding plate. It is important to distinguish this rollback rate from the net rollback rate, which is the observed rate of advance of the trench axis. The net rollback rate, which is equal to the absolute motion of the overriding plate plus any back-arc spreading rate, is hypothesized to equal the spontaneous rollback rate when back-arc spreading is present. Spontaneous rollback can only move the trench axis oceanward, with a rate $V_r = V_g$ cot DipD, where DipD is the deep dip and V_g is the vertical sinking velocity, which is a function of the age-dependent gravitational instability of the slab. This model makes several predictions that are readily testable with modern subduction zones:

1. All net rollback rates must be positive, i.e., trench axes always move seaward.
2. Net rollback rates correlate with slab age for subduction zones with back-arc spreading.
3. Net rollback rates for subduction zones lacking back-arc spreading are faster than net rollback rates for subduction zones with back-arc spreading, if slab ages are comparable.
4. The angle of descent of a point on the deep slab is always intermediate between the deep slab dip and vertical, with older slabs descending at an angle closer to vertical than younger slabs.
5. The strain regime in the overriding plate is highly correlated with slab age and absolute motion of the overriding plate.

Net rollback rates are tabulated in Table 1. Most are consistent with the first prediction, but New Zealand, Izu-Bonin, Yap, and Palau are clearly inconsistent, with large negative (landward) "rollbacks." Makran, Alaska Peninsula, Nicaragua, Marianas, and Sumatra have rollback rates that may be negative but are not statistically distinguishable from zero. Net rollback rates are plotted as a function of slab age in Figure 13. Contrary to prediction, rates are consistently higher for subduction zones with back-arc spreading than for those without back-arc spreading. Too few examples of back-arc spreading are available for a reliable fit of rollback rate to slab age, but the apparent trend is for faster rollback with younger slabs, the opposite of the predicted trend. Similarly, no correlation of increasing slab age with increasing trench rollback is evident among subduction zones lacking back-arc spreading. The latter observation does not disprove the concept of spontaneous age-dependent rollback, because V_{oa} may mask the possible correlation with age of V_r. However, it suggests that spontaneous rollback, if real, is less than 2 cm/yr even in the oldest slabs.

The angle of descent of a point on the deep slab is readily calculable from the deep dip, convergence velocity including back-arc spreading, and net rollback rate, assuming that the deep dip is not changing with time. These angles are tabulated in Table 1. Unfortunately, descent angles can only be calculated for 23 of the 39 subduction zones, primarily because many subduction zones are too short for reliable estimation of deep dip. Furthermore, calculated descent angles are quite sensitive to the absolute motion model assumed, as evidenced by differences between the *Chase* [1978*a*] and *Minster and Jordan* [1978] columns of Table 1.

Figure 14 plots slab descent angles as a function of deep slab dip. According to the model of Dewey, all points should lie within the envelope corresponding to angles between deep dip and vertical. Subduction zones with older slabs should plot closer to the horizontal line (corresponding to vertical sinking), and those with younger slabs should plot closer to the diagonal line (corresponding to no spontaneous rollback). Although uncertainties in computed angle of slab descent are large, no correlation between slab age and the two envelope extremes is apparent. Several subduction zones lie significantly outside the predicted envelope. New Zealand and Izu-Bonin lie significantly to the right of the envelope, implying landward advance of the slab. Rollback rates in the Solomon and particularly New Hebrides and South Sandwich subduction zones are so rapid that descent angles of points on the slab are actually opposite in sign to the dip of the slab.

Unless absolute rates are substantially in error for the Solomon, New Hebrides, South Sandwich, New Zealand, and Izu-Bonin subduction zones, downward gravitational force can be excluded as the only factor causing a difference between descent angle and deep dip. Descent angles for these subduction zones seem to require an active horizontal force at 100- to 400-km depth. The only plausible source of such a force is deep convective mantle flow. Thus rather than spontaneous rollback causing mantle flow, mantle flow may be causing spontaneous rollback.

The apparent dependence of rollback rates on mantle flow (at least in some subduction zones) is discouraging, as we can never hope to know mantle flow patterns as well as relative or absolute plate motions. *Hager and O'Connell* [1978] have modelled worldwide mantle flow resulting from mass flux between trenches and ridges; they discuss the uncertainties in such models. The possible implications of such models for prediction of deep dip are discussed in a subsequent section.

It is important to note that the relationship of slab dip to slab injection angle used here is markedly different from relationships determined in previous papers [*Hager and O'Connell*, 1978; *Dewey*, 1980]. This difference is subtle for many subduction zones but is quite large for some (e.g., Solomon and South Sandwich, Figure 15). The velocity of descent

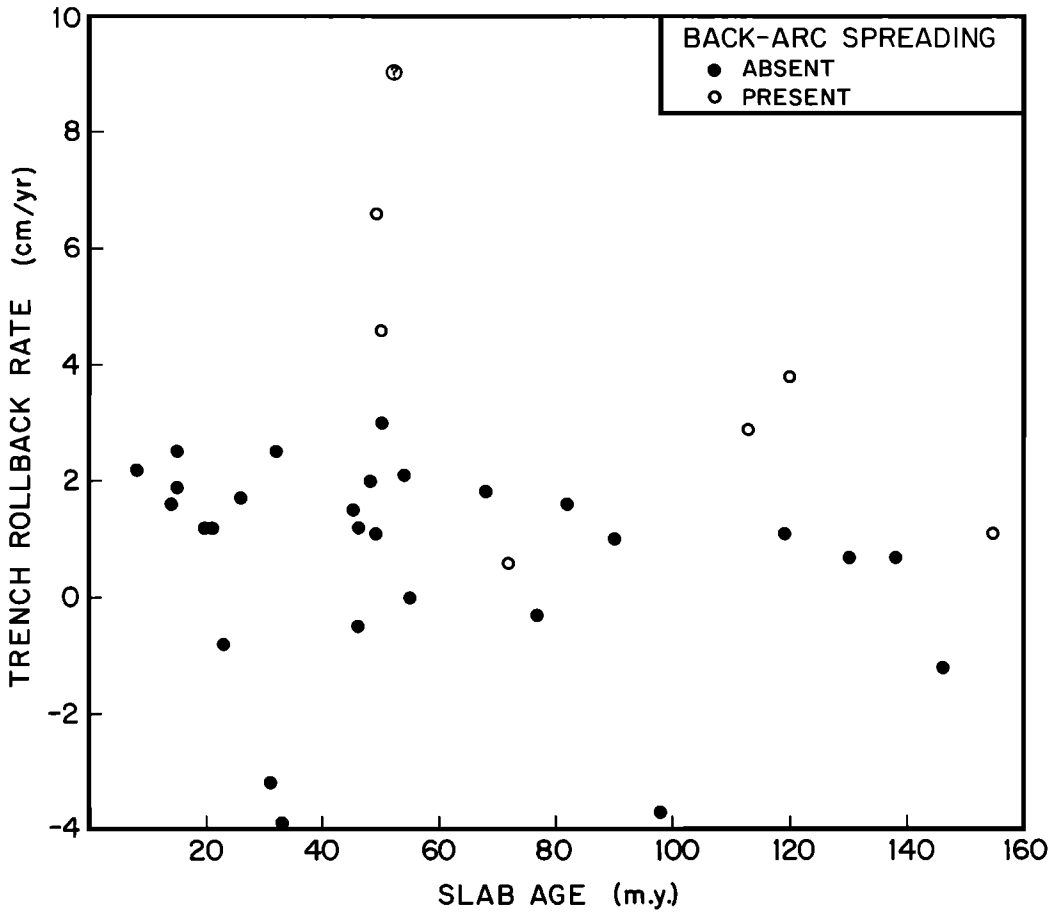

Fig. 13. Cross plot of trench rollback rate versus slab age at the trench, for modern subduction zones. Note that the fastest rollback rates occur in subduction zones with back-arc spreading. Note also that modern subduction zones show no tendency toward increasing rollback rate associated with increasing slab age. These observations indicate that rollback rate is not controlled by a combination of slab age and an advancing overriding plate.

parallel to the slab dip is simply the total convergence rate at the trench (V_{us}, or the convergence rate between overriding and underriding plates plus any back-arc spreading). The angle of injection into the mantle of a point on the slab (V_i) is the vector sum of V_{us} (the velocity parallel to the slab) and V_{sa} (the rollback rate of the trench axis, equivalent to the absolute motion of the forearc).

As recognized by *Hager and O'Connell* [1978], V_i is equivalent to the absolute motion of a point on the underriding plate (V_{ua}). Both the angle and the rate of V_{ua} are different for points on the slab than on the unsubducted portion of the underriding plate. If one assumes that the rate is unchanged [*Hager and O'Connell*, 1978], then the velocity triangle $V_{us} + V_{sa} = V_{ua}$ does not close (Figure 15). For the Solomon example, V_{us} is underestimated by about 30%, while for the South Sandwich example, no rate of subduction parallel to the slab or angle of injection can be reconciled with the known magnitudes of V_{sa} and V_{ua}.

In the model of *Dewey* [1980], V_{ua} for the slab is incorrectly assumed to be parallel to the slab (Figure 15). Rollback is thought to impart an additional downward component V_g to a point on the slab. For the very steep dip and moderately fast rollback in the Solomons, a near-vertical injection rate of 35–40 cm/yr is implied; this rate is clearly inconsistent with the 12-cm/yr rate at which lithosphere is entering the trench. For the South Sandwich example the discrepancy is less extreme, with predicted slab sinking at a rate about double the rate that available slab enters the trench. Thus one must question the existence of an additional sinking component V_g caused by rollback, except to the extent that increased rollback increases convergence rates.

Though the analyses above have failed to detect evidence of age-dependent rollback, both slab age and absolute motion of the overriding plate may still control strain regime in the overriding plate. Coupling at the contact between overriding and underriding plates may be affected by both slab age and absolute motion, with an increase in horizontal compressive stress possible due to either an increase in absolute motion or a decrease in slab age. However, when multiple regression of strain regime on both absolute motion and slab age is undertaken, the resulting regression does not account for significantly more of the variance in strain regime than does absolute motion alone (Table 9). In view of the significant correlation of strain regime with both absolute motion and slab age when considered separately, a strong covariance between the effects of slab age and absolute motion is implied. We may conclude that strain regime is not controlled by the combination of slab age and absolute motion of the overriding plate.

Convergence Rate and Slab Age

Successful prediction of earthquake magnitude, based on convergence rate and slab age, was discussed in a previous

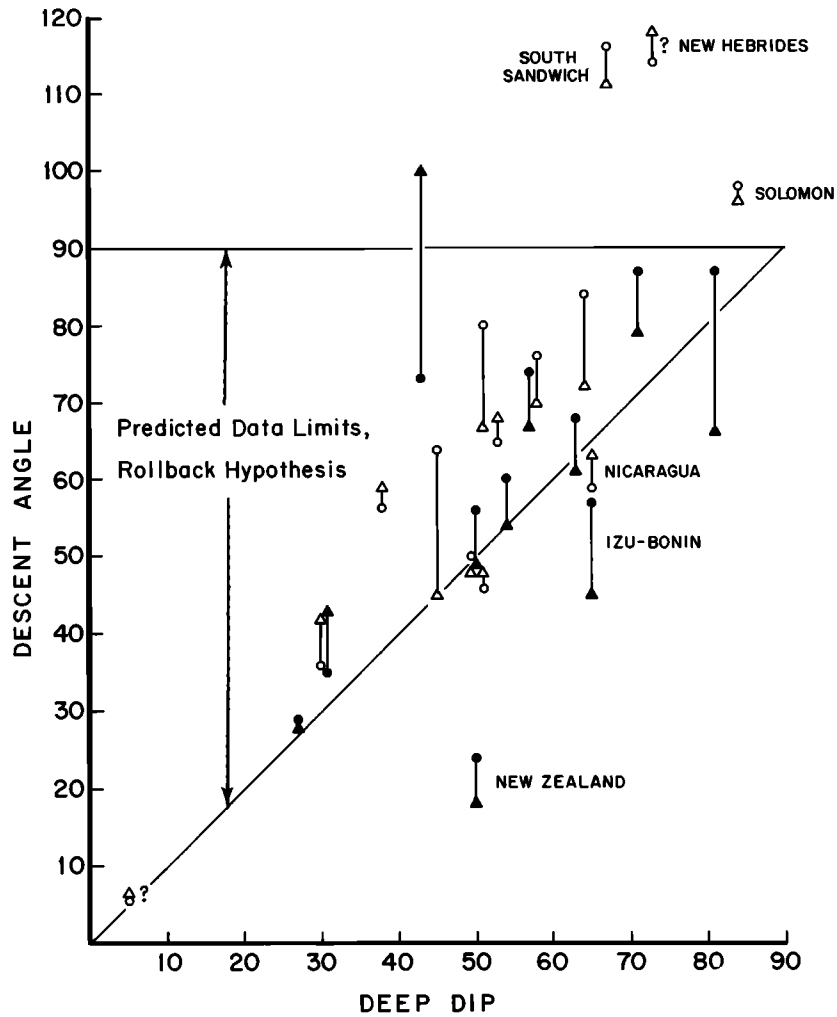

Fig. 14. Descent angle of the deep slab versus deep slab dip, for modern subduction zones. Solid symbols indicate slabs older than 70 m.y.; open symbols indicate slabs younger than 70 m.y. Descent angles calculated from the global motion models of *Chase* [1978*a*] and *Minster and Jordan* [1978] are indicated by circles and triangles, respectively. Note that few deep slabs sink at an angle parallel to the deep dip (diagonal line); more often, they descend at an angle between the deep dip and vertical, as predicted by the rollback models of *Molnar and Atwater* [1978] and *Dewey* [1980]. However, some deep slabs sink at an angle shallower than deep dip or greater than 90°. Also, no tendency is seen for open symbols to plot near the diagonal line and closed symbols to plot near the horizontal line. Both observations are inconsistent with a model in which greater slab age gravitationally swings the descent angle toward vertical.

section. Although M_w and M_w' were the only measures of coupling quantitatively analyzed by *Ruff and Kanamori* [1980], a similar effect of coupling on the strain regime in the overriding plate may be present. *Uyeda and Kanamori* [1979] found a qualitative correlation between strain regime in the overriding plate and maximum earthquake magnitude. *Ruff and Kanamori* [1980] found that subduction zones with active back-arc spreading were generally associated with predicted magnitudes of less than 8 from their regression equation. They concluded that back-arc spreading is most likely in subduction zones with slow subduction of old slabs.

This correlation between coupling (as measured by M_w') and back-arc spreading can be extended to a more comprehensive correlation between coupling and strain regime (Figure 16). A moderate correlation between M_w' and strain regime ($R = 0.579$) is improved to a good correlation ($R = 0.694$) if two extreme points are omitted. Some of the variance in Figure 16 is undoubtedly attributable to the long recurrence time between major earthquakes and to uncertainties in strain regime. However, some of the variance may also be due to different variables affecting M_w' and strain regime.

When the semiquantitative strain regime of this study is considered as the dependent variable, the independent variables V_c and slab age are together a moderately successful predictor of strain regime (Table 9). With a correlation coefficient of 0.78, the combination of convergence rate and slab age accounts for 62% of the total variance in strain regime. Thus these two variables together appear to be about as successful as absolute motion of the overriding plate in predicting strain regime. Because both slab age and convergence rate are somewhat correlated with absolute motion for the subduction zones of Table 1, further analysis is required to determine which of the two relationships is the primary causal relation. In a subsequent section we will see that significant improvement is achieved by adding a third variable (intermediate dip) to the strain regime equation based on convergence rate and slab age.

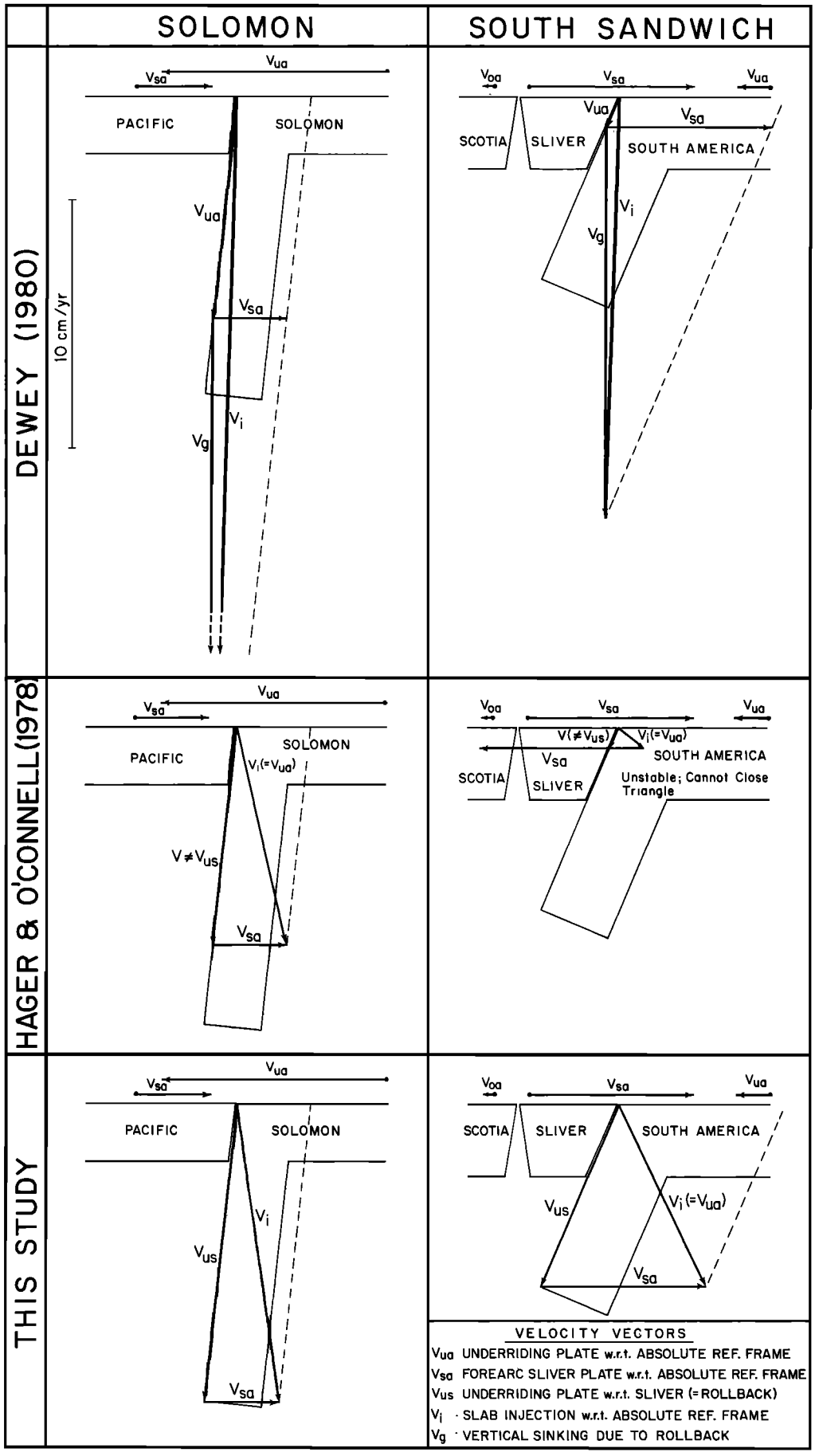

Fig. 15. Three different methods of determining the injection (or descent) angle of the slab into the mantle. Note that the assumptions made by *Dewey* [1980] lead to extremely high slab injection rates in the Solomon and South Sandwich regions and that the assumptions made by *Hager and O'Connell* [1978] break down in the South Sandwich case of large V_{sa}. These two subduction zones are extreme examples; more often, the differences between the three methods are much smaller.

TABLE 9. Strain Regressions

Regression Equation (Strain =)	Comment*	Velocity Source†	F Ratios				R^2	R
			Regression	First Term	Second Term	Third Term		
$0.862 + 0.469 \times V_c$	1	C	14.2	...	...	...	0.3717	0.610
$3.71 + 0.706 \times V_{oa}$	1	C	24.0	...	...	...	0.5003	0.707
$4.07 + 0.429 \times V_c - 0.124 \times$ DipI	1	C	17.6	17.8	13.5	...	0.6042	0.777
$6.25 + 0.619 \times V_{oa} - 0.106 \times$ DipI	1	C	22.8	25.3	11.3	...	0.6652	0.816
$1.95 + 0.519 \times V_c - 0.018 \times A_s$	1	M	12.9	19.8	6.4	...	0.5284	0.727
$5.19 + 0.464 \times V_c - 0.122 \times$ DipI $- 0.021 \times A_s$	1	C	25.1	34.5	21.9	16.4	0.7736	0.880
$4.52 + 0.275 \times V_c - 0.105 \times$ DipI $+ 0.459 \times V_{oa}$	1	C	24.2	9.6	15.2	15.4	0.7671	0.876
$5.18 + 0.494 \times V_c - 0.130 \times$ DipI $- 0.018 \times A_s$	1	M	26.7	37.4	26.1	13.0	0.7845	0.886
$3.65 + 0.662 \times V_{oa}$	2	C	30.1	...	...	...	0.5092	0.714
$3.95 + 0.468 \times V_{oa}$	2	M	35.6	...	...	...	0.5508	0.742

*Comment 1: delete 13 subduction zones with missing data. Comment 2: all possible data used in correlations; equivalent to deleting subduction zones with missing data when only one term in regression.

†C, *Chase* [1978*a*]. M, *Minster and Jordan* [1978]. Both revised as indicated in text.

Slab Dip

The Benioff zones of the highly compressional Andes are among the most shallowly dipping of modern subduction zones. Indeed, in two segments of the Andes, Peru and Central Chile, the slab flattens at about 100-km depth and apparently travels horizontally along the lower surface of the South American lithosphere. In contrast, subduction zones with back-arc spreading include some of the steepest slab dips. This apparent correlation has led several authors to infer that slab dip controls strain regime in the overriding plate.

Low-angle subduction beneath the Andes of Peru and Central Chile [*Barazangi and Isacks*, 1976] is often considered the best evidence for an effect of slab dip on strain regime in the overriding plate [e.g., *Barazangi and Isacks*, 1976; *Megard and Philip*, 1976; *Pilger*, 1981; *Mercier*, 1981]. The low-angle subduction is thought to greatly facilitate the transmission of compressive stress to the overriding plate, through increased contact area between plates. *Jordan et al.* [1983] have thoroughly documented the association between Benioff zone geometry and modern structural style in the Andes. However, structural style along the Andes is also clearly associated with Paleozoic paleogeographic features [*Allmendinger et al.*, 1983]. Thus it is possible that paleogeographic features influence not only modern structural style but also the geometry of the subducted plate [*Allmendinger et al.*, 1983].

Laramide deformation of western North America is in many respects similar to modern Andean deformation [*Jordan et al.*, 1983]. The Laramide orogeny was apparently also associated with very shallow slab dip based on magmatic patterns in the western United States [*Coney and Reynolds*, 1977; *Keith*, 1978; *Dickinson and Snyder*, 1978; *Cross and Pilger*, 1978]. In New Zealand a gradual change from middle Miocene foreland deformation to the present mildly extensional environment was similarly associated with a change from very shallow to moderate dip [*Kamp*, 1984]. A cause-and-effect relationship between low-angle subduction and pervasive intraplate deformation in both the Andes and western North America seems relatively well established, with the proviso that one of the conditions favoring low-angle dip may be the paleogeographic character of the overriding plate.

Association between strain regime and the steeper dips more commonly found in Benioff zones is less well established. The strain classes of this study exhibit a moderate inverse correlation with shallow dip ($R = -0.492$), intermediate dip ($R = -0.570$), and deep dip ($R = -0.583$). This apparently significant relationship (Figures 17 and 18) is substantially improved if a single extreme point (the Solomon subduction zone) is excluded; the correlation coefficients are then -0.549, -0.633, and -0.670, respectively. However, examination of Figure 2 shows that Benioff zone geometry cannot be the only factor influencing strain regime.

Correlation between dip and strain regime may arise from the effect of shallow dip on the degree of coupling at the contact between overriding and underriding plates [*Cross and Pilger*, 1982; *Jarrard*, 1984]. Resistance to motion on this interface is $\tau S/\sin D_c$, where τ is the shear stress, S is the thickness of the overriding plate, and D_c is the average dip along the contact. This relationship may greatly underestimate the frictional resistance in the extreme case of very low angle subduction; for example, in Peru and Central Chile an intermediate dip of 13°–14° changes to near zero at about 100 km, where the underriding plate drags along the bottom surface of the upper plate. Further, D_c is not equivalent to DipI, because the thickness of the overriding plate, though usually not known, is probably somewhat less than 100 km. Nevertheless, it may be appropriate to use 1/sin (DipI) as the independent variable rather than DipI. However, for the shallow dips of modern subduction, the relation of sin (DipI) to DipI is nearly linear, making it impossible to distinguish between the two on the basis of regression goodness of fit. Variations in both overriding plate thickness and particularly shear stress are probably much more important sources of the variance in Figure 17. Dip alone is an inadequate predictor of strain regime.

Shear stress at the base of the accretionary prism is much lower than at the base of the overriding lithosphere. This difference will tend to obscure any possible relationship between dip and strain regime, because two subduction zones with the same DipI may have very different widths of accretionary prism (e.g., Alaska Peninsula and Peru). Unfortunately, width of the accretionary prism is often not reliably known.

The opposite relationship between slab dip and strain regime has also been proposed or implied. In his initial consideration of back-arc spreading, *Karig* [1971] suggested that one effect of back-arc spreading would be to decrease the dip of the slab. In the model of *Dewey* [1980], slab age and abso-

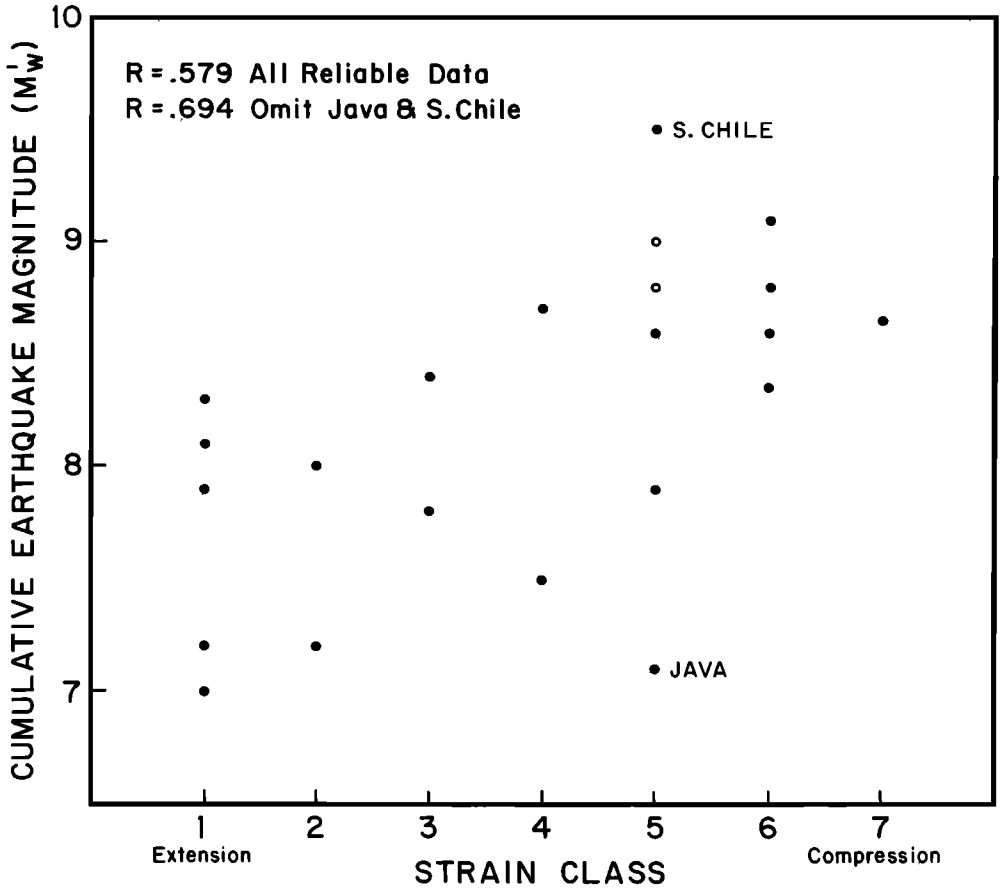

Fig. 16. Cross plot of cumulative earthquake moment (M_w') versus strain class, for modern subduction zones. Note the fair to good correlation between the two, which suggests that coupling between underriding and overriding plates is one factor controlling the strain regime of the overriding plate. Data dispersion is probably too high for coupling to be the only factor controlling strain regime.

lute motion of the overriding plate are the primary controls on strain regime. Deep slab dip is also a factor in this model, because it controls the amount of rollback caused by gravitational sinking of the slab. A doubling of slab dip causes about a 60% reduction in rollback for lithosphere of the same age, substantially increasing compressive stress whenever the overriding plate is advancing. *Ruff and Kanamori* [1980] proposed that strain regime is controlled by the effect of convergence rate and slab age on coupling at the interface between the two plates. Convergence rate and slab age together determine a preferred trajectory for the shallow slab; if this trajectory is shallower than the dip of the interface, compression results. The deeper dip of the slab, beyond the interface, is thought to be controlled by slab age, convergence rate, and possibly other parameters. An inverse correlation between deep dip and compression would result, caused by the effect of convergence rate and slab age on both parameters. Thus the *Ruff and Kanamori* [1980] model predicts that strain regime is positively correlated with shallow dip and inversely correlated with deep dip. Except for the observed inverse correlation with deep dip, none of these predictions is substantiated by this study.

Convergence Rate, Intermediate Dip, and Either Slab Age or Absolute Motion

Stepwise multiple regression indicates that the best prediction of strain regime occurs with a combination of three independent variables: convergence rate, slab age, and intermediate dip. The resulting regression equation (Table 9), with a correlation coefficient of 0.88, accounts for 77% of the observed variance in strain classes (Figure 19). The overall correlation coefficient is higher (0.93) if subduction zones with incomplete data are included in the analysis, but the more conservative approach of using only complete data is considered preferable.

Residuals to this regression equation may be systematic (Figure 19). The data appear to be better fit by a curve than a linear regression, possibly suggesting that the seven strain classes are not equally spaced points on the extension/compression continuum. The regression equation is much better at accounting for variations in compressional states than for variations in extensional states; it does not attempt to account for variations in back-arc spreading rates within class 1 zones.

This relationship can be thought of as a small but significant refinement of the previously discussed relationship of strain regime to slab age and convergence rate. According to this model, slab age and convergence rate determine the shear stress at the plate boundary, while intermediate dip is a measure of the contact area over which this stress acts.

DipI is only an approximate measure of the most important contact area, that between rigid lithospheres of the overriding and subducting plates. That contact area is not generally determinable, because neither the width of the accretionary

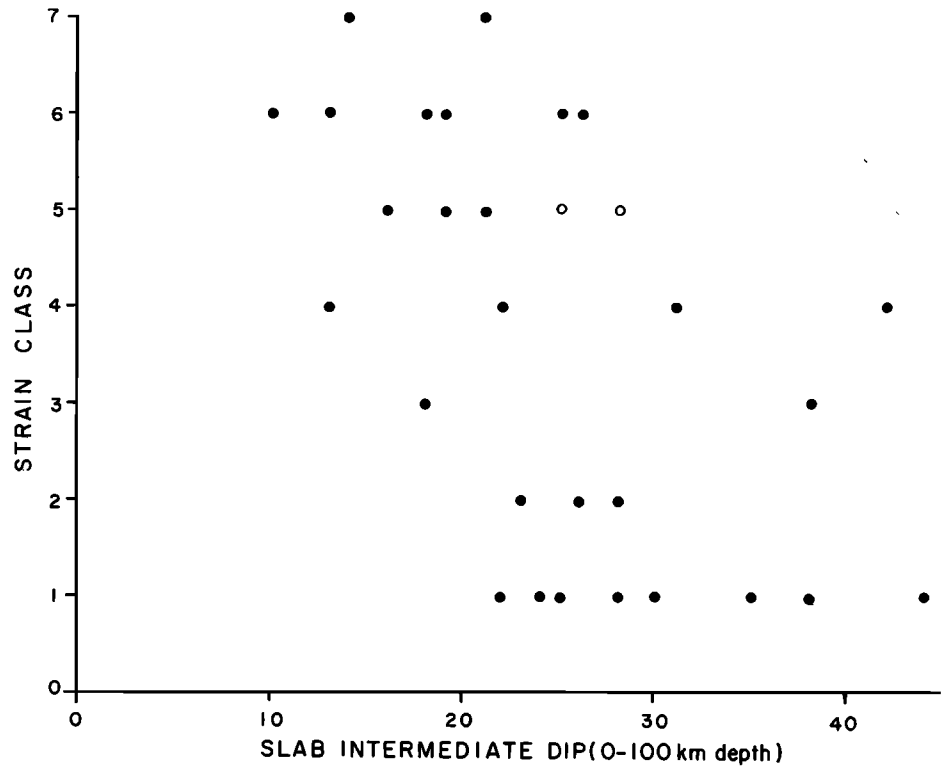

Fig. 17. Cross plot of strain class (Table 2) versus slab intermediate dip for modern subduction zones. See Figure 10 for an explanation of symbols. The correlation between the two is only fair, indicating that slab intermediate dip is not the only factor controlling strain regime of the overriding plate.

prism nor the thickness of the overriding plate is known for most subduction zones. Sediments in accretionary prisms are often highly overpressured [e.g., *von Huene*, 1984] and deform at very low shear stresses (e.g., W.-L. Zhao et al., unpublished manuscript, 1986). We may anticipate that the strain regime equation will ultimately be modified to include convergence rate, slab age, width of the accretionary prism, and width of the lithospheric contact zone.

The success of convergence rate, slab age, and DipI in accounting for variations in strain regime does not imply that coupling and contact area are the only two factors controlling strain regime. The relative magnitudes of the V_c and A_s coefficients in the strain regime equation are different than in the equation for earthquake moment. Further, decreased coupling does not account for the rapid rollback associated with back-arc spreading (Figure 13). As previously discussed, this rollback does not seem to be a simple function of slab age. An additional horizontal force may be required; deep mantle flow and asthenospheric counterflow [*Toksöz and Hsui*, 1978] are possible sources of this force, but more model studies are required to evaluate their contribution.

England and Wortel [1980] present a theoretical analysis of the ways in which these three parameters may interact to affect the net force favoring or resisting subduction at a subduction zone. This total force is the sum of four forces: (1) the driving force from ridge push, (2) the driving force from slab pull, (3) the resisting force from friction at the contact between plates, and (4) the resisting force from compositional buoyancy of the slab. *England and Wortel* [1980] hypothesize that a net force favoring subduction might be expected to lead to slab rollback and back-arc spreading. In contrast, a net force resisting subduction may result in increased coupling with the overriding plate and consequent compression.

To avoid acceleration, the forces acting on the slab must sum to zero. *England and Wortel* [1980] apparently assume that the net force favoring or resisting subduction is equal to the frictional and gravitational forces involved in crustal thinning (back-arc spreading) or thickening (thrusting) of the overriding plate. However, this net force may also be balanced by frictional drag at the base of the underriding plate or by trench suction on the overriding plate.

Quantitative determination of the four forces is plagued by major uncertainties in key parameters. However, at least a semiquantitative comparison of the empirical strain equation and the model of *England and Wortel* [1980] is warranted. The two major forces whose variation may affect strain regime are slab pull and interface friction.

The slab pull force is dominated by a very strong dependence on slab age: for example, 100 m.y. old crust has a factor of 2 or 3 greater slab pull than 30 m.y. crust at high convergence rates (10 cm/yr) and a factor of 4 greater for slow convergence (3 cm/yr). This effect is augmented slightly by the age dependence of the weaker ridge push force. A weaker but still strong dependence on convergence rate is expected: fast convergence (10 cm/yr) causes roughly twice the slab pull force of slow convergence (3 cm/yr) for young crust, and 50% more for old crust. The observed range in deep slab dips causes only a 40% range in slab pull.

In contrast, only shallow dip explicitly affects interface friction. For the range of shallow dips in modern subduction zones, the effect is nearly linear: a doubling of dip decreases the interface friction about 50%. The possible effect of slab

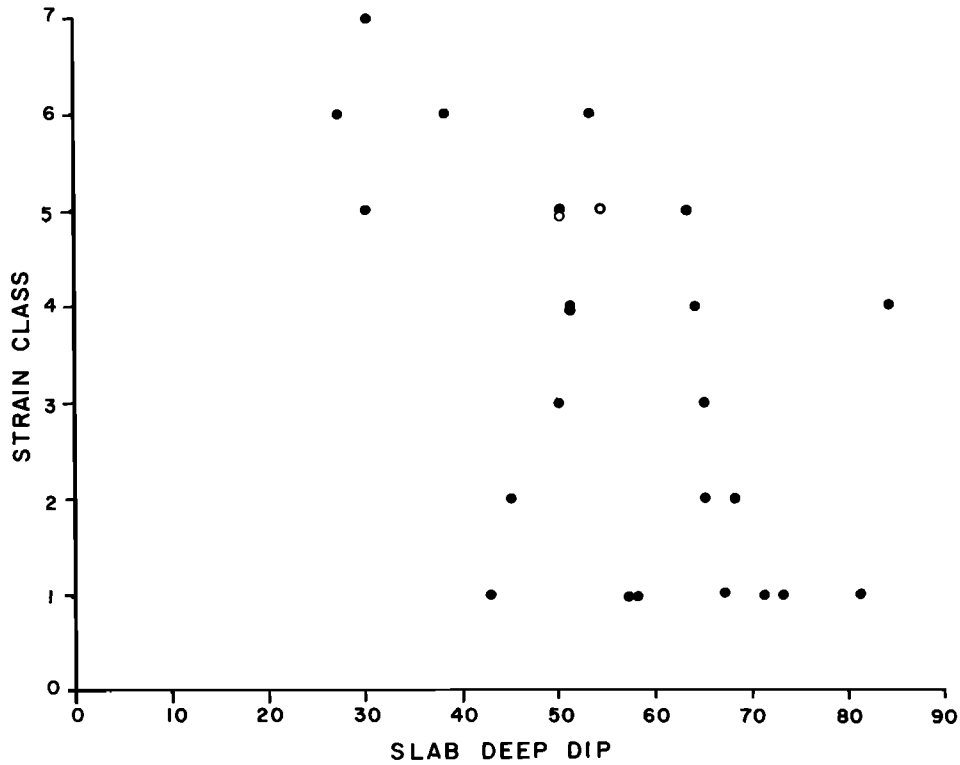

Fig. 18. Cross plot of strain class (Table 2) versus slab deep dip. See Figure 10 for an explanation of symbols. The correlation between the two is poor, indicating that deep slab dip probably has no effect on the strain regime of the overriding plate.

age and convergence rate on shear stress at the interface [*Ruff and Kanamori*, 1980] was not specifically considered by the model of *England and Wortel* [1980].

The model of *England and Wortel* [1980] therefore predicts that the empirical strain regime equation should show a very strong inverse correlation with slab age, a strong inverse correlation with convergence rate, a moderate inverse correlation with deep dip, and a moderate inverse correlation with shallow dip. The sign of the slab age and shallow dip correlations is as predicted, though the slab age term is less dominant than expected. The sign of the convergence rate correlation is the opposite of model prediction. This conflict is present not only for the empirical strain regime equation, but also for the empirical earthquake moment equation.

The proposed relationship between strain regime and resistance to subduction can also be tested by a crossplot of slab age versus vertical sinking rate [*England and Wortel*, 1980]. On such a plot, a line corresponding to a resisting force of 8×10^{12} N/m was thought [*England and Wortel*, 1980] to separate extensional and compressional subduction zones. Figure 20 shows that this expected pattern is poorly displayed by the data of Table 1. Differences between Figure 20 and the corresponding figure of *England and Wortel* [1980] are primarily attributed to the substantial improvements in strain classifications and the greater number of subduction zones in the present study.

One may tentatively conclude that coupling at the interface between plates is more important to strain regime in the overriding plate than is slab pull. Theoretical calculations cannot predict the effect of slab age and convergence rate on shear stress at this boundary. However, the three parameters that emerge from stepwise regression all operate in directions consistent with the hypothesis that coupling is the dominating influence on strain regime.

A possibly surprising result of this stepwise regression is the absence of absolute motion of the overriding plate, particularly because this variable shows the highest individual correlation with strain regime. As the three other variables are gradually added to the regression, the contribution of absolute motion gradually sinks to a nonsignificant level. This results from the correlation of absolute motion with the three other independent variables: inverse correlations with intermediate dip and slab age and positive correlation with convergence rate. The mechanism for all three of these fair to poor correlations is obscure, if indeed they are even real. The combined effect of these correlations on the stepwise regression is too large for the statistical technique to unambiguously isolate the variables affecting strain regime.

An alternative stepwise regression endpoint suggests that strain regime is affected by convergence rate, intermediate dip, and absolute motion of the overriding plate. The regression equation (Table 9), with a correlation coefficient of 0.88, accounts for 76% of the observed variance in strain class (Figure 19). This fit is as high as that achieved by the combination of convergence rate, intermediate dip, and slab age. Thus multivariate analysis is capable of indicating that two of the three variables affecting strain class are convergence rate and intermediate dip; it is not capable of distinguishing whether absolute motion or slab age is the third variable.

Two observations suggest that slab age is more likely than absolute motion to be the third variable. First, nearly all of the empirical subduction relations previously discussed in-

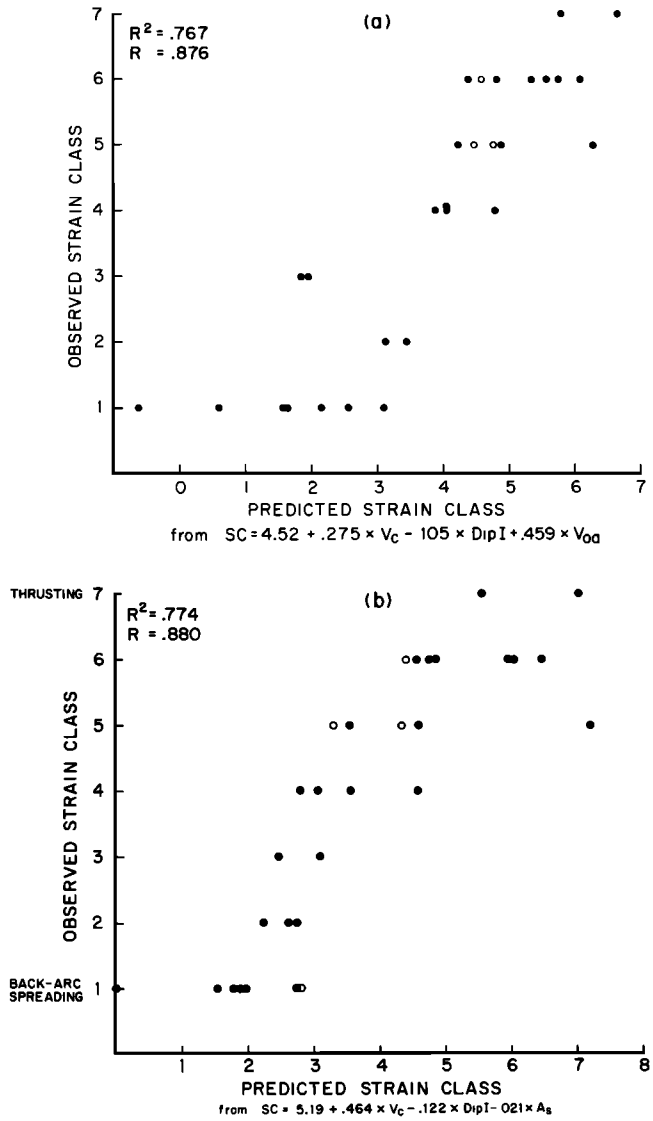

Fig. 19. Cross plots of strain class (Table 2) versus predicted strain class. Predicted strain classes are based on regressions in which the independent variables are convergence rate, intermediate dip, and either (*b*) slab age or (*a*) absolute motion of the overriding plate. Both regression results are very successful in accounting for modern variations in strain regime. Analysis of modern subduction zones cannot determine with confidence whether slab age or absolute motion is the third causal variable. See Figure 10 for an explanation of symbols. Note the possibility that the data in each plot would be better fit by a curve than by the linear fit used. This observation may suggest that the strain classes are not equally spaced points along the continuum from extension to compression.

volve some combination of convergence rate, slab age, and intermediate dip. Absolute motion is consistently absent from these other relations, though each statistical analysis included absolute motions of both overriding and underriding plates as potential independent variables. Second, M_w', which is affected by slab age and convergence rate, is correlated with strain class. Neither observation proves that slab age, rather than absolute motion, affects strain class. Thus neither of the two regression equations can be accepted until they are both tested on other (presumably pre-Quaternary) data.

Strain regimes of modern subduction zones are indirectly correlated with crustal type in the overriding plate. All overriding plates composed of oceanic crust are extensional or neutral, while continental overriding plates are more often compressional than extensional (Table 1). This correlation is a sampling artifact, resulting from three factors: (1) strain regime is affected by DipI (as discussed above), (2) DipI is affected by duration of subduction, and (3) continental overriding plates have much longer subduction durations than oceanic overriding plates. The latter two factors are explored more thoroughly in the next section.

Slab Dip Models

The factors influencing slab dip are not yet known with certainty. The search for the primary causes of slab dip variations has been hampered by four limitations: (1) changes in dip with depth within each subduction zone, (2) limited data concerning paleodips, (3) correlation between possible causative factors, and (4) unknown values for parameters in theoretical models.

Almost all subduction zones show a gradual steepening of the Benioff zone with increasing depth, at least to 100- to 200-km depth (Figure 2). Thus the dip of a Benioff zone is not readily characterized by a single value. It is probably inappropriate to use the average dip of the entire Benioff zone to characterize slab dip, because the search for factors controlling slab dip is then contaminated by factors controlling slab length. In this paper, slab dip is parameterized into three somewhat arbitrary measures: (1) DipS, the average shallow dip to 60-km depth, (2) DipI, the average dip for the more intermediate depth range of 0 to 100 km, and (3) DipD, the more constant dip of the deeper slab, generally in the interval from about 150 km to 400 km. It has been suggested that there is no correlation between shallow dip and deep dip [*Karig et al.*, 1976], indicating that entirely different causes may be responsible for DipS and DipD. However, DipS and DipD are moderately correlated ($R = 0.560$) and therefore probably not independent. Apparently either some of the same factors control both deep and shallow dip, or either deep or shallow dip is partly controlled by the dip of the other part of the slab.

Analysis of deep slab dips is entirely limited to present Benioff zones. This limitation may be serious, as we cannot assume a priori that observed present deep dips are in an equilibrium state rather than a state of constant major change. Such an assumption may be safely made only a posteriori, if it is found that observed deep dips can be accurately predicted from independent variables that change only gradually (e.g., V_c, V_{oa}, or A_s). Paleodip estimation is possible for DipI, based on potassium content of ancient arc volcanics [*Dickinson*, 1972; *Lipman et al.*, 1972] or correlation between Benioff zone depth and other measures of arc composition [*Keith*, 1978]. However, these paleodip estimates must be treated with caution, as factors other than Benioff zone depth can have major impact on arc composition [*Gill*, 1981; *Glazner and Supplee*, 1982; *Foden*, 1983].

The problem of correlation between possible causative variables is not unique to dip models, as previously discussed. It is, however, more severe for dip and strain regime models than for some other models (e.g., slab length) because qualitative relationships to more potential independent variables are plausible.

Quantitative theoretical models of slab dip have met with very limited success because key parameters affecting flow and force balances within the mantle are too poorly known. Slab

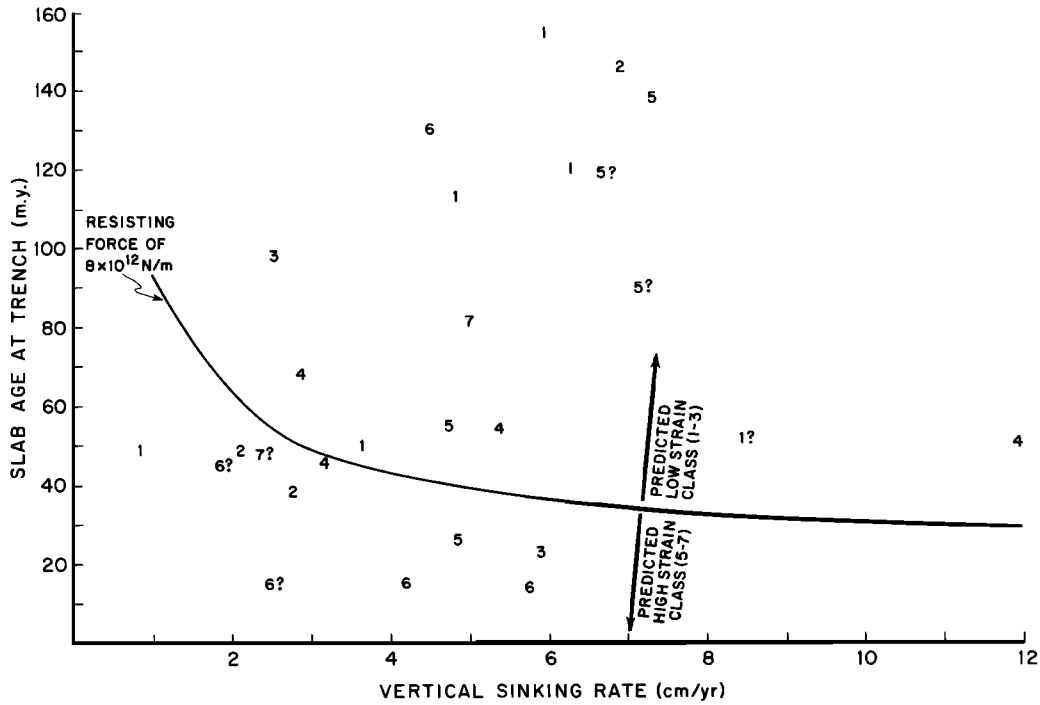

Fig. 20. Cross plot of slab age versus vertical sinking rate of the slab. The strain class of each subduction zone is indicated by a number between 1 and 7; question marks indicate less reliable data. According to the model of *England and Wortel* [1980], strain class is expected to increase from the upper right to the lower left of the plot. The line representing a resisting force of 8×10^{12} N/m was thought to separate extensional (classes 1–3) from compressional (classes 5–7) subduction zones. Note the poor fit of the data to this predicted pattern.

dip models are therefore largely dependent on empirical correlation to possible independent variables. Given reliable empirical correlations, it may then be possible to place limits on appropriate theoretical models. For example, *Hager and O'Connell* [1978] modelled mantle flow patterns based on three different sets of viscosity assumptions and compared their results to observed slab dips as a test of these assumptions.

Radius of Curvature

Subduction-related bending of a part of the earth's spherical lithospheric cap imposes internal stresses on the slab. The slab dip that minimizes internal stress is simply twice the radius of curvature of the plate boundary [*Frank*, 1968]. Benioff zone geometry may therefore be analogous to a dent in a ping pong ball, except that in the ping pong ball the radius of curvature is free to change in response to the imposed dip, whereas the shape of an overriding plate imposes a radius of curvature which may control slab dip. Several studies have sought to establish an empirical relationship between radius of curvature and dip [*Aoki*, 1974; *DeFazio*, 1974; *Laravie*, 1975], usually using radius of curvature of the trench rather than of the arc and average dip of the entire Benioff zone instead of shallow or deep dip. *Tovish and Schubert* [1978] showed that the correlation between arc radius of curvature and deep dip is poor. In this analysis, logarithm of radius of curvature is used, because both the distribution of radii of curvature and uncertainties in individual RC's are approximately log normally distributed. The conclusion of *Tovish and Schubert* [1978] is not changed by the present study ($R = 0.100$ for DipS, $R = -0.256$ for DipD). Though *Frank*'s [1968] relationship is clearly not a primary control on slab dip, the relation may still be useful as an indicator of stress within the slab [*Laravie*, 1975].

Convergence Rate

Luyendyk [1970] suggested that convergence rate may be an important control of slab dip, based on examination of the Tonga, Kermadec, Java, and Kamchatka-Kurile subduction zones. Faster convergence was thought to cause shallower dip, following the relation sin (dip) = sinking rate/convergence rate. Similarly, *Roeder* [1975] proposed that convergence rate changes may cause dip changes. However, *Tovish and Schubert* [1978] compared deep dips to convergence rate for most of the subduction zones of Table 1 and found little correlation between the two for convergence rates of less than 10 cm/yr. The present analysis confirms this result: a small positive correlation between V_{cba} and dip is found, and a small inverse correlation between V_c and dip is found (Table 6). These correlations do not disprove the relationship proposed by *Luyendyk* [1970]; if it is valid, sinking rate must be much more variable than originally suggested.

Slab Age

South America has both shallower dips and younger subducted lithosphere than many western Pacific subduction zones. Because older lithosphere is more gravitationally unstable than younger lithosphere, it might be expected to sink more rapidly, causing greater dips. *Wortel and Vlaar* [1978] suggested that dip variations along South America may be caused by variations in slab age. Similarly, *Barazangi and Isacks* [1979] suggested that the youth of the slab beneath Peru is one possible cause of flat subduction there. *Jordan et al.* [1983] indicated a possible association between decrease in

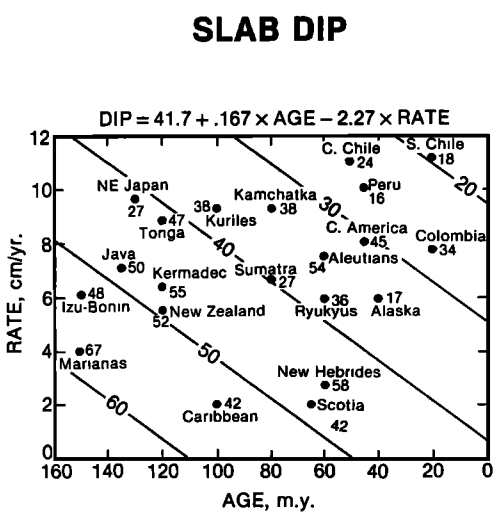

Fig. 21. Observed dips for a subset of modern subduction zones, shown on a cross plot of total convergence rate versus slab age [*Jarrard*, 1984]. Diagonal lines indicate the regression plane of predicted dips. The good fit of observed to predicted dips seen here is not confirmed by the revised data of Table 1.

dip from North Chile to Central Chile and decreasing slab age; they noted, however, that the even younger slab beneath South Chile is not shallowly dipping. When all the subduction zones of Table 1 are considered, the correlations between slab age and both DipI and DipD are negligible ($R < 0.3$, Table 6).

Convergence Rate and Slab Age

Increase in gravitational instability with slab age suggests a possible modification of the relation proposed by *Luyendyk* [1970]: $\sin(\text{dip}) = k \times A_s/V_{cba}$. This simple geometrical relationship indicates that the dip depends only on the amount of sinking that accompanies a given period of convergence and that this sinking rate is proportional to slab age. However, no correlation of A_s/V_{cba} is found with either the sine of DipD ($R = 0.14$) or the sine of DipI ($R = -0.24$). A somewhat similar relationship was suggested by *Ruff and Kanamori* [1980]. They noted that Benioff zone maximum depth is moderately correlated with slab age and that maximum horizontal extent of the Benioff zone is moderately correlated with convergence rate.

Based on the subduction zones tabulated by *Ruff and Kanamori* [1980], *Jarrard* [1984] found through multiple regression that

$$\text{DipA} = 41.7 + 0.17 \times A_s - 0.23 \times \text{Rate}$$

where DipA is the average dip of the entire Benioff zone and Rate is the convergence rate, not just the component perpendicular to the trench, excluding back-arc spreading. This empirical relationship, with a correlation coefficient of 0.717, is shown in Figure 21. *Jarrard* [1984] tested this equation by using Late Cretaceous and Tertiary variations in A_s and Rate for western North America [*Engebretson*, 1982] to generate predicted dips. Comparison of these predicted dips with those independently determined by *Keith* [1982], on the basis of locations of dated andesitic volcanism, shows a strong agreement (Figure 22).

Two lines of evidence indicate that this apparent confirmation of the relationship of *Jarrard* [1984] is only a coincidence. First, the hypothesized Late Tertiary slab steepening inferred from patterns of andesitic volcanism [*Coney and Reynolds*, 1977; *Keith*, 1978] appears to be an artifact of latitudinal sweep in the location of volcanism [*Glazner and Supplee*, 1982]. Second, because of Benioff zone curvature (Figure 2), the physical significance of average Benioff zone dip is not obvious. A more appropriate dip for comparison with locations of andesitic volcanism is DipI, the average dip to 100 km. However, Table 6 shows that the correlations of DipI with A_s, V_c, and V_{cba} are negligible. This decrease in quality of fit may be partly attributable to the increase in number of subduction zones analyzed and improved estimates of dip, V_c, and A_s. Perhaps more important is the change from average Benioff zone dip to DipI.

Thermal modelling of the flexural rigidity of the subducted slab has been used to infer a different dependence of DipI on convergence rate and slab age [*Furlong et al.*, 1982], with greater DipI resulting from slower V_c or younger A_s. Based on thermal modelling of each of 12 subduction zones, a different relationship of dip to V_c and A_s was found for six subduction zones with continental overriding plates than for six oceanic ones. *Furlong et al.* [1982] find an overall correlation coefficient of 0.9 between observed and predicted dips. Because of the small number of subduction zones analyzed, a more rigid test of this hypothesis requires thermal modelling of each subduction zone omitted from the original analysis. Such a test is not attempted here, partially because it has not been possible to successfully reproduce shallow dips, initial effective elastic thicknesses, or even convergence rates for the examples described by *Furlong et al.* [1982]. The hypothesized effect of convergence rate and slab age is not expected to accurately fit the form of a regression equation, but a good fit of DipI to the product of convergence rate and slab age is predicted. Subduction zones with continental overriding plates show no correlation of DipI with $V_{cba} \times A_s$ ($R = 0.06$), V_{cba} ($R = 0.07$), or A_s ($R = -0.08$). Subduction zones with oceanic overriding plates show no correlation with $V_{cba} \times A_s$ ($R = -0.12$) but fair correlations with A_S ($R = -0.51$) and V_{cba} ($R = 0.58$). The apparent correlation with V_{cba} is the inverse of that predicted by the model of *Furlong et al.* [1982]. Similar correlations are found using V_c instead of V_{cba}. Thus no confirmation of the model of *Furlong et al.* [1982] is found in the much larger data set of Table 1.

Convergence Rate, Slab Age, and Absolute Motion

Cross and Pilger [1982] suggest that slab dip is controlled by four factors: absolute motion of the overriding plate, convergence rate, slab age, and subduction of aseismic ridges. The possible influence of subduction of aseismic ridges is discussed in a subsequent section. *Cross and Pilger* [1982] also suggest that accretion plays a secondary role in modifying shallow dip; accretion too is discussed in a subsequent section.

In the model of *Cross and Pilger* [1982], both increased convergence rate and decreased slab age cause shallower dip, as in the models just discussed. Absolute motion is also hypothesized to affect dip, with rapid trenchward advance causing a shallower dip through overriding of the subducted slab. A similar effect of advancing absolute motion on shallow dip was suggested by *Dewey* [1980]. Both studies infer that retreating absolute motion of the overriding plate has no effect on dip. *Lliboutry* [1974] hypothesized that dip is dependent on absolute motion and rate of vertical sinking. If vertical

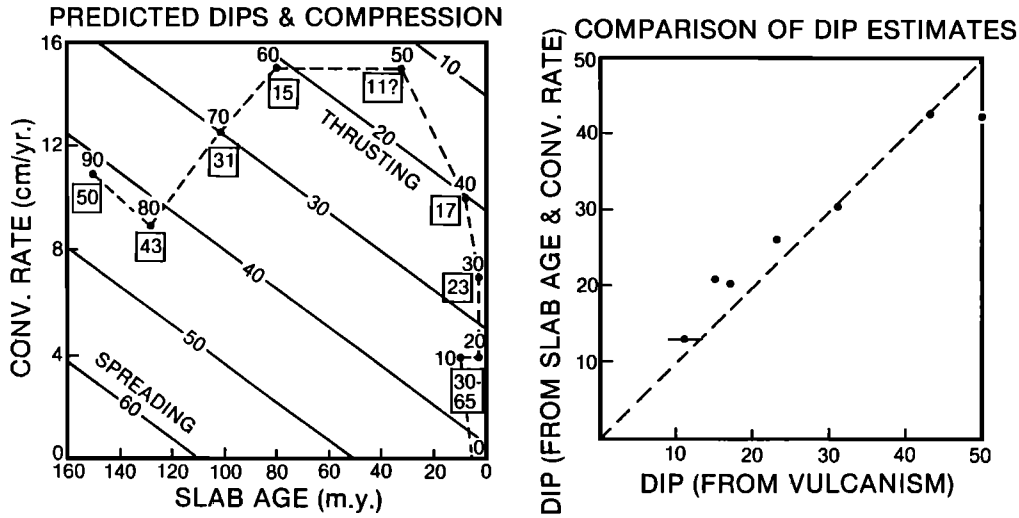

Fig. 22. Application of the dip relationship of Figure 21 to the prediction of Late Cretaceous and Tertiary dips for western North America [*Jarrard*, 1984]. (Left) Changes in convergence rate and slab age from 90 m.y. to present, overlain on the regression plane of corresponding dips; numbers in boxes are dips independently determined by *Keith* [1978] based on dated arc volcanism. (Right) Cross plot comparing dips of *Keith* [1978] with predicted dips based on slab age and convergence rate.

sinking rate depends on convergence rate and slab age [*England and Wortel*, 1980], then the model of *Lliboutry* [1974] is similar to that of *Cross and Pilger* [1982], except that higher convergence rate would cause steeper rather than shallower dip.

Cross and Pilger [1982] documented the possible effect of these three independent variables through examination of regions in which only one of the three variables changes. For example, a shallowing of dip from southwest Mexico to southeast Mexico may be attributable to the 1.3- to 1.4-cm/yr faster convergence in the latter. The gradual dip shallowing from north to south along the South Sandwich subduction zone [*Brett*, 1977] may be attributable to the much younger lithosphere in the southern half of the slab than in the northern half. Much shallower dips in Mexico compared with Nicaragua may be related to the differences in absolute motion of the North American and Caribbean plates.

An alternative approach to determining the importance of these three variables to slab dip is multiple regression. With DipD as the dependent variable, absolute motion of the overriding plate (V_{oa}) is the most important of these three possible independent variables. With an F of 5.5, V_{oa} is marginally significant and accounts for 19% of the observed variance in DipD. Virtually zero ($F < 0.1$) residual correlation with convergence rate and slab age is found. The correlation with V_{oa} results almost entirely from the fact that South American subduction zones have both a rapid advance in V_{oa} and shallow dips; the Solomon subduction zone, with a rapid advance in V_{oa} and the steepest DipD, conflicts with the South American data and substantially degrades the correlation. The major difference between South American and Solomon deep dips occurs despite generally similar convergence rates, slab ages, and absolute motions of overriding plates.

With DipI as the dependent variable, all three of the variables V_{oa}, V_c, and A_s show very low correlations; V_{oa}, the best of the three, has a correlation coefficient of only -0.160 (Table 6). It therefore appears unlikely that the primary controls on either DipI or DipD are convergence rate, slab age, and absolute motion of the overriding plate.

Mantle Flow

Observed plate motions require net mantle flow from subduction zones to ridges. *Hager and O'Connell* [1978] have modelled global flow patterns based on current mass fluxes at ridges and trenches and three different sets of viscosity assumptions. Resulting flow directions at subduction zones can be compared with descent angles of subducted slabs, based on the assumption that deep dip is controlled by mantle flow. A good fit of observed to predicted descent angles can then be taken as an indication that deep dip is controlled by mantle flow.

Based on 10 subduction zones, *Hager and O'Connell* [1978] find that observed deep dips correlate with dips predicted by their "Cathles" model with a correlation coefficient of 0.91. The "Cathles" model has constant viscosity throughout almost the entire mantle, with a narrow low-viscosity layer just below the lithosphere. Their model effectively predicts both the polarity of subduction and the amount of dip; thus both seismic and predicted dips go from 0 to 180°. For seven of the ten subduction zones considered, the overriding plate is continental, thereby precluding subduction of the opposite polarity. For consistency with other tests of causes of dip, it is probably more appropriate to consider only amount of dip rather than both polarity and dip. The correlation between observed and Cathles predicted dips is then 0.78.

Two factors indicate that a revised analysis of the consistency of flow models with observed dips is warranted. First, newer data on Benioff zone geometry change some deep dips. For nine of the ten subduction zones, the deep dips of Table 1 are within 10° of those used by *Hager and O'Connell* [1978]. For New Zealand the difference is 21°, because *Adams and Ware* [1977] showed that the dip estimate of *Ansell and Smith* [1975] was biased by faster velocities in the slab. A more significant revision is in the transformation between descent angle and deep dip. As discussed in the section on strain regime models and shown in Figure 15, *Hager and O'Connell* [1978] apparently incorrectly assumed that the rate of absolute motion of the underriding plate is the same for the slab as for the unsubducted portion of the plate.

Correlation of the descent angles of Table 1 with predicted descent angles based on the Cathles model yields correlation coefficients of 0.417 and 0.414 for the *Chase* [1978*a*] and *Minster and Jordan* [1978] motion models, respectively. The fit is much better for the constant mantle viscosity model of *Hager and O'Connell* [1978]: 0.742 and 0.724, respectively. Comparing the two models by fit to individual subduction zones, six of the ten show a better fit to the constant model, two show a better fit to the Cathles model, and two show approximately equal fits. However, descent angles for two subduction zones are highly tentative and not even shown in Table 1. Estimated descent angles for New Hebrides (114° for *Chase* [1978*a*]; 118° for *Minster and Jordan* [1978]) are highly dependent on the uncertain velocities for this region, though a descent angle of >90° seems likely. The descent angle of 6° used for Peru assumes a deep dip of 5°; this dip determination requires a relaxation of the requirement that deep dips be measured for portions of the slab deeper than 150 km.

Most analyses indicate that a constant viscosity mantle is less likely than a mantle with a low-viscosity asthenosphere [e.g., *Richter and McKenzie*, 1978]; the correlation coefficient of 0.4 between observed and predicted dips suggests that mantle flow is not the primary control on deep dip. An analysis of more than ten subduction zones seems warranted, but such an analysis is not possible from the figures shown by *Hager and O'Connell* [1978].

The flow models of *Hager and O'Connell* [1978] do not include the possible effect of density contrast of the downgoing slab on either flow or slab dip. *Tovish et al.* [1978] modelled corner flows associated with the slab and found that pressures induced by flow generally act to lift the slab, offsetting the tendency of gravity to make the slab vertical. As dip is decreased, a dip is reached beyond which these pressure forces cannot be balanced and the only stable configuration is a dip of about zero. This may explain the lack of dips between 10° and 25° [*Tovish et al.*, 1978]. Further, this result implies that the substantial dip variation along South America may not reflect much difference in whatever factors primarily control dip.

Aseismic Ridges

Subduction of aseismic ridges is occurring or about to occur at several of the subduction zones considered in this study: Roo Rise (Java), Izu-Bonin Ridge (southwest Japan), Pratt-Welker Chain (Alaska Peninsula), Carnegie Ridge (Ecuador), Nazca Ridge (Peru), San Fernandez Ridge (Central Chile), and Tiburon Ridge (Lesser Antilles). Aseismic ridges are also subducting several hundred kilometers away from the transects of Table 1 for some subduction zones: Louisville Ridge (Tonga-Kermadec), Oki-Daito Ridge (Ryukyu), Marcus-Necker Seamounts (Izu-Bonin), and Emperor Seamounts (Kamchatka).

All of these ridges are likely to have greater than normal crustal thicknesses [*Kelleher and McCann*, 1976; *Detrick and Watts*, 1979]. *Kelleher and McCann* [1976] suggested that the increased crustal thickness of aseismic ridges decreases the gravitational instability of the slab, thereby decreasing slab dip. At a depth of about 60 km the basalt of oceanic crust undergoes a phase transformation to eclogite [*Ahrens and Schubert*, 1975], with a corresponding major increase in density. Therefore aseismic ridge subduction is predicted to cause a shallowing of dip above 60 km and a steepening of dip below 60 km.

The effect of aseismic ridge subduction on the accretionary prism is dramatic, with a strong association between aseismic ridge collision and both uplift and deformation of the accretionary prism (W. R. McCann and Haberman, unpublished manuscript, 1986). Several authors have suggested that shallow dips along portions of the South American margin may result from aseismic ridge subduction [e.g., *Kelleher and McCann*, 1976; *Barazangi and Isacks*, 1979; *Pilger*, 1981; *Pennington*, 1981]. Evidence for dip shallowing in other subduction zones due to aseismic ridges is summarized by *Cross and Pilger* [1982]. No evidence has been found for anomalously steep subduction of the deeper slab in such regions; in fact, only below 60 km does the anomalously shallow subduction of Peru and Central Chile become evident. Thus a major discrepancy appears to exist between experimental geochemistry and the hypothesized effect of aseismic ridges on slab dip below 60 km. *Cross and Pilger* [1982] suggest that either the transformation to eclogite does not occur for aseismic ridges or the aseismic ridge is sheared away from the slab. However, such shearing would presumably occur above 60–100 km and would still leave an anomalously thick crustal root.

In summary, aseismic ridge subduction probably has a substantial impact on the accretionary prism. Effects on both intraplate and interplate earthquakes have also been amply demonstrated [*Kelleher and McCann*, 1976; *Barazangi and Isacks*, 1979]. A possible role of aseismic ridge subduction in modifying slab dip has been demonstrated. However, quantitative evaluation of this effect must await reconciliation with experimental geochemical data and isolation of the factors controlling dip of normal oceanic lithosphere.

Accretion, Arc Age, and Mantle Flow

The uppermost portion of the Benioff zone may be flattened by an accretionary prism [*Karig and Sharman*, 1975; *Karig et al.*, 1976]. Gravity modelling indicates that the load of the accretionary prism is sufficient to depress the overriding plate [*Karig et al.*, 1976], thus modifying both DipS and DipI. Accretion cannot be the only factor affecting shallow dip, as substantial dip variations occur even among subduction zones with virtually no accretionary prisms.

Karig et al. [1976] tabulated the widths of accretionary prisms for many subduction zones. However, recent DSDP sites in forearcs often yielded surprising and major revisions in the widths of accretionary prisms [e.g., *von Huene*, 1984]. Unfortunately, only a few forearcs have been drilled as yet. In the absence of either deep drilling or very high quality multichannel profiling, estimation of the location of the transition from crust to accretionary prism is often hazardous. Consequently, no estimates of width of the accretionary prism are included in Table 1.

Nevertheless, it appears safe to conclude that certain subduction zones have particularly wide accretionary prisms: Alaska [*Jacob et al.*, 1977], Alaska Peninsula [*Jacob et al.*, 1977], Makran [*Farhoudi and Karig*, 1977; *White*, 1979], New Zealand [*Katz*, 1982], North Sulawesi [*Silver et al.*, 1983*a*], Java-Sumatra-Andaman [*Hamilton*, 1979], Kamchatka [*Dickinson*, 1973], Lesser Antilles [*Biju-Duval et al.*, 1981], southwest Japan, Aegean, and Cascades. Examination of Table 1 shows that these subduction zones are consistently lower in both DipS and DipI than nearly all other subduction zones; low-accretion Peru and possibly low-accretion South Chile are notable exceptions. No correlation of the high-accretion subduction zones with DipD is expected or observed. Because accretion affects shallow dip but is difficult to quantify, subduction zones with higher accretion are omitted from subsequent regressions in which DipI is the dependent variable. It

TABLE 10. Dip Regressions

Regression Equation	Comment*	Velocity Source†	F Ratios: Regression	F Ratios: First Variable	F Ratios: Second Variable	R^2	R
DipD = 32.3 + 0.939 × DipI‡	1	···	16.8	···	···	0.412	0.642
DipD = 46.4 + 0.604 × DipI − 0.0653 × A_a	1	···	13.6	6.1	6.5	0.542	0.736
DipD = 34.2 + 0.838 × DipI − 1.21 × V_{oa}	1	M	11.4	14.2	3.9	0.498	0.706
DipD = 31.6 + 0.972 × DipI	2	···	16.9	···	···	0.424	0.651
DipD = 37.3 + 0.814 × DipI	3	···	13.6	···	···	0.392	0.626
DipI = 35.2 − 0.081 × A_a	1	···	22.1	···	···	0.538	0.733
DipI = 41.7 − 1.64 × $(A_a)^{1/2}$	1	···	31.8	···	···	0.626	0.791
DipI = 42.8 − 1.92 × $(A_a)^{1/2}$‡	4	···	64.3	···	···	0.791	0.889

*Comment 1: all possible data used in correlations; equivalent to deleting subduction zones with missing data when only one term in regression. Comment 2: delete New Britain. Comment 3: delete South America; eliminates all correlation with V_{oa}. Comment 4: delete Colombia and Middle America.

†M, *Minster and Jordan* [1978]. Revised as indicated in text.

‡Preferred model.

should be noted, however, that an appreciable effect of accretion on DipI is probable even among the nominally "low accretion" subduction zones. This currently unknown accretion contribution is expected to degrade the quality of fit of DipI to any other factors that control dip.

Dickinson [1973] compiled estimates of arc-trench gap and arc age for many of the subduction zones of Table 1. He found an approximately linear relationship between the two variables and concluded that arc-trench gap tends to increase at a rate of about 1 km/m.y. A similar pattern of increasing arc-trench gap with time is often found within individual subduction zones [*Dickinson*, 1973]. A combination of accretion and retrograde motion of the arc (of unknown cause) was suggested as the factors causing this relationship.

Because arc volcanism nearly always occurs above the portion of the Benioff zone that is about 125 km in depth, arc-trench gap bears a very close relationship to DipI ($R = -0.824$, and $R = 0.907$ for 1/tan (DipI)). If the correlation between arc-trench gap and arc age is significant, then either (1) arc age affects arc-trench gap, which affects DipI, or (2) arc age affects DipI, which affects arc-trench gap. The latter seems much more plausible.

When multiple regression is applied to prediction of DipI for the subset of subduction zones with "low" accretion, the most significant correlation is with arc age (A_a). The resulting regression equation (Table 10), with a correlation coefficient of −0.73, accounts for only 53% of the variance in DipI. With the exception of DipS and DipD, no other potential independent variable shows a significant correlation with either DipI or regression residuals. The relationship between DipI and A_a may not be linear; a better fit is observed for the square root of A_a (Table 10 and Figure 23). Seventy-nine percent of the variance in DipI for "low-accretion" subduction zones is accounted for by a regression on the square root of arc age, if two anomalous points (Colombia and Middle America) are omitted.

The conclusion that arc age is the primary variable of Table 1 affecting DipI is unchanged if all subduction zones are considered, rather than just the "low-accretion" subduction zones. The correlation coefficient is degraded from −0.73 to −0.54, because variance in DipI associated with accretion is no longer even partly removed. With the exception of DipS and DipD, regression residuals show very low correlation with all other possible independent variables.

With DipD as the dependent variable, both DipI and arc age show approximately equally high correlations (0.64 and −0.65, respectively). No other potential independent variable of Table 1 shows a significant primary correlation with DipD. However, the quality of fit of DipD to DipI and arc age is comparable to the fit achieved for a small subset of subduction zones by the constant-viscosity mantle convection model of *Hager and O'Connell* [1978]. Arc age is unlikely to directly affect DipD; more likely, arc age affects DipI, and the trajectory initiated by DipI has a strong impact on DipD. With DipI as the primary independent variable, there is a small residual correlation with arc age, but this residual correlation is entirely attributable to South American subduction zones (Table 10).

In summary, regression analysis indicates that the primary factors controlling average dip to 100-km depth (DipI) are accretion and duration of subduction (i.e., arc age). A gradual shallowing of DipI with time is predicted for most subduction zones, because duration of subduction will always increase with time (unless arc polarity reversal occurs) and accretion will usually increase with time (though erosion may occur). Because the width of the accretionary prism is often unknown, a single regression equation combining the two effects is not attempted. Deep dip is probably a result of DipI and mantle convection: the slab trajectory established at shallow depths is modified at greater depth by mantle flow patterns. Because estimates of present mantle flow patterns are highly dependent on viscosity assumptions, it is not currently possible to reliably establish the impact of mantle flow on DipD or include it with DipI in a regression equation predicting DipD.

Other variables often considered to affect slab dip (e.g., convergence rate, slab age, and absolute motion of the overriding plate) do not show any systematic relationship to either DipD or DipI. A subsidiary role of one of these variables cannot be excluded, however. It was not possible to combine arc age and accretion in a single equation to predict DipI, nor to combine DipI and mantle flow in a single equation to predict DipD. Therefore the possibility of a significant residual correlation to another variable could not be fully investigated.

The mechanism for a decrease in dip with increasing duration of subduction is not known with certainty. Gradual thinning of the lithosphere of the overriding plate with time is implied. Whether this thinning is a result of active abrasion [*Smith*, 1976] or of frictional heating [*Dickinson*, 1973] is diffi-

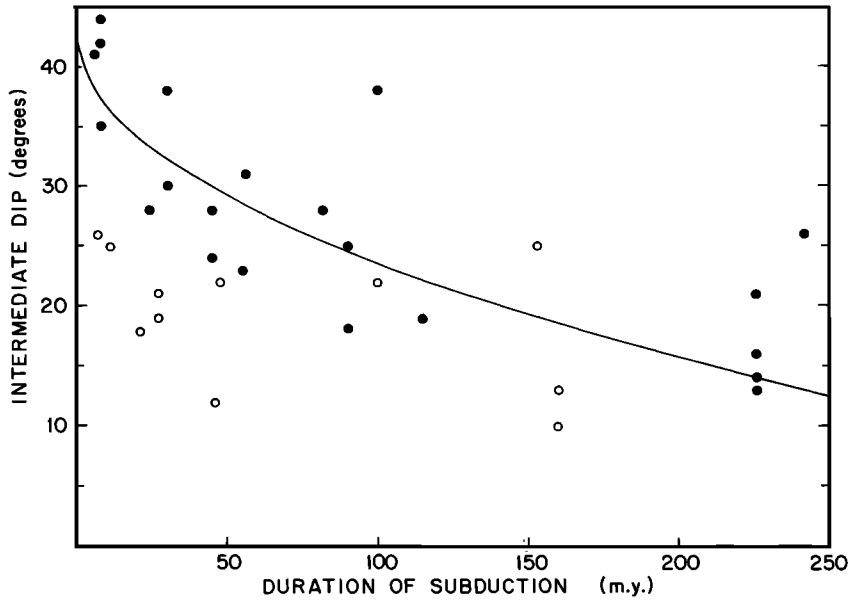

Fig. 23. Cross plot of intermediate slab dip versus duration of subduction, as indicated by maximum age of arc-related rocks. Solid circles are subduction zones with narrow or moderate accretionary prisms; open circles are subduction zones with wide accretionary prisms. The best fit regression line (Table 10) assumes that intermediate dip depends on the square root of subduction duration; this line is based on solid circles only and excludes two points. Presence of a wide accretionary prism causes a shallower intermediate dip than would be expected otherwise. The influence of both duration of subduction and accretion on intermediate dip indicates that the slab conforms to the cross-sectional shape of the overriding plate.

cult to determine without a better knowledge of the shear stresses and strength of the overriding plate. In the very old arcs of South America, active erosion of the overriding plate is required by the fact that the oldest arc is at or seaward of the present coast [*James*, 1971]. This erosion affects even the uppermost part of the South American overriding plate and does not necessarily imply erosion-related shallowing of dip.

The better regression fit achieved by the square root of A_a, compared with a linear fit to A_a, suggests that gradual heating of the overriding plate may be the primary factor causing shallowing of dip with time. The temperature of the top surface of the slab is independent of slab age upon entering the trench, and the slab acts as a heat sink rather than a heat source within the zone of contact with the overriding plate [*Furlong et al.*, 1982]. Therefore the cause of heating of the overriding plate is likely to be friction at the interface between plates rather than heat from within the slab. Consequently no correlation between DipI and slab age is expected. However, subduction of a spreading center is expected to involve accelerated heating of the overriding plate and therefore anomalously shallow DipI. Unfortunately, ridge crest subduction also implies little or no Benioff zone, so that this prediction of the model is not readily testable.

This model for DipI is very different in mechanism from models discussed in preceding sections. All of the previous models (e.g., V_c, A_s, V_{oa}, and aseismic ridges) implicitly treat the cross-sectional shape of the overriding plate as a point indenter. In contrast, if accretion and arc age control DipI, then the slab must follow the leading edge of the overriding plate, regardless of other forces acting on the slab. Earthquake epicenters strongly suggest that contact is usually maintained down to at least 60-km depth. The difficulty in precisely locating the top of the slab at shallow depths is a consequence of this contact and resultant earthquakes within the overriding plate. Possible contact within the depth range from about 60 km to the base of the overriding plate is not determinable, because these depths are below the brittle/ductile transition in the overriding plate.

Jischke [1975] examined the physics of stresses involved at the contact between plates and concluded that nonhydrostatic pressure force and viscous shear force are sufficient to maintain contact down to the base of the overriding plate. Flexural rigidity of the slab will also act to minimize dip and maintain contact. However, our knowledge of some forces acting on the slab is insufficient to permit reliable determination of the relative magnitudes of all forces. The empirical correlation of DipI with accretion and arc age suggests that the dominant forces are buoyant at depths less than the base of the overriding plate. Apparently, horizontal forces associated with convergence rate and vertical forces associated with age-dependent negative buoyancy of the slab are insufficient to affect DipI, though they can affect both earthquake magnitude and stress in the overriding plate.

A gradual shallowing of DipI is usually but not invariably accompanied by an increase in arc-trench gap. In New Zealand the arc has moved seaward during the Neogene [*Kamp*, 1984]. Similarly, a major Laramide landward migration of volcanism in western North America was followed by a swing back toward the trench [e.g., *Coney and Reynolds*, 1977; *Keith*, 1978]. In both cases, near-horizontal subduction of the portion of the slab deeper than about 80–100 km apparently occurred. Thus the general validity of the DipI and DipD relations may not be invalidated by these observations; the subhorizontal slab could result from the combination of shallow DipI and mantle flow. In New Zealand the shallow DipI presumably resulted primarily from the very wide sedimentary prism, because the subduction was newly established. In contrast, Laramide subduction beneath western North America

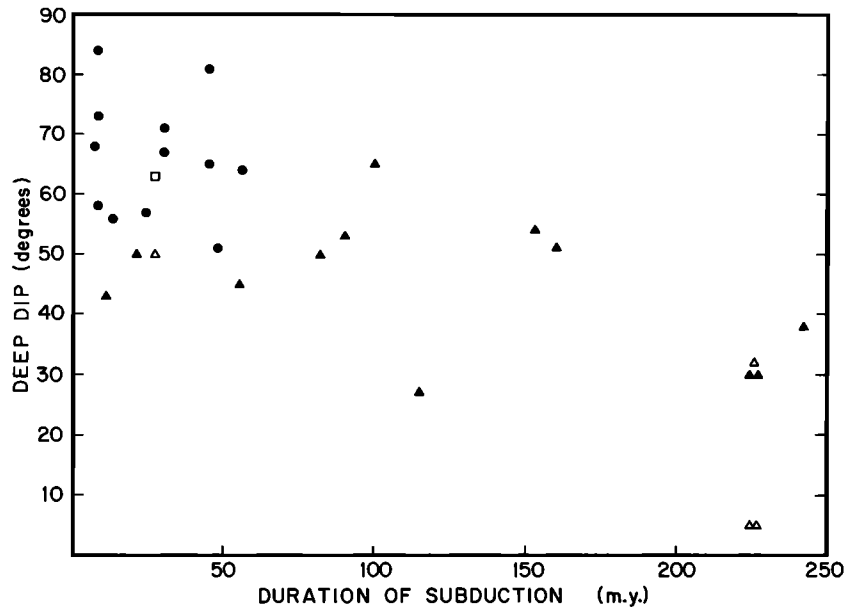

Fig. 24. Cross plot of deep slab dip versus duration of subduction. The crustal type of the overriding plate is indicated by triangles for continental crust, squares for transitional crust, and circles for oceanic crust. Open symbols indicate less reliable data than solid symbols. Subduction zones with continental overriding plates have generally shallower deep dips than those with oceanic overriding plates, probably because they are older.

occurred beneath an old arc with an accretionary prism of unknown width.

The Laramide and New Zealand examples highlight an oversimplification of the model. The 100-km depth selection for DipI does not have a unique physical significance; it is merely a compromise between the 100- to 150-km depth of origin of arc volcanism and the 50- to 100-km thickness of overriding plates. Unfortunately, the thickness of the overriding plate is usually not accurately known. One would expect, however, that the base of the overriding plate is the depth at which accretion and duration of subduction cease controlling dip and mantle flow begins to have an effect. Dip change above the base of the overriding plate may be possible only when the overriding plate is gradually heated or abraded.

The apparent association between paleogeography and both low-angle subduction and segmentation in South America may be speculatively explained by the DipI and DipD models above. Duration of the present period of Andean subduction is constant from Peru to South Chile. However, the variable Paleozoic subduction and structural histories in the four segments may have permitted variations between these segments in amount of late Mesozoic and Cenozoic abrasion of the overriding plates. The result is slight differences in DipI. As *Tovish et al.* [1978] have shown, there may be a critical dip beyond which pressure forces cannot be balanced and near-horizontal subduction occurs. Because of the long duration of subduction (and therefore abrasion) and the landward mantle flow beneath South America, these subduction segments may be near the critical dip. Such speculation is hazardous, however; it must be remembered that the preferred models for dip are neither as quantitative nor as successful as models for some other subduction parameters.

Crust of Overriding Plate

In an examination of DipD for 16 subduction zones, *Furlong et al.* [1982] noted a possible correlation between deep dip and the crustal type in the overriding plate. Slabs beneath continental overriding plates had a mean DipD of 53°, while those beneath oceanic overriding plates had a mean dip of 65°. The mantle down to about 400 km exhibits systematic differences in shear velocity between oceanic and continental lithosphere [*Sipkin and Jordan*, 1980]. *Furlong et al.* [1982] hypothesize that the differences in DipD may indicate that mantle material properties affecting DipD may also differ between suboceanic and subcontinental mantle.

The difference in DipD for slabs beneath continental and oceanic lithosphere is confirmed by the larger number of subduction zones in the present study. Only one subduction zone with a continental overriding plate (Middle America) has a deep dip steeper than 55°; crustal type in the Nicaragua portion of Middle America is not known with certainty. Only one subduction zone with an oceanic overriding plate (Lesser Antilles) has a deep dip shallower than 55°. The median DipD beneath continental overriding plates (40.5°) is much less than the median DipD beneath oceanic overriding plates (66°).

The difference in DipD for slabs beneath continental and oceanic lithosphere does not necessarily imply a difference in sublithospheric mantle properties. Instead, the difference may be an artifact, caused by differences in duration of subduction between continental and oceanic subduction zones. In the preceding section we showed an apparent dependence of DipI on accretion and duration of subduction and dependence of DipD on DipI and mantle flow. Thus DipD also correlates with duration of subduction (Figure 24), though this correlation does not imply a primary causal relationship. Because duration of subduction is greater for nearly all continental overriding plates than for oceanic ones, deep dips are generally shallower beneath continental plates (Figure 24). The excellent correlation between DipD and crustal type in the overriding plate therefore must be treated with caution.

TRENCH DEPTH MODELS

Maximum trench depth is strongly correlated with regional seafloor depth away from the trench [*Grellet and Dubois,*

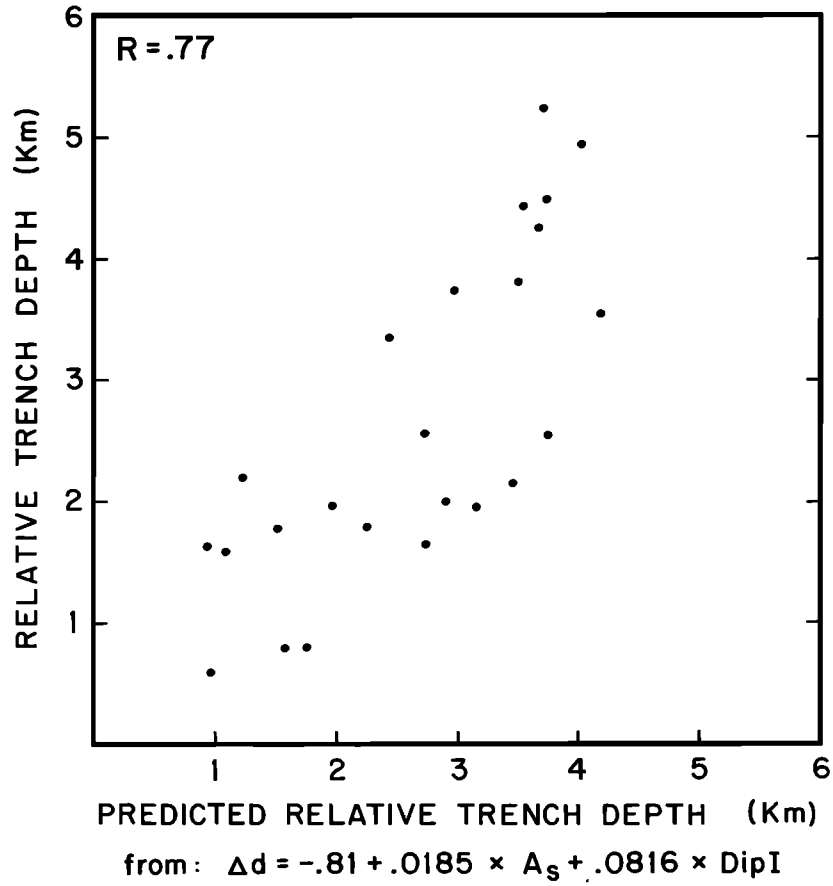

Fig. 25. Comparison of relative trench depths with those predicted from a regression (Table 11) in which the independent variables are slab age and intermediate dip.

1982; *Hilde and Uyeda*, 1983]; this obvious correlation is removed by analyzing only relative depth (Δd), the difference between maximum trench depth and regional crustal depth.

Causes of variations in Δd have only recently been investigated in detail. *Melosh* [1978] and *Grellet and Dubois* [1982] correlated trench depth with convergence rate. *Grellet and Dubois* [1982] found that trench depth changes along 8 of 11 subduction zones showed positive correlations with convergence rate changes, though regression coefficients were quite different for different subduction zones. They also found a correlation between Δd for eight subduction zones and convergence rates. Both *Melosh* [1978] and *Grellet and Dubois* [1982] suggest that this correlation may result from viscous flow in the lower lithosphere of the subducting plate. *Hilde and Uyeda* [1983] suggest an alternative explanation for this correlation: age of the subducting slab affects both Δd and convergence rate. Thus the correlation of Δd with convergence rate is interpreted by them as simply another confirmation of the effect of slab pull on convergence rate [*Forsyth and Uyeda*, 1975; *Carlson et al.*, 1983].

A strong correlation has been found between maximum trench depth and age of the slab at the trench [*Grellet and Dubois*, 1982; *Hilde and Uyeda*, 1983]. *Grellet and Dubois* [1982] fit a curve to all subduction zones analyzed. In contrast, *Hilde and Uyeda* [1983] fit a straight line to half of their subduction zones and consider the other half to be anomalous. Most of these anomalous subduction zones are subducting lithosphere of marginal basins. *Hilde and Uyeda* [1983] suggest that marginal basin subduction may result in anomalously deep trenches because of compensation of nonequilibrated subducted lithosphere within the mantle of these regions.

Statistical analysis of the larger number of subduction zones of Table 1 confirms the correlation of Δd with both slab age ($R = 0.57$) and total subduction rate V_{cba} ($R = 0.45$ for the models of both *Minster and Jordan* [1978] and *Chase* [1978*a*]). Relative trench depth is also moderately correlated with intermediate slab dip ($R = 0.52$). As suggested by *Hilde and Uyeda* [1983], the correlation with subduction rate arises largely or entirely from the correlation between slab age and subduction rate. When the slab age correlation is accounted for by stepwise regression, the residual correlation with V_{cba} is degraded ($R = 0.32$ for the Minster and Jordan model; $R = 0.29$ for the Chase model) while the residual correlation with DipI is improved to 0.61. When both A_s and DipI are then included in the regression, the residual correlation to V_{cba} is insignificant ($R = 0.07$ for the Minster and Jordan model; $R = 0.14$ for the Chase model). Other possible independent variables show no significant contribution to Δd.

Stepwise regression therefore indicates that relative trench depth (Δd) is affected by slab age at the trench and the dip of the interface between overriding and underriding plates (DipI). An increase in either A_s or DipI appears to cause an increase in Δd. The overall correlation coefficient is 0.77 (excluding subduction zones with missing data), indicating that these two independent variables account for 60% of the variance in Δd (Figure 25). *Hilde and Uyeda* [1983] have suggested that sub-

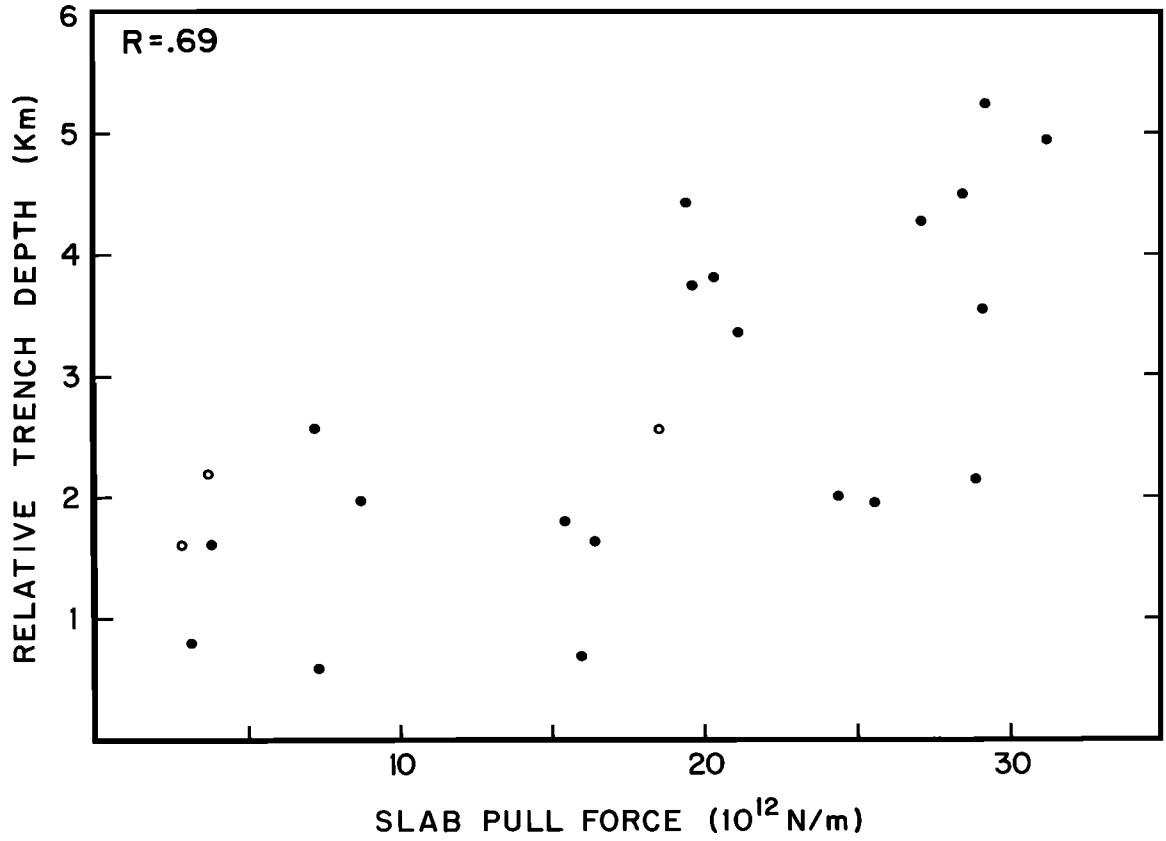

Fig. 26. Comparison of relative trench depth with local slab pull force; the latter is calculated from slab age, convergence rate, and deep dip as described in text. Solid symbols, based on more reliable data than open symbols, are subduction zones used for determination of correlation coefficient.

duction of marginal basin lithosphere is associated with anomalously deep trenches. No such relationship is indicated by Figure 25; nor is it evident in the analysis of *Grellet and Dubois* [1982]. This discrepancy is attributable to variations in crustal ages assumed by different investigators.

The height and wavelength of the outer rise of the subducting plate are well fit by a simple elastic flexural model, particularly when effective age of the lithosphere is considered instead of true age [*McNutt*, 1984]. Effective age, which can be estimated from basement depth, is often less than true age because of lithospheric reheating. Relative trench depth might also be expected to be flexurally controlled. However, the observed positive correlation between Δd and A_s is the opposite of the inverse relationship expected from a simple flexural model. *Hilde and Uyeda* [1983] suggest that this apparent contradiction is explicable in terms of variations between trenches in amount of effective load on the subducting plate. The effective load on the plate includes both the load due to the overriding plate and that due to the slab pull. Only if the effective load is relatively constant in different trenches is an inverse relationship between Δd and slab age expected. If regional variations in slab age cause much larger variations in slab pull force than in flexural rigidity, then a positive correlation between Δd and slab age can result [*Hilde and Uyeda*, 1983].

The slab pull force per unit length of trench segment (F_s) was derived by *Richter and McKenzie* [1978] and modified for a nonvertical dip of the slab by *England and Wortel* [1980]. Following *England and Wortel* [1980] and using their estimates of physical constants,

$$F_S = K_1 S^3 V_{cba} \sin(\text{DipD})[1 - \exp(K_2/S^2 V_{cba} \sin(\text{DipD}))]$$

where V_{cba} is in km/m.y., $K_1 = 2.37 \times 10^6$, $K_2 = -1.74 \times 10^5$, and S is the thickness of the lithosphere, determined from

$$S = 8.19(A_S)^{1/2}$$

for $A_S \leq 70$ m.y., or

$$S = 91.3 - 74.9 \exp(-A_s/62.8)$$

for $A > 70$ m.y. *England and Wortel* [1980] do not include back-arc spreading rate in convergence rate. Because the critical velocity parameter is vertical sinking rate into the mantle, V_{cba} is considered here to be more appropriate than V_c.

Accurate determination of F_S is not possible, due to major uncertainties in many physical parameters required for the determination of K_1 and K_2. Nevertheless, the equations above permit a general estimation of the relative magnitudes of trench pull among different subduction zones. Based on the values of V_{cba}, DipD, and A_S in Table 1, calculated slab pull forces are plotted as a function of Δd in Figure 26. The correlation between the two is better than the correlation between Δd and A_S and similar to the regression of Figure 25. The hypothesis that trench depth is directly correlated with slab pull [*Hilde and Uyeda*, 1983] is therefore consistent with this analysis.

Slab pull force on the portion of underthrusting plate at the trench axis is directed nearly parallel to the slab and therefore subhorizontally. A more relevant force to the effective load on

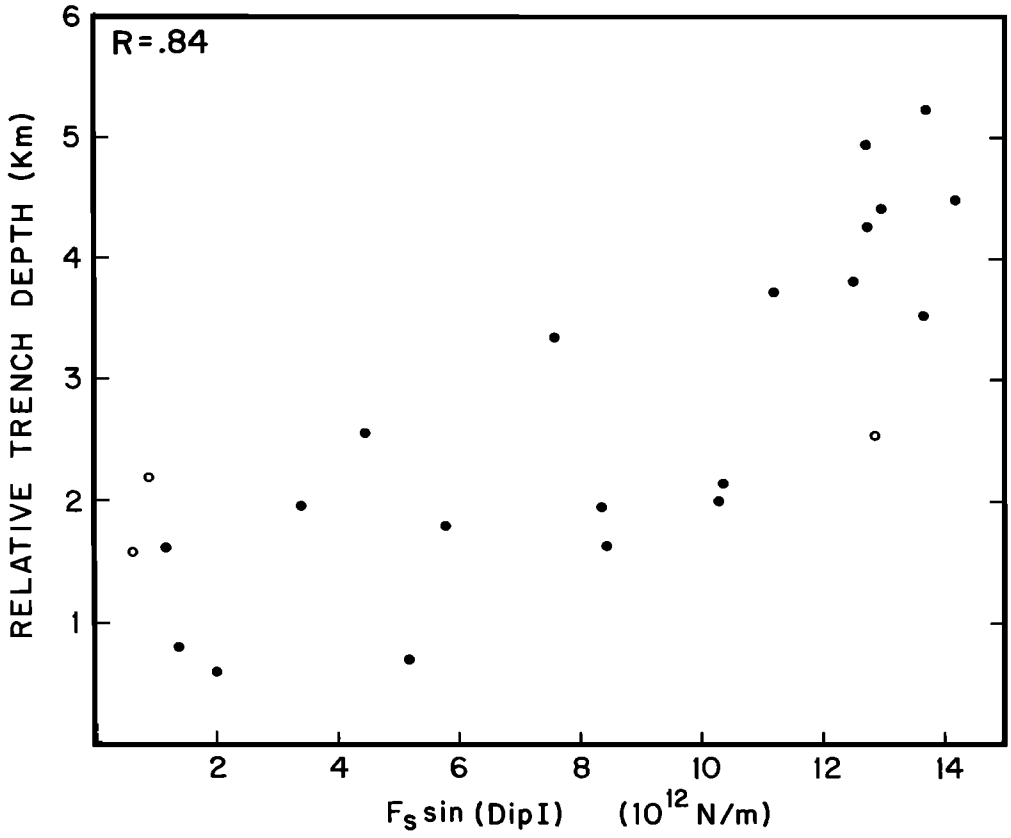

Fig. 27. Comparison of relative trench depth with vertical component of the slab pull force at the interface between plates. The latter is calculated from slab age, convergence rate, deep dip, and intermediate dip as described in text. Solid symbols, based on more reliable data than open symbols, are subduction zones used in regression (Table 11). Note the similarity to Figures 25 and 26 but smaller dispersion than either.

the slab may be the vertical component of slab pull beneath the overriding plate. This vertical force, which is equal to the product of F_S and sin (DipI), is plotted as a function of Δd in Figure 27. The correlation coefficient of 0.84 is substantially better than that for the stepwise regression above. This correlation is considered to be very good, in view of the fact that individual estimates of vertical component of trench pull are subject to the combined uncertainties of physical "constants" and four variables: V_{cba}, A_S, DipI, and DipD.

Although vertical component of trench pull is influenced by V_{cba}, A_S, DipI, and DipD, it is strongly dominated by A_S and DipI. Thus the stepwise regression (Figure 25) and physical model (Figure 27) are consistent. We conclude that relative trench depth is controlled by flexure of the underthrusting plate. Variations in relative trench depth arise primarily from variations in the loading effect of the vertical component of the trench pull force beneath the overriding plate.

For regions with wide accretionary prisms, this loading effect is generally concealed beneath the accretionary prism. In such regions the trench axis is only slightly loaded by accretionary prism; the near-horizontal slab there has negligible vertical component of slab pull. Most of these regions have already been excluded from Table 1 and the analysis above because of the dominating influence of sediments.

CONCLUSIONS

Modern subduction zones constitute a rich data source for the determination of relations among subduction parameters. Based on a detailed review of the literature, 26 parameters (variables) were determined for each of 39 modern subduction zone segments. Not all parameters are known for every subduction zone. Stepwise regression analysis was applied to portions of this data set, in order to determine empirical quantitative equations indicating the most likely cause-and-effect relationships. Table 11 summarizes the final empirical equations which result from this analysis. Published models were tested primarily through regression, but also through a comparison of model-based predictions with the observed variations among subduction zones. This analysis is not meant to substitute for theoretical analyses, but to complement them and perhaps focus them.

A surprising result of this analysis is that most of the dependent variables are accounted for by one or more of only three independent variables: convergence rate (V_c or V_{cba}), slab age (A_s or A_t), and intermediate dip (DipI). Though absolute motions of the overriding and underriding plates were included as potential independent variables in all stepwise regressions, only one possibly significant relationship was found: a correlation of absolute motion with strain regime. Duration of subduction (A_a) only affects one dependent variable, DipI. The dominance of convergence rate, slab age, and DipI has two implications for future research: (1) development of theoretical physical models will be aided by the knowledge that these three independent variables are the primary factors controlling subduction characteristics; and (2) if values for the dependent variables are known for a subduction zone, the independent variables can be estimated by solution of simultaneous equations.

TABLE 11. Preferred Empirical Models

Variable Predicted	Regression Equation	Comment*	F Ratio: Regression	First Variable	Second Variable	Third Variable	R^2	R
Slab length	$L_s = 302.9 + 0.0671 \times V_c \times A_t$	1, 2	156.6	156.6	···	···	0.858	0.926
	$L_s = 396.6 + 0.0669 \times V_c \times A_t - 3.91 \times \text{DipI}$	1, 2	89.8	174.6	4.1	···	0.878	0.937
Earthquake moment	$M_w' = 8.01 - 0.0105 \times A_s + 0.159 \times V_c$		14.5	19.6	17.0	···	0.605	0.778
Strain class	$\text{strain} = 5.19 + 0.464 \times V_c - 0.122 \times \text{DipI} - 0.021 \times A_s$		25.1	34.5	21.9	16.4	0.774	0.880
Intermediate dip	$\text{DipI} = 42.8 - 1.92 \times (A_a)^{1/2}$	3	64.3	64.3	···	···	0.791	0.889
Deep dip	$\text{DipD} = 32.3 + 0.939 \times \text{DipI}$	4	16.8	16.8	···	···	0.412	0.642
Arc-trench gap	$\text{gap} = 51. + 81.4/\tan(\text{DipI})$		147.7	147.7	···	···	0.822	0.907
Trench relative depth	$\Delta d = -0.81 + 0.0185 \times A_s + 0.0816 \times \text{DipI}$		15.4	18.7	13.3	···	0.595	0.772
	$\Delta d = 0.36 + 2.87 \times 10^{-13} \times F_s \times \sin(\text{DipI})$		60.4	60.4	···	···	0.707	0.841

*Comment 1: delete NE Japan. Comment 2: for units consistency within this equation, velocities are in km/m.y.; all other velocities in this table and text are in cm/yr. Comment 3: delete all subduction zones with wide accretionary wedges; also delete Colombia and Middle America. Comment 4: also possible correlation with mantle flow.

An excellent correlation ($R = 0.93$) is found between Benioff zone length and the product of slab age and convergence rate. On the basis of a conductive heating model, *Molnar et al.* [1979] predicted such a correlation; however, the present analysis results in substantial modification of their relationship. Slab heating is much slower during passage beneath the accretionary prism and overriding plate than when the slab is adjacent to deeper mantle. This equation can be used to estimate either slab age or convergence rate, when the other variable and slab length are known. Significant second-order effects on Benioff zone length may result from width of the accretionary prism, trench rollback rate, and slab dip.

Uncertainties in determination of forces acting on both overriding and underriding plates have prevented similarly precise theoretical analyses of strain and strike-slip faulting in the overriding plate, maximum earthquake magnitude, and slab dip. The strain regime of the overriding plate cannot even be accurately quantified. However, one can classify individual subduction zones into one of seven strain classes, along a continuum from strongly extensional (back-arc spreading) to strongly compressional (active folding and thrusting). Stepwise regression indicates that these semiquantitative strain classes can be accounted for with an accuracy of about ± 1 class ($R = 0.88$) by the combined effect of three variables: convergence rate, intermediate slab dip, and either slab age or absolute motion of the overriding plate. Other observations suggest that slab age, not absolute motion, is the third variable. However, data from modern subduction zones cannot unambiguously isolate this third variable.

Convergence rate and slab age affect strain regime through their effect on coupling between plates. This effect is confirmed by a high correlation ($R = 0.78$) of maximum earthquake magnitude with the combination of convergence rate and slab age [*Ruff and Kanamori*, 1980]. The physical mechanism of intermediate dip affecting strain regime is less certain; two possibilities are (1) stress in the overriding plate depends on the contact area between plates, which is proportional to intermediate dip, or (2) intermediate dip affects the asthenospheric return flow and therefore affects shear traction on the base of the overriding plate.

Relative trench depth, the difference between maximum trench depth and depth of the nearby abyssal plain, is strongly affected by slab age and intermediate slab dip. The vertical component of the slab pull force in the vicinity of a trench is dominated by these two variables. This vertical force, in conjunction with the load of the overriding plate, determines the flexural deflection of the underriding plate and thereby the depth of the trench.

Development of empirical equations for the prediction of intermediate and deep slab dip is hampered by limited knowledge of two key variables: width of the accretionary prism and mantle flow patterns. Nevertheless, intermediate dip is clearly strongly dependent on width of the accretionary prism. When subduction zones with moderate to narrow accretionary prisms are analyzed, a dependence of intermediate dip on duration of subduction is found. The correlation coefficient ($R = 0.71$) is degraded by two factors: (1) variable accretion among the subduction zones used and (2) uncertain durations of subduction for many subduction zones. Intermediate dip shallows with increasing duration of subduction, due to abrasion and/or heating of the overriding plate. Arc-trench gap is almost entirely controlled by intermediate dip. Deep slab dip is affected by the mantle trajectory established by intermediate dip ($R = 0.64$), but this trajectory is probably modified by mantle flow patterns. Unfortunately, mantle viscosities are not known with sufficient precision to permit reliable estimation of mantle flow patterns for all subduction zones. Stepwise regression indicates that convergence rate, slab age, and absolute motion of the overriding plate have little or no direct effect on slab dip.

The study of strike-slip faulting in the overriding plate is less amenable to regression analysis. Nevertheless, several physical insights result from a global survey of strike-slip faulting behind subduction zones. The combination of oblique convergence and strong coupling between overriding and underriding plates causes the development of sliver plates, with the forearc separated from the remainder of the overriding plate by a zone of arc-parallel strike-slip faults. Modern offset directions are nearly always consistent with the sense of oblique convergence, and strike-slip faulting is almost exclusively confined to compressive (strain classes 5–7) subduction zones. The location of the strike-slip fault(s) is generally along the arc, which is the portion of the overriding plate that is weakest due to high thermal gradient, thin lithosphere, and

thick crust. Two thirds of modern subduction zones with an overriding plate composed of continental crust exhibit active strike-slip faulting near the arc, while only one fifth of oceanic overriding plates have similar faulting. The much more common occurrence of strike-slip faulting in continental lithosphere than in oceanic lithosphere is a consequence of the greater strength of oceanic lithosphere. Once a strike-slip fault has been established due to oblique convergence, subsequent stress is readily accommodated along this zone of weakness, resulting in dip-slip, reverse faulting, and transpressional or transtensional faulting. Lateral relative motion of a forearc sliver often causes compression and mountain building at the leading edge and crustal extension at the trailing edge.

Though focal mechanisms of shallow underthrusting earthquakes are used in global inversions to determine relative plate motions, they actually reflect motion between the underriding and sliver plate, not between the underriding and major back-arc plate. If the convergence direction between a pair of major plates is reliably known, this direction can be compared to slip vectors, in order to detect the presence of systematic slip vector residuals. These slip vector residuals can then be used to estimate the rates of strike-slip motion of sliver plates: these rates are usually less than 2 cm/yr, but in Sumatra the inferred strike-slip rate is 3.6 ± 0.5 cm/yr. The hypothesized "Bering plate" is an artifact of slip vector residuals resulting from strike-slip faulting in the Aleutians. The hypothesized Southeast Asia plate is real and is moving eastward with respect to Eurasia, based on analysis of slip vectors in the Sunda Trench.

Terrane motions can occur as a response to several distinctive conditions. The type of terrane motion most often considered is transport of an aseismic ridge or continental fragment on oceanic crust, followed by collision and accretion at a subduction zone [e.g., *Nur*, 1983]. This study suggests that two other types of terrane motion are much more common though smaller in rate: (1) strike-slip motion of forearc sliver plates and (2) back-arc spreading and collapse of back-arc basins. Both are expected to be highly variable with time, because of changes in azimuth and rate of convergence and in slab age. The resulting complex mosaic of terranes may include many regions that were formerly continuous but have experienced relative motions of less than 100 km.

The results summarized above justify optimism that three longer-term goals are achievable: (1) a better theoretical understanding of the interrelations between subduction parameters, partially guided by empirical equations, (2) application of the equations to estimate unknown parameters in modern subducton zones, and (3) utilization of geological data from ancient subduction zones (e.g., Tethys) to infer the plate tectonic setting. First, however, we should test the predictive power of the empirical relations on other data.

Acknowledgments. I thank D. M. Davis, D. W. Forsyth, M. A. Hobart, and L. Ruff for their careful and helpful reviews of the manuscript. I also thank the many other persons with whom I discussed individual subduction zones or subduction relations. This research was partially supported by Atlantic Richfield, grant ARCO363401. Lamont-Doherty Geological Observatory contribution 3957.

REFERENCES

Adams, R. D., and D. E. Ware, Subcrustal earthquakes beneath New Zealand; Locations determined with a laterally inhomogeneous velocity model, *N. Z. J. Geol. Geophys.*, *20*, 59–83, 1977.

Ahrens, T. J., and G. Schubert, Gabbro-eclogite reaction rate and its geophysical significance, *Rev. Geophys.*, *13*, 383–400, 1975.

Allen, C. R., Circum-Pacific faulting in the Philippines-Taiwan region, *J. Geophys. Res.*, *67*, 4795–4812, 1962.

Allmendinger, R. W., V. A. Ramos, J. E. Jordan, M. Palma, and B. L. Isacks, Paleogeography and Andean structural geometry, northwest Argentina, *Tectonics*, *2*, 1–16, 1983.

Alvarez, W., D. V. Kent, I. Premoli-Silva, R. A. Schweickert, and R. A. Larson, Franciscan Complex limestone deposited at 17° south paleolatitude, *Geol. Soc. Am. Bull.*, *91*, 476–484, 1980.

Ansell, J. H., and E. G. C. Smith, Detailed structure of a mantle seismic zone using the homogeneous station method, *Nature*, *253*, 518–520, 1975.

Aoki, H., Pressure effects on the deformation of slabs descending below island arcs, *J. Seismol. Soc. Jpn.*, *27*, 110–119, 1974.

Arabasz, W. J., Geological and geophysical studies of the Atacama Fault Zone in northern Chile, Ph.D. thesis, 275 pp., Calif. Inst. of Technol., Pasadena, 1971.

Arthurton, R. S., G. S. Alam, S. Anisuddin-Admad, and S. Iqbal, Geological history of the Alamreg-Mashki Chah area, Chagai District, Baluchistan, in *Geodynamics of Pakistan*, edited by A. Farah and K. A. DeJong, pp. 295–304, Geological Survey of Pakistan, Quetta, 1979.

Atwater, T., and P. Molnar, Relative motion of the Pacific and North American plates deduced from sea-floor spreading in the Atlantic, Indian, and South Pacific oceans, in *Proceedings of the Conference on Tectonic Problems of the San Andreas Fault System*, *Publ. 13*, edited by R. L. Kovach and A. Nur, pp. 136–148, Stanford University Press, Palo Alto, Calif., 1973.

Auden, J. B., Afghanistan-Pakistan, in *Mesozoic-Cenozoic Orogenic Belts*, edited by A. M. Spencer, pp. 235–253, Scottish Academic Press, Edinburgh, 1974.

Avdeiko, G. P., Evolution of geosynclines on Kamchatka, *Pac. Geol.*, *3*, 1–14, 1971.

Ballance, P. F., Evolution of the upper Cenozoic magmatic arc and plate boundary in northern New Zealand, *Earth Planet. Sci. Lett.*, *28*, 356–370, 1976.

Bandy, W. L., and T. W. C. Hilde, Structural features of the Bonin Arc: Implications for its tectonic history, *Tectonophysics*, *99*, 331–353, 1983.

Barazangi, M., and B. L. Isacks, Spatial distribution of earthquakes and subduction of the Nazca plate beneath South America, *Geology*, *4*, 686–692, 1976.

Barazangi, M., and B. L. Isacks, Subduction of the Nazca plate beneath Peru: Evidence from spatial distribution of earthquakes, *Geophys. J. R. Astron. Soc.*, *57*, 537–555, 1979.

Barker, P., A spreading centre in the East Scotia Sea, *Earth Planet. Sci. Lett.*, *15*, 123–132, 1972.

Barker, P., and D. H. Griffiths, The evolution of the Scotia Ridge and Scotia Sea, *Philos. Trans. R. Soc. London, Ser. A*, *271*, 151–183, 1972.

Barker, P., and I. A. Hill, Back-arc extension in the Scotia Sea, *Philos. Trans. R. Soc. London, Ser. A*, *300*, 249–262, 1981.

Beck, M. E., Jr., Paleomagnetic record of plate margin tectonic processes along the western edge of North America, *J. Geophys. Res.*, *85*, 7115–7131, 1980.

Ben-Avraham, Z., and S. Uyeda, Entrapment origin of marginal seas, in *Geodynamics of the Western Pacific–Indonesian Region*, *Geodyn. Ser.*, vol. 11, edited by T. W. C. Hilde and S. Uyeda, pp. 91–104, AGU, Washington, D. C., 1983.

Bevis, M., and B. L. Isacks, Hypocentral trend surface analysis: Probing the geometry of Benioff zones, *J. Geophys. Res.*, *89*, 6153–6170, 1984.

Bibee, L. D., G. G. Shor, and R. S. Lu, Inter-arc spreading in the Mariana Trough, *Mar. Geol.*, *35*, 183–197, 1980.

Biju-Duval, B., et al., Premiers resultats des forages IPOD implatés lors de la croisiére 78A du Glomar Challenger au NE de la ride de la Barbade (arc des Petites Antilles), *C. R. Acad. Sci. Paris*, *293*, 621–628, 1981.

Bloomer, S. H., Distribution and origin of igneous rocks from the landward slopes of the Mariana Trench: Implications for its structure and evolution, *J. Geophys. Res.*, *88*, 7411–7428, 1983.

Bowin, C., G. M. Purdy, C. Johnston, G. G. Shor, L. Lawver, H. M. S. Hartono, and P. Jezek, Arc-continent collision in Banda Sea region, *Am. Assoc. Pet. Geol. Bull.*, *64*, 868–915, 1980.

Bowland, C. L., Seismic stratigraphy and structure of the western Colombian Basin, Caribbean Sea, M.A. thesis, 164 pp., Univ. of Tex., Austin 1984.

Brett, C. P., Seismicity of the South Sandwich Islands region, *Geophys. J. R. Astron. Soc.*, *51*, 453–464, 1977.

Buffler, R. R., R. J. Schaub, J. S. Watkins, and J. L. Worzel, Anatomy of the Mexican ridges, southwestern Gulf of Mexico, Geological

and Geomorphological Investigations of Continental Margins, *Mem. Am. Assoc. Pet. Geol., 29*, 319–328, 1979.
Burbach, G. V., C. Frohlich, W. D. Pennington, and T. Matumoto, Seismicity and tectonics of the subducted Cocos plate, *J. Geophys. Res., 89*, 7719–7735, 1984.
Burke, K., and J. T. Wilson, Is the African plate stationary?, *Nature, 239*, 387–390, 1972.
Burke, K., W. S. F. Kidd, and J. T. Wilson, Relative and latitudinal motion of Atlantic hotspots, *Nature, 245*, 133–137, 1973.
Byrne, T., Late Paleocene demise of the Kula-Pacific spreading center, *Geology, 7*, 341–344, 1979.
Campbell, C. J., Colombian Andes, in *Mesozoic-Cenozoic Orogenic Belts*, edited by A. M. Spencer, pp. 705–724, Scottish Academic Press, Edinburgh, 1974*a*.
Campbell, C. J., Ecuadorian Andes, in *Mesozoic-Cenozoic Orogenic Belts*, edited by A. M. Spencer, pp. 725–732, Scottish Academic Press, Edinburgh, 1974*b*.
Cande, S. C., Nazca–South America plate interactions 80 m.y. B.P. to present (abstract), *Eos Trans. AGU, 64*, 865, 1983.
Cardwell, R. K., and B. L. Isacks, Geometry of the subducted lithosphere beneath the Banda Sea in eastern Indonesia from seismicity and fault plane solutions, *J. Geophys. Res., 87*, 2825–2838, 1978.
Cardwell, R. K., B. L. Isacks, and D. E. Karig, The spatial distribution of earthquakes, focal mechanism solutions, and subducted lithosphere in the Philippine and northeastern Indonesian Islands, in *The Tectonic and Geologic Evolution of Southeast Asian Seas and Islands, Part 1, Geophys. Monogr. Ser.*, vol. 23, edited by D. E. Hayes, pp. 1–35, AGU, Washington, D. C., 1980.
Carlson, R. L., T. W. C. Hilde, and S. Uyeda, The driving mechanism of plate tectonics: Relation to age of the lithosphere at trenches, *Geophys. Res. Lett., 10*, 297–300, 1983.
Carney, J. N., and A. Macfarlane, Geological evidence bearing on the Miocene to Recent structural evolution of the New Hebrides Arc, The Evolution of the India-Pacific Plate Boundaries, *Tectonophysics, 87*, 147–175, 1982.
Carter, R. M., and R. J. Norris, Cainozoic history of southern New Zealand: An accord between geological observations and plate tectonic predictions, *Earth Planet. Sci. Lett., 31*, 85–94, 1976.
Chael, E. P., and G. S. Stewart, Recent large earthquakes along the Middle America Trench and their implications for the subduction process, *J. Geophys. Res., 87*, 329–338, 1982.
Chase, C. G., Plate kinematics: The Americas, East Africa and the rest of the world, *Earth Planet. Sci. Lett., 37*, 355–368, 1978*a*.
Chase, C. G., Extension behind island arcs and motions relative to hot spots, *J. Geophys. Res., 83*, 5385–5387, 1978*b*.
Chase, C. G., and D. R. Sprowl, Proper motion of hotspots: Pacific plate (abstract), *Eos Trans. AGU, 65*, 1099, 1984.
Chinn, D., Accurate source depths and focal mechanisms of shallow earthquakes in western South America and in the New Hebrides Island Arc, Ph.D. thesis, Cornell, Univ., Ithaca, N. Y., 1982.
Choi, D. R., Late Permian–Early Triassic paleogeography of northern Japan: Did Pacific microplates accrete to Japan?, *Geology, 12*, 728–731, 1984.
Chotin, P., A. Giret, J. P. Rampnoux, L. Rasplus, Suminta, and Sumarso, Etude de la fracturation de l'île de Java, Indonésie, *Bull. Soc. Geol. Fr.*, in press, 1985.
Christiansen, R. L., and P. W. Lipman, Cenozoic volcanism and plate-tectonic evolution of the western United States, II, Late Cenozoic, *Philos. Trans. R. Soc. London, Ser. A, 271*, 249–284, 1972.
Christofferson, E., Plate model of the collapsing Caribbean continental margin of Nicaragua and the adjacent San Andres Island Trough, *Caribb. Geol. Conf. Trans. 10th*, 32, 1983.
Clague, D. A., and R. D. Jarrard, Tertiary Pacific plate motion deduced from the Hawaiian-Emperor chain, *Geol. Soc. Am. Bull., 84*, 1135–1154, 1973.
Cole, W. S., R. Todd, and C. G. Johnson, Conflicting age determinations suggested by Foraminifera on Yap, Caroline Islands, *Bull. Am. Paleontol., 41*, 77–112, 1960.
Coleman, P. J., and B. D. Hackman, Solomon Islands, in *Mesozoic-Cenozoic Orogenic Belts*, edited by A. M. Spencer, pp. 453–461, Scottish Academic Press, Edinburgh, 1974.
Coleman, R. G., Tectonic setting for ophiolite obduction in Oman, *J. Geophys. Res., 86*, 2497–2508, 1981.
Coney, P. J., Cordilleran tectonics and North America plate motion, *Am. J. Sci., 272*, 603–628, 1972.
Coney, P. J., and S. J. Reynolds, Cordilleran Benioff zones, *Nature, 270*, 403–406, 1977.
Cormier, V. F., Composite focal mechanism solution of the Near Islands (Aleutian Islands) earthquakes of February 2, 1975 (abstract), *Eos Trans. AGU, 56*, 393, 1975.
Cox, A., and D. C. Engebretson, Change in motion of Pacific plate at 5 Ma (abstract), *Eos Trans. AGU, 65*, 1099, 1984.
Creager, K. C., and T. H. Jordan, Slab penetration into the lower mantle beneath the Mariana island arc (abstract), *Eos Trans. AGU, 66*, 298, 1985.
Cross, T. A., and R. H. Pilger, Jr., Constraints on absolute motion and plate interaction inferred from Cenozoic igneous activity in the western United States, *Am. J. Sci., 278*, 865–902, 1978.
Cross, T. A., and R. H. Pilger, Controls of subduction geometry, location of magmatic arcs, and tectonics of arc and back-arc regions, *Geol. Soc. Am. Bull., 93*, 545–562, 1982.
Crosson, R. S., and J.-W. Lin, A note on the Mt. Rainier earthquake of April 20, 1974, *Bull. Seismol. Soc. Am., 65*, 549–556, 1975.
Csejtey, B., D. P. Cox, R. C. Evarts, G. D. Stricker, and H. L. Foster, The Cenozoic Denali Fault System and the Cretaceous accretionary development of southern Alaska, *J. Geophys. Res., 87*, 3741–3754, 1982.
Curray, J. R., F. J. Emmel, D. G. Moore, and R. W. Raitt, Structure, tectonics and geological history of the northeastern Indian Ocean, in *The Ocean Basins and Margins*, vol. 6, *The Indian Ocean*, edited by A. E. M. Nairn and F. G. Stehli, pp. 399–450, Plenum, New York, 1982.
Dalmayrac, B., and P. Molnar, Parallel thrust and normal faulting in Peru and constraints on the state of stress, *Earth Planet. Sci. Lett., 55*, 473–481, 1981.
Dalrymple, G. B., M. A. Lanphere, and D. A. Clague, Conventional and $^{40}Ar/^{39}Ar$ K-Ar ages of volcanic rocks from Ōjin (site 430), Nintoku (site 432), and Suiko (site 433) seamounts and the chronology of volcanic propagation along the Hawaiian-Emperor chain, *Initial Rep. Deep Sea Drill. Proj., 55*, 659–676, 1980.
Dalziel, I. W. D., Back-arc extension in the southern Andes: A review and critical reappraisal, *Philos. Trans. R. Soc. London, Ser. A, 300*, 319–335, 1981.
Davies, H. L., P. A. Symonds, and I. D. Ripper, Structure and evolution of the southern Solomon Sea region, *BMR J. Aust. Geol. Geophys., 9*, 49–68, 1984.
Davis, D. M., and S. C. Solomon, Variations in the velocities of the major plates since the Late Cretaceous, *Tectonophysics, 79*, 189–208, 1981.
Davis, D. M., J. Suppe, and F. A. Dahlen, Mechanics of fold-and-thrust belts and accretionary wedges, *J. Geophys. Res., 88*, 1153–1172, 1983.
Dean, B. W., and C. L. Drake, Focal mechanism solutions and tectonics of the Middle America Arc, *J. Geol., 86*, 111–128, 1978.
DeFazio, T. L., Island-arc and underthrust-plate geometry, *Tectonophysics, 23*, 149–154, 1974.
Deffeyes, K. S., Plume convection with an upper-mantle temperature inversion, *Nature, 240*, 539–544, 1972.
Dengo, G., and O. Bohnenberger, Structural development of northern Central America, *Mem. Am. Assoc. Pet. Geol., 11*, 203–220, 1969.
Detrick, R. S., and A. B. Watts, An analysis of isostasy in the world's oceans, 3, Aseismic ridges, *J. Geophys. Res., 84*, 3637–3653, 1979.
Dewey, J. F., Episodicity, sequence and style at convergent plate boundaries, The Continental Crust and Its Mineral Deposits, *Spec. Pap. Geol. Assoc. Can., 20*, 553–573, 1980.
Dewey, J. F., and J. M. Bird, Mountain belts and the new global tectonics, *J. Geophys. Res., 75*, 2625–2647, 1970.
Dewey, J. W., and S. T. Algermissen, Seismicity of the Middle America arc-trench system near Managua, Nicaragua, *Bull. Seismol. Soc. Am., 64*, 1033–1048, 1974.
Dickinson, W. R., Evidence for plate-tectonic regimes in the rock record, *Am. J. Sci., 272*, 551–576, 1972.
Dickinson, W. R., Widths of modern arc-trench gaps proportional to past duration of igneous activity in associated magmatic arcs, *J. Geophys. Res., 78*, 3376–3389, 1973.
Dickinson, W. R., and W. S. Snyder, Laramide folding associated with basement block faulting in the western United States, Plate Tectonics of the Laramide Orogeny, *Mem. Geol. Soc. Am., 151*, 355–366, 1978.
Dubois, J., J. Launay, J. Recy, and J. Marshall, New Hebrides Trench: Subduction rate from associated lithospheric bulge, *Can. J. Earth Sci., 14*, 250–255, 1977.
Dubois, J., F. Dugas, A. Lapouille, and R. Louat, The troughs at the rear of the New Hebrides island arc: Possible mechanisms of formation, *Can. J. Earth Sci., 15*, 351–360, 1978.
Duncan, R. A., Hotspots in the southern oceans—An absolute frame

of reference for motion of the Gondwana continents, *Tectonophysics, 74*, 29–42, 1981.
Dykstra, J. D., and R. W. Birnie, Segmentation of the Quaternary subduction zone under the Baluchistan region of Pakistan and Iran, in *Geodynamics of Pakistan*, edited by A. Farah and K. A. DeJong, pp. 319–323, Geological Survey of Pakistan, Quetta, 1979.
Elsasser, W. M., Sea floor spreading as thermal convection, *J. Geophys. Res., 76*, 1101–1112, 1971.
Engdahl, E. R., Seismicity and plate subduction in the central Aleutians, in *Island Arcs, Deep Sea Trenches, and Back-Arc Basins, Maurice Ewing Ser.*, vol. 1, edited by M. Talwani and W. C. Pitman III, pp. 259–271, AGU, Washington, D. C., 1977.
Engdahl, E. R., N. H. Sleep, and M.-T. Lin, Plate effects in north Pacific subduction zones, *Tectonophysics, 37*, 95–116, 1977.
Engebretson, D. C., Relative motions between oceanic and continental plates in the Pacific Basin, Ph.D. thesis, Stanford Univ., Stanford, Calif., 1982.
England, P., and R. Wortel, Some consequences of the subduction of young slabs, *Earth Planet. Sci. Lett., 47*, 403–415, 1980.
Enslein, K., A. Ralston, and H. S. Wilf (Eds.), *Statistical Methods for Digital Computers*, John Wiley, New York, 1977.
Ewart, A., and W. B. Bryan, Petrography and geochemistry of the igneous rocks from Eua, Tongan Islands, *Geol. Soc. Am. Bull., 83*, 3281–3298, 1972.
Farhoudi, G., and D. E. Karig, Makran of Iran and Pakistan as an active arc system, *Geology, 5*, 664–668, 1977.
Farrar, E., and R. M. Lowe, Age-length dependence of inclined seismic zones, *Nature, 273*, 292–293, 1978.
Fisher, M. A., Structure and tectonic setting of the continental shelf southwest of Kodiak Island, Alaska, *Am. Assoc. Pet. Geol. Bull., 63*, 301–310, 1979.
Fitch, T. J., Plate convergence, transcurrent faults, and internal deformation adjacent to Southeast Asia and the western Pacific, *J. Geophys. Res., 77*, 4432–4460, 1972.
Foden, J. D., The petrology of the calcalkaline lavas of Rindjani volcano, East Sunda Arc: A model for island arc petrogenesis, *J. Petrol., 24*, 98–130, 1983.
Forbes, R. B., T. E. Smith, and D. L. Turner, A solution to the Denali Fault offset problem, in *Alaska Division of Geological and Geophysical Survey Annual Report, 1973*, pp. 25–27, College, 1974.
Forsyth, D. W., Fault plane solutions and tectonics of the South Atlantic and Scotia Sea, *J. Geophys. Res., 80*, 1429–1443, 1975.
Forsyth, D. W., and S. Uyeda, On the relative importance of the driving forces of plate motion, *Geophys. J. R. Astron. Soc., 43*, 163–200, 1975.
Forsythe, R., and E. Nelson, Geological manifestations of ridge collision: Evidence from the Golfo de Penas-Taitao Basin, southern Chile, *Tectonics, 4*, 477–495, 1985.
Frank, F. G., Curvature of island arcs, *Nature, 220*, 363, 1968.
Furlong, K. P., D. S. Chapman, and P. W. Alfeld, Thermal modeling of the geometry of subduction with implications for the tectonics of the overriding plate, *J. Geophys. Res., 87*, 1786–1802, 1982.
Gill, J. B., *Orogenic Andesites and Plate Tectonics*, Springer-Verlag, New York, 1981.
Glazner, A. F., and J. A. Supplee, Migration of Tertiary volcanism in the southwestern United States and subduction of the Mendocino fracture zone, *Earth Planet. Sci. Lett., 60*, 429–436, 1982.
Gnibidenko, H. S., and I. I. Khvedchuk, The tectonics of the Okhotsk Sea, *Mar. Geol., 50*, 155–198, 1982.
Grange, F., D. Hatzfeld, P. Cunningham, P. Molnar, S. W. Roecker, G. Suárez, A. Rogrígues, and L. Ocola, Tectonic implications of the microearthquake seismicity and fault plane solutions in southern Peru, *J. Geophys. Res., 89*, 6139–6152, 1984.
Green, T. H., Island arc and continent-building magmatism—A review of petrogenic models based on experimental petrology and geochemistry, *Tectonophysics, 63*, 367–385, 1980.
Grellet, C., and J. Dubois, The depth of trenches as a function of the subduction rate and age of lithosphere, *Tectonophysics, 82*, 45–56, 1982.
Hager, B. H., Slab dip and length and the dynamics of back-arc opening or closing (abstract), *Eos Trans. AGU, 64*, 845–846, 1983.
Hager, B. H., and R. J. O'Connell, Subduction zone dip angles and flow driven by plate motion, *Tectonophysics, 50*, 111–133, 1978.
Hamilton, W., Tectonics of the Indonesian region, *U.S. Geol. Surv. Prof. Pap., 1078*, 345 pp., 1979.
Hammond, P. E., A tectonic model for the evolution of the Cascade Range, *Soc. Econ. Paleontol. Mineral., Pac. Sect., 3*, 219–237, 1979.
Hanus, V., and J. Vanek, Tonga-Lau system: Deep collision of subducted lithospheric plates, *J. Geophys., 44*, 473–480, 1978.
Hasegawa, A., and I. S. Sacks, Subduction of the Nazca plate beneath Peru as determined from seismic observations, *J. Geophys. Res., 86*, 4971–4980, 1980.
Hasegawa, A., N. Umino, and A. Takagi, Double-planed structure of the deep seismic zone in the northeastern Japan Arc, *Tectonophysics, 47*, 43–58, 1978.
Hegarty, K. A., J. K. Weissel, and D. E. Hayes, Convergence at the Caroline-Pacific plate boundary: Collision and subduction, in *The Tectonic and Geologic Evolution of Southeast Asian Seas and Islands, Part 2, Geophys. Monogr. Ser.*, vol. 27, edited by D. E. Hayes, pp. 326–348, AGU, Washington, D. C., 1982.
Herman, B. M., R. N. Anderson, and M. Truchan, Extensional tectonics in the Okinawa Trough, Geological and Geophysical Investigations of Continental Margins, *Mem. Am. Assoc. Pet. Geol., 29*, 199–208, 1979.
Hervé, F., J. Fuenzaleda, E. Araya, and A. Solano, Edades radiometricas y tectonica Neogena en el sector Costero de Chiloe Continental, Xa region, in *Acta II Congreso Geológico Chileno, Aug. 1979*, pp. F1–F18, Arica, Chile, 1979.
Hilde, T. W. C., Sediment subduction versus accretion around the Pacific, *Tectonophysics, 99*, 381–397, 1983.
Hilde, T. W. C., and S. Uyeda, Trench depth: Variation and significance, in *Geodynamics of the Western Pacific–Indonesian Region, Geodyn. Ser.*, vol. 11, edited by T. W. C. Hilde and S. Uyeda, pp. 75–89, AGU, Washington, D. C., 1983.
Hochstein, M. P., J. C. Schofield and G. G. Shor, Jr., Tonga-Kermadec-Lau, in *Mesozoic-Cenozoic Orogenic Belts*, edited by A. M. Spencer, pp. 417–423, Scottish Academic Press, Edinburgh, 1974.
House, L. S., and K. H. Jacob, Earthquakes, plate subduction, and stress reversals in the eastern Aleutian Arc, *J. Geophys. Res., 88*, 9347–9373, 1983.
Huchon, P., and X. Le Pichon, Sunda Strait and Central Sumatra Fault, *Geology, 12*, 668–672, 1984.
Hussong, D. M., and S. Uyeda, Tectonic processes and the history of the Mariana Arc: A synthesis of the results of Deep Sea Drilling leg 60, *Initial Rep. Deep Sea Drill. Proj., 60*, 909–929, 1982.
Hyndman, R. D., Plate motions relative to the deep mantle and the development of subduction zones, *Nature, 238*, 263–265, 1972.
Ichikawa, M., Mechanism of earthquakes in and near Japan, 1950–1962, *Pap. Meteorol. Geophys., 16*, 201–229, 1966.
Ichikawa, M., Some problems in the focal mechanism in and near Japan, *Geophys. Mag., 39*, 1–22, 1980.
IHO/IOC/CHS, GEBCO—General bathymetric chart of the oceans, 5th ed., 74 pp., Int. Hydrogr. Org. of Intergov. Oceanogr. Comm./Can. Hydrogr. Serv., Ottawa, Ont., 1984.
Isacks, B. L., Topography and tectonics of the central Andes (abstract), *Eos Trans. AGU, 66*, 375, 1985.
Isacks, B. L., and M. Barazangi, Geometry of Benioff zones: Lateral segmentation and downwards bending of the subducted lithosphere, in *Island Arcs, Deep Sea Trenches, and Back-Arc Basins, Maurice Ewing Ser.*, vol. 1, edited by M. Talwani and W. C. Pitman III, pp. 99–114, AGU, Washington D. C., 1977.
Isacks, B. L., and P. Molnar, Distribution of stresses in the descending lithosphere from a global survey of focal mechanism solutions of mantle earthquakes, *Rev. Geophys., 9*, 103–174, 1971.
Isacks, B. L., J. Oliver, and L. R. Sykes, Seismology and the new global tectonics, *J. Geophys. Res., 73*, 5855–5899, 1968.
Jachens, R. C., and A. Griscom, Three-dimensional geometry of the Gorda plate beneath northern California, *J. Geophys. Res., 88*, 9375–9392, 1983.
Jacob, K. H., and R. L. Quittmeyer, The Makran region of Pakistan and Iran: Trench-arc system with active plate subduction, in *Geodynamics of Pakistan*, edited by A. Farah and K. A. DeJong, pp. 305–317, Geological Survey of Pakistan, Quetta, 1979.
Jacob, K. H., K. Nakamura, and J. N. Davies, Trench-volcano gap along the Alaska-Aleutian Arc: Facts and speculations on the role of terrigenous sediments for subduction, in *Island Arcs, Deep Sea Trenches, and Back-Arc Basins, Maurice Ewing Ser.*, vol. 1, edited by M. Talwani and W. C. Pitman III, pp. 243–258, AGU, Washington, D. C., 1977.
James, D. E., Plate tectonic model for the evolution of the central Andes, *Geol. Soc. Am. Bull., 82*, 3325–3346, 1971.
Jarrard, R. D., Prediction of continental structural style from plate tectonic parameters (abstract), *Eos Trans. AGU, 65*, 1095, 1984.

Jarrard, R. D., and S. Sasajima, Paleomagnetic synthesis for Southeast Asia: Constraints on plate motions, in *The Tectonic and Geologic Evolution of Southeast Asian Seas and Islands, Part 1, Geophys. Monogr. Ser.*, vol. 23, edited by D. E. Hayes, pp. 293–316, AGU, Washington, D. C., 1980.

Jischke, M. C., On the dynamics of descending lithospheric plates and slip zones, *J. Geophys. Res., 80*, 4809–4813, 1975.

Jordan, T. E., B. L. Isacks, R. W. Allmendinger, J. A. Brewer, V. A. Ramos, and C. J. Ando, Andean tectonics related to the geometry of subducted Nazca plate, *Geol Soc. Am. Bull., 94*, 341–361, 1983.

Jordan, T. H., The present-day motions of the Caribbean plate, *J. Geophys. Res., 80*, 4433–4439, 1975.

Jung, D., M. O. C. Kursten, and M. Tarkin, Post-Mesozoic volcanism in Iran and its relation to the subduction of the Afro-Arabian under the Eurasian plate, in *Afar Between Continental and Oceanic Rifting*, edited by A. Pilger and A. Rosler, pp. 173–181, E. Schweizerbartsche, Stuttgart, Federal Republic of Germany, 1976.

Jurdy, D. M., Relative plate motions and the formation of marginal basins, *J. Geophys. Res., 84*, 6796–6802, 1979.

Jurdy, D. M., and M. Stefanick, Flow models for back-arc spreading, Convergence and Subduction, *Tectonophysics, 99*, 191–206, 1983.

Kaizuka, S., A tectonic model for the morphology of arc-trench systems, especially for the echelon ridge and mid-arc faults, *Jpn. J. Geol. Geogr., 45*, 9–28, 1975.

Kamp, P. J. J., Neogene and Quaternary extent and geometry of the subducted Pacific plate beneath North Island, New Zealand: Implications for Kaikoura tectonics, *Tectonophysics, 108*, 241–266, 1984.

Kanamori, H., Tectonic implications of the 1944 Tonankai and the 1946 Nankaido earthquakes, *Phys. Earth Planet. Inter., 5*, 129–139, 1972.

Kappel, E. S., Plate convergence in the Sunda and Banda arcs, B.A. thesis, Cornell Univ., Ithaca, N. Y., 1980.

Karig, D. E., Origin and development of marginal basins in the western Pacific, *J. Geophys. Res., 76*, 2542–2561, 1971.

Karig, D. E., Plate convergence between the Philippines and the Ryukyu Islands, *Mar. Geol., 14*, 153–168, 1973.

Karig, D. E., Basin genesis in the Philippine Sea, *Initial Rep. Deep Sea Drill. Proj., 31*, 857–879, 1975.

Karig, D. E., and J. Mammerickx, Tectonic framework of the New Hebrides island arc, *Mar. Geol., 12*, 187–205, 1972.

Karig, D. E., and G. F. Moore, Tectonic complexities in the Bonin Arc system, *Tectonophysics, 27*, 97–118, 1975.

Karig, D. E., and G. F. Sharman III, Subduction and accretion in trenches, *Geol. Soc. Am. Bull., 86*, 377–389, 1975.

Karig, D. E., et al., *Initial Reports of the Deep Sea Drilling Project*, vol. 31, 927 pp., U.S. Government Printing Office, Washington, D. C., 1975.

Karig, D. E., J. G. Caldwell, and E. M. Parmentier, Effects of accretion on the geometry of the descending lithosphere, *J. Geophys. Res., 81*, 6281–6291, 1976.

Karig, D. E., M. B. Lawrence, G. F. Moore, and J. R. Curray, Structural framework for the fore-arc basin, NW Sumatra, *J. Geol. Soc. London, 137*, 1–15, 1980.

Katili, J. A., Large transcurrent faults in Southeast Asia with special reference to Indonesia, *Geol. Rundsch., 59*, 581–600, 1970.

Katili, J. A., On fitting certain geological and geophysical features of the Indonesian island arc to the new global tectonics, in *The Western Pacific, Island Arcs, Marginal Seas, Geochemistry*, edited by P. J. Coleman, pp. 287–305, Crane, Russak, New York, 1973.

Katili, J. A., Sumatra, in *Mesozoic-Cenozoic Orogenic Belts*, edited by A. M. Spencer, pp. 317–331, Scottish Academic Press, Edinburgh, 1974.

Katili, J. A., and F. Hehuwat, On the occurrence of large transcurrent faults in Sumatra, Indonesia, *J. Geosci. Osaka City Univ., 10*, 1–17, 1967.

Katsumata, M., and L. R. Sykes, Seismicity and tectonics of the western Pacific: Izu-Mariana-Caroline and Ryukyu-Taiwan regions, *J. Geophys. Res., 74*, 5923–5948, 1969.

Katz, H. R., Plate margin transition from oceanic arc-trench to continental system: The Kermadec–New Zealand example, The Evolution of the India-Pacific Plate Boundaries, *Tectonophysics, 87*, 49–64, 1982.

Kaula, W. M., Absolute plate motions by boundary velocity minimization, *J. Geophys. Res., 80*, 244–248, 1975.

Kawano, Y., and Y. Ueda, Periods of the igneous activities of the granitic rocks in Japan by K/Ar dating method, *Tectonophysics, 4*, 523–530, 1967.

Kazmi, A. H., Active fault systems in Pakistan, in *Geodynamics of Pakistan*, edited by A. Farah and K. A. DeJong, pp. 285–294, Geological Survey of Pakistan, Quetta, 1979.

Keith, S. B., Paleosubduction geometries inferred from Cretaceous and Tertiary magmatic patterns in southwestern North America, *Geology, 6*, 516–521, 1978.

Keith, S. B., Paleoconvergence rates determined from K_2O/SiO_2 ratios in magmatic rocks and their application to Cretaceous and Tertiary tectonic patterns in southwestern North America, *Geol. Soc. Am. Bull., 93*, 524–532, 1982.

Kelleher, J., and W. McCann, Buoyant zones, great earthquakes, and unstable boundaries of subduction, *J. Geophys. Res., 81*, 4885–4896, 1976.

Klitgord, K. D., and J. Mammerickx, Northern East Pacific Rise: Magnetic anomaly and bathymetric framework, *J. Geophys. Res., 87*, 6725–6750, 1982.

Kobayashi, K., and N. Isezaki, Magnetic anomalies in the Sea of Japan and the Shikoku Basin: Possible tectonic implications, in *The Geophysics of the Pacific Ocean Basin and Its Margin, Geophys. Monogr. Ser.*, vol. 19, edited by G. H. Sutton, M. H. Manghnani, and R. Moberly, pp. 235–251, AGU, Washington, D. C., 1976.

Kroenke, L. W., and R. Scott, Old questions answered—And new ones asked, *Geotimes, 23*(7), 20–23, 1978.

Lahr, J., Detailed seismic investigation of Pacific–North America plate interaction in southern Alaska, Ph.D. thesis, 141 pp., Columbia Univ., New York, 1975.

Laravie, J. A., Geometry and lateral strain of subducted plates in island arcs, *Geology, 3*, 484–486, 1975.

Larson, R. L., W. C. Pitman III, X. Golovchenko, S. C. Cande, J. F. Dewey, W. F. Haxby, and J. L. LaBrecque, *The Bedrock Geology of the World*, W. H. Freeman, New York, 1985.

Lathram, E. H., Aleutian Arc, in *Mesozoic-Cenozoic Orogenic Belts*, edited by A. M. Spencer, pp. 553–561, Scottish Academic Press, Edinburgh, 1974.

Lathram, E. H., A. Grantz, D. F. Barnes, D. A. Brew, A. T. Ovenshine, G. Plafker, R. L. Detterman, H. L. Foster, M. Churkin, Jr., W. W. Patton, Jr., J. M. Hoare, I. L. Tailleur, W. P. Brosgé, T. P. Miller, and C. L. Sainsbury, Alaska, in *Mesozoic-Cenozoic Orogenic Belts*, edited by A. M. Spencer, pp. 563–589, Scottish Academic Press, Edinburgh, 1974.

Lawver, L. A., and J. R. Curray, Evolution of the Andaman Sea (abstract) *Eos Trans. AGU, 62*, 1044, 1981.

Lee, C. S., G. Shor, L. D. Bibee, R. S. Lu, and T. W. C. Hilde, Okinawa Trough: Origin of a back-arc basin, *Mar. Geol., 35*, 219–241, 1980.

Le Pichon, X., Seafloor spreading and continental drift, *J. Geophys. Res., 73*, 3661–3697, 1968.

Le Pichon, X., and J. Angelier, The Aegean Sea, *Philos. Trans. R. Soc. London, Ser. A, 300*, 357–372, 1981.

Letouzey, J., and M. Kimura, Okinawa Trough genesis: Structure and evolution of a backarc basin developed in a continent, *Mar. Pet. Geol.*, in press, 1985.

Lipman, P. W., H. J. Prostka, and R. L. Christiansen, Cenozoic volcanism and plate-tectonic evolution of the western United States, I, Early and middle Cenozoic, *Philos. Trans. R. Soc. London, Ser. A, 271*, 217–248, 1972.

Lliboutry, L., Plate movement relative to rigid lower mantle, *Nature, 250*, 298–300, 1974.

Lohmann, H. H., Outline of tectonic history of Bolivian Andes, *Am. Assoc. Pet. Geol. Bull., 54*, 735–757, 1970.

Luhr, J. F., S. A. Nelson, J. F. Allan, and I. S. E. Carmichael, Active rifting in southwestern Mexico: Manifestations of an incipient eastward spreading-ridge jump, *Geology, 13*, 54–57, 1985.

Luyendyk, B. P., Dips of downgoing lithospheric plates beneath island arcs, *Geol. Soc. Am. Bull., 81*, 3411–3416, 1970.

Maki, T., Spatial variation of earthquake-generating stress in and around the Kanto District, central Japan, *Bull. Earthquake Res. Inst. Univ. Tokyo, 58*, 591–646, 1983.

Malahoff, A., R. H. Feden, and H. S. Fleming, Magnetic anomalies and tectonic fabric of marginal basins north of New Zealand, *J. Geophys. Res., 87*, 4109–4125, 1982.

Malfait, B. T., and M. G. Dinkelman, Circum-Caribbean tectonic and igneous activity and the evolution of the Caribbean plate, *Geol. Soc. Am. Bull., 83*, 251–272, 1972.

Malumián, N., and V. A. Ramos, Magmatic intervals, transgression-regression cycles and oceanic events in the Cretaceous and Tertiary

of southern South America, *Earth Planet. Sci. Lett.*, *67*, 228–237, 1984.

Markhinin, E. K., Volcanism as an agent of formation of the earth's crust, in *The Crust and Upper Mantle of the Pacific Area, Geophys. Monogr. Ser.*, vol. 12, edited by L. Knopoff, edited by L. Knopoff, C. L. Drake, and P. J. Hart, pp. 412–423, AGU, Washington, D. C., 1968.

Martin, S., A review of oil exploration and stratigraphy of sedimentary basins of the Philippines, *CCOP Tech. Bull.*, *10*, 55–102, 1976.

Maruyama, S., S. Banno, T. Matsuda, and T. Nakajima, Kurosegawa zone and its bearing on the development of the Japanese Islands, *Tectonophysics*, *110*, 47–60, 1984.

Matsuda, T., and N. Kitamura, Northeast Japan, In *Mesozoic-Cenozoic Orogenic Belts*, edited by A. M. Spencer, pp. 543–552, Scottish Academic Press, Edinburgh, 1974.

Matsuda, T., K. Nakamura, and A. Sugimura, Late Cenozoic orogeny in Japan, *Tectonophysics*, *4*, 349–366, 1966.

Matsumoto, T., and T. Kimura, Southwest Japan, in *Mesozoic-Cenozoic Orogenic Belts*, edited by A. M. Spencer, pp. 513–541, Scottish Academic Press, Edinburgh, 1974.

Mattson, P. H., Mesozoic and Tertiary lithosphere plate interactions in the northern Caribbean, *Trans. Caribb. Geol. Conf.*, *7*, 79–85, 1976.

Mattson, P. H., Subduction, buoyant breaking, flipping, and strike-slip faulting in the northern Caribbean, *J. Geol.*, *87*, 293–304, 1979.

McBirney, A. R., and H. Williams, Volcanic history of Nicaragua, *Univ. Calif. Berkeley Publ. Geol. Sci.*, *55*, 73 pp., 1965.

McCann, W. R., and L. R. Sykes, Subduction of aseismic ridges beneath the Caribbean plate: Implications for the tectonics and seismic potential of the northeast Caribbean, *J. Geophys. Res.*, *89*, 4493–4519, 1984.

McGetchin, T. R., K. C. Burke, G. A. Thompson, and R. A. Young, Mode and mechanism of plateau uplifts, in *Dynamics of Plate Interiors, Geodyn. Ser.*, vol. 1, edited by A. W. Bally, P. L. Bender, T. R. McGetchin, and R. I. Walcott, pp. 99–110, AGU, 1980.

McKenzie, D. P., Speculations on the consequences and causes of plate motions, *Geophys. J. R. Astron. Soc.*, *18*, 1–32, 1969.

McKenzie, D. P., Active tectonics of the Alpine-Himalayan belt: The Aegean Sea and surrounding regions, *Geophys. J. R. Astron. Soc.*, *55*, 217–254, 1978.

McNutt, M. K., Lithospheric flexure and thermal anomalies, *J. Geophys. Res.*, *89*, 11,180–11,194, 1984.

Megard, F., and H. Philip, Plio-Quaternary tectono-magmatic zonation and plate tectonics in the central Andes, *Earth Planet. Sci. Lett.*, *33*, 231–238, 1976.

Melosh, H. L., Dynamic support of the outer rise, *Geophys. Res. Lett.*, *5*, 321–324, 1978.

Mercier, J. L., Extensional-compressional tectonics associated with the Aegean Arc: Comparison with the Andean Cordillera of south Peru–north Bolivia, *Philos. Trans. R. Soc. London, Ser. A*, *300*, 337–355, 1981.

Minster, J. B., and T. H. Jordan, Present-day plate motions, *J. Geophys. Res.*, *83*, 5331–5354, 1978.

Minster, J. B., T. H. Jordan, P. Molnar, and E. Haines, Numerical modelling of instantaneous plate tectonics, *Geophys. J. R. Astron. Soc.*, *36*, 541–576, 1974.

Mizoue, M., T. Yokota, and I. Nakamura, High angle reverse faultings in the interaxial zone of active folds in the inner belt of northeast Japan, *Bull. Earthquake Res. Inst. Univ. Tokyo*, *57*, 359–377, 1982.

Moberly, R., Origin of lithosphere behind island arcs, with reference to the western Pacific, Studies in Earth and Space Sciences, *Mem. Geol. Soc. Am.*, *132*, 35–56, 1972.

Molnar, P., and T. Atwater, Relative motion of hot spots in the mantle, *Nature*, *246*, 288–291, 1973.

Molnar, P., and T. Atwater, Interarc spreading and Cordilleran tectonics as alternates related to the age of subducted oceanic lithosphere, *Earth Planet. Sci. Lett.*, *41*, 330–340, 1978.

Molnar, P., and J. Francheteau, The relative motion of "hot spots" in the Atlantic and Indian oceans during the Cenozoic, *Geophys. J. R. Astron. Soc.*, *43*, 763–774, 1975.

Molnar, P., and L. R. Sykes, Tectonics of the Caribbean and middle America regions from focal mechanisms and seismicity, *Geol. Soc. Am. Bull.*, *80*, 1639–1684, 1969.

Molnar, P., and P. Tapponnier, Cenozoic tectonics of Asia—Effects of a continental collision, *Science*, *189*, 419–426, 1975.

Molnar, P., D. Freedman, and J. Shih, Lengths of intermediate and deep seismic zones and temperatures in downgoing slabs of lithosphere, *Geophys. J. R. Astron. Soc.*, *56*, 41–54, 1979.

Morgan, W. J., Plate motions and deep mantle convection, Studies in Earth and Space Sciences, *Mem. Geol. Soc. Am.*, *132*, 7–22, 1972.

Morgan, W. J., Hotspot tracks and the opening of the Atlantic and Indian oceans, in *The Sea*, vol. 7, pp. 443–487, edited by C. Emiliani, John Wiley, New York, 1980.

Mrozowski, C. L., and D. E. Hayes, The evolution of the Parece Vela Basin, eastern Philippine Sea, *Earth Planet. Sci. Lett.*, *46*, 49–67, 1979.

Mrozowski, C. L., S. D. Lewis, and D. E. Hayes, Complexities in the tectonic evolution of the West Philippine Basin, *Tectonophysics*, *82*, 1–24, 1982.

Mukhopadhyay, M., Seismotectonics of subduction and back-arc rifting under the Andaman Sea, *Tectonophysics*, *108*, 229–239, 1984.

Nakamura, K., Volcanoes as possible indicators of tectonic stress orientation—Principle and proposal, *J. Volcanol. Geotherm. Res.*, *2*, 1–16, 1977.

Nakamura, K., and S. Uyeda, Stress gradient in arc and backarc regions and plate subduction, *J. Geophys. Res.*, *85*, 6419–6428, 1980.

Nakamura, K., G. Plafker, K. H. Jacob, and J. N. Davies, A tectonic stress trajectory map of Alaska using information from volcanoes and faults, *Bull. Earthquake Res. Inst. Univ. Tokyo*, *55*, 89–100, 1980.

Ness, G., and S. Johnson, Subduction geometry of the Nazca–South American convergence (abstract), *Eos Trans. AGU*, *57*, 334, 1976.

Norris, R. J., and R. M. Carter, Fault-bounded blocks and their role in localizing sedimentation and deformation adjacent to the Alpine Fault, southern New Zealand, The Evolution of the India-Pacific Plate Boundaries, *Tectonophysics*, *87*, 11–23, 1982.

Nozawa, T., Radiometric ages of granitic rocks in outer zone of southwest Japan and its extension: 1968 summary and north-shift hypothesis of igneous activity, *J. Geol. Soc. Jpn.*, *74*, 485–489, 1968.

Nur, A., Accreted terranes, *Rev. Geophys.*, *21*, 1779–1785, 1983.

Okada, A., Active faulting of the median tectonic line (in Japanese), *Kagaku Tokyo*, *41*, 666–669, 1971.

Okayama, T., The relations between the geomorphic and geologic structure of the Japanese Islands, in *Geographical Papers in Commemoration of Professor T. Tsujimura's 70th Birthday*, pp. 50–67, 1961.

Ozima, M., I. Kaneoka, and H. Ujiie, ^{40}Ar-^{39}Ar age of rocks, and the development mode of the Philippine Sea, *Nature*, *267*, 816–818, 1977.

Packham, G. H., and D. A. Falvey, An hypothesis for the formation of marginal seas in the western Pacific, *Tectonophysics*, *11*, 79–109, 1971.

Page, B. G. N., J. D. Bennett, N. R. Cameron, D. M. Bridge, D. H. Jeffery, W. Keats, and J. Thaib, A review of the main structural and magmatic features of northern Sumatra, *J. Geol. Soc. London*, *136*, 569–579, 1979.

Page, R. W., and R. J. Ryburn, K-Ar ages and geological relations of intrusive rocks in New Britain, *Pac. Geol.*, *12*, 99–105, 1977.

Pallister, J. S., Structure of the sheeted dike complex of the Samail ophiolite near Ibra, Oman, *J. Geophys. Res.*, *86*, 2661–2672, 1981.

Paquin, C., J. Bloyet, and C. Angelidis, Tectonic stresses on the boundary of the Aegean domain: "In situ" measurements by overcoring, *Tectonophysics*, *110*, 145–150, 1984.

Parrish, R. R., Cenozoic thermal evolution and tectonics of the Coast Mountains of British Columbia, 1, Fission track dating, apparent uplift rates, and patterns of uplift, *Tectonics*, *2*, 601–631, 1983.

Pascal, G., Seismotectonics of the Papua New Guinea–Solomon Islands region, *Tectonophysics*, *57*, 7–34, 1979.

Pennington, W., Subduction of the eastern Panama Basin and seismotectonics of northwestern South America, *J. Geophys. Res.*, *86*, 10,753–10,770, 1981.

Philip, H., and F. Megard, Structural analysis of the superficial deformation of the 1969 Pariahuanca earthquakes (central Peru), *Tectonophysics*, *38*, 259–278, 1977.

Pilger, R. H., Jr., Plate reconstructions, aseismic ridges, and low-angle subduction beneath the Andes, *Geol. Soc. Am. Bull., Part I*, *92*, 448–456, 1981.

Quittmeyer, R. C., A. Farah, and K. H. Jacob, The seismicity of Pakistan and its relation to surface faults, in *Geodynamics of Pakistan*, edited by A. Farah and K. A. DeJong, pp. 271–284, Geological Survey of Pakistan, Quetta, 1979.

Reed, B. L., and M. A. Lanphere, Age and chemistry of Mesozoic and Tertiary plutonic rocks in south-central Alaska, *Geol. Soc. Am. Bull.*, *80*, 23–43, 1969.

Reed, B. L., and M. A. Lanphere, Offset plutons and history of movement along the McKinley segment of the Denali Fault System, Alaska, *Geol. Soc. Am. Bull.*, *85*, 1883–1892, 1974.

Richardson, R. M., S. C. Solomon, and N. H. Sleep, Tectonic stress in the plates, *Rev. Geophys.*, *17*, 981–1019, 1979.

Richter, F. M., and D. P. McKenzie, Simple plate models of mantle convection, *J. Geophys.*, *44*, 441–471, 1978.

Richter, I., and K. Strobach, Benioff zones of the Aegean Arc, in *Alps, Apennines, Hellenides*, edited by H. Closs, D. Roeder, and K. Schmidt, pp. 410–414, E. Schweizerbartsche Verlagsbuchhandlung, Stuttgart, Federal Republic of Germany, 1978.

Ripper, I. D., Seismicity of the Indo-Australian/Solomon Sea plate boundary in the southeast Papua region, The Evolution of India-Pacific Plate Boundaries, *Tectonophysics*, *87*, 355–369, 1982.

Roeder, D. H., Tectonic effects of dip changes in subduction zones, *Am. J. Sci.*, *275*, 252–264, 1975.

Ruff, L., and H. Kanamori, Seismicity and the subduction process, *Phys. Earth Planet. Inter.*, *23*, 240–252, 1980.

Rutland, R. W. R., Andes: Antofagasta segment (20°–25°S), in *Mesozoic-Cenozoic Orogenic Belts*, edited by A. M. Spencer, pp. 733–743, Scottish Academic Press, Edinburgh, 1974.

Sacks, I. S., The subduction of young lithosphere, *J. Geophys. Res.*, *88*, 3355–3366, 1983.

Scholl, D., E. Buffington, and M. Marlow, Plate tectonics and the structural evolution of the Aleutian–Bering Sea region, *Spec. Pap. Geol. Soc. Am.*, *151*, 1–31, 1975.

Sebrier, M., D. Huaman, J. L. Blanc, J. Machare, D. Bonnot, and J. Cabrera, Observaciones acerca de la neotectonica del Peru, Contrib. IGP-LGDI, Inst. Geophys. del Peru, Lima, 1982.

Seno, T., The instantaneous rotation vector of the Philippine Sea plate relative to the Eurasian plate, *Tectonophysics*, *42*, 209–226, 1977.

Shepherd, G. L., and R. Moberly, Coastal structure of the continental margin, northwest Peru and southwest Ecuador, Nazca Plate: Crustal Formation and Andean Convergence, *Mem. Geol. Soc. Am.*, *154*, 351–391, 1981.

Shih, T.-C., Marine magnetic anomalies from the western Philippine Sea: Implications for the evolution of marginal basins, in *The Tectonic and Geologic Evolution of Southeast Asian Seas and Islands, Part 1, Geophys. Monogr. Ser.*, vol. 23, edited by D. E. Hayes, pp. 49–76, AGU, Washington, D. C., 1980.

Silver, E. A., and J. C. Moore, The Molucca Sea collision zone, Indonesia, *J. Geophys. Res.*, *83*, 1681–1691, 1978.

Silver, E. A., R. McCaffrey, and R. B. Smith, Collision, rotation, and the initiation of subduction in the evolution of Sulawesi, Indonesia, *J. Geophys. Res.*, *88*, 9407–9418, 1983*a*.

Silver, E. A., D. Reed, R. McCaffrey, and Y. Joyodiwiryo, Back arc thrusting in the eastern Sunda Arc, Indonesia: A consequence of arc-continent collision, *J. Geophys. Res.*, *88*, 7429–7448, 1983*b*.

Sipkin, S. A., and J. H. Jordan, Multiple *ScS* travel times in the western Pacific: Implications for mantle heterogeneity, *J. Geophys. Res.*, *85*, 853–861, 1980.

Skewes, M. A., and C. R. Stern, Petrology and geochemistry of alkali basalts and ultramafic inclusions from the Palei-Aike volcanic field in southern Chile and the origin of the Patagonian plateau lavas, *J. Volcanol. Geotherm. Res.*, *6*, 3–25, 1979.

Smith, A. G., Plate tectonics and orogeny: A review, *Tectonophysics*, *33*, 215–285, 1976.

Smith, E. G. C., and F. J. Davey, Joint hypocentre determination of intermediate depth earthquakes in Fiordland, New Zealand, *Tectonophysics*, *104*, 127–144, 1984.

Smith, S. W., and J. S. Knapp, The northern termination of the San Andreas Fault, Studies of the Sea Andreas Fault Zone in Northern California, *Spec. Rep. Calif. Div. Mines Geol.*, *140*, 153–164, 1980.

Solomon, S. C., and N. H. Sleep, Some simple physical models for absolute plate motions, *J. Geophys. Res.*, *79*, 2557–2567, 1974.

St. Amand, P., and C. R. Allen, Strike-slip faulting in northern Chile, *Geol. Soc. Am. Bull.*, *71*, 1965, 1960.

Stauder, W., Subduction of the Nazca plate under Peru as evidenced by focal mechanisms and by seismicity, *J. Geophys. Res.*, *80*, 1053–1064, 1975.

Stauder, W., and L. Mualchin, Fault motion in the larger earthquakes of the Kurile-Kamchatka Arc and of the Kurile-Hokkaido corner, *J. Geophys. Res.*, *81*, 297–308, 1976.

Stein, S., and R. G. Gordon, Statistical tests of additional plate boundaries from plate motion inversions, *Earth Planet. Sci. Lett.*, *69*, 401–412, 1984.

Stephens, C. D., K. A. Fogleman, J. C. Lahr, and R. A. Page, Wrangell Benioff zone, southern Alaska, *Geology*, *12*, 373–376, 1984.

Stern, T. A., A back-arc basin formed within continental lithosphere: The central volcanic region of New Zealand, Structures and Processes in Subduction Zones, *Tectonophysics*, *112*, 385–409, 1985.

Stoiber, R. E., and M. J. Carr, Quaternary volcanic and tectonic segmentation of Central America, *Bull. Volcanol.*, *37*, 304–325, 1973.

Stone, D. B., B. C. Panuska, and D. R. Packer, Paleolatitudes versus time for southern Alaska, *J. Geophys. Res.*, *87*, 3697–3707, 1982.

Suárez, G., P. Molnar, and B. C. Burchfiel, Seismicity, fault plane solutions, depth of faulting, and active tectonics of the Andes of Peru, Ecuador, and southern Colombia, *J. Geophys. Res.*, *88*, 10,403–10,428, 1983.

Sugi, N., and S. Uyeda, Subduction of young oceanic plates without deep focus earthquakes, *Bull. Soc. Geol. Fr.*, *26*, 245–254, 1984.

Sykes, L. R., and M. Ewing, The seismicity of the Caribbean region, *J. Geophys. Res.*, *70*, 5065–5074, 1965.

Sykes, L. R., and M. L. Sbar, Intraplate earthquakes, lithospheric stresses and the driving mechanism of plate tectonics, *Nature*, *245*, 298–302, 1973.

Sykes, L. R., W. R. McCann, and A. L. Kafka, Motion of Caribbean plate during the last 7 million years and implications for earlier Cenozoic movements, *J. Geophys. Res.*, *87*, 10,656–10,676, 1982.

Taylor, B., Bismarck Sea: Evolution of a back-arc basin, *Geology*, *7*, 171–174, 1979.

Taylor, B., and G. D. Karner, On the evolution of marginal basins, *Rev. Geophys.*, *21*, 1727–1741, 1983.

Taylor, B., D. Hussong, and P. Fryer, Rifting of the Bonin Arc (abstract) *Eos Trans. AGU*, *65*, 1006, 1984.

Tharp, T. M., Mechanical analysis of the Mexican Ridges foldbelt (abstract) *Eos Trans. AGU*, *66*, 376, 1985.

Thornburg, T., and L. D. Kulm, Sedimentary basins of the Peru continental margin: Structure, stratigraphy, and Cenozoic tectonics from 6°S to 16°S latitude, Nazca Plate: Crustal Formation and Andean Convergence, *Mem. Geol. Soc. Am.*, *154*, 393–422, 1981.

Tilton, G. R., C. A. Hopson, and J. E. Wright, Uranium-lead isotopic ages of the Samail ophiolite, with applications to Tethyan ocean ridge tectonics, Oman, *J. Geophys. Res.*, *86*, 2763–2775, 1981.

Times, *Atlas of the World*, Times Books, London, 1975.

Tjia, H. D., The Lembang Fault, West Java, *Geol. Mijnbouw*, *47*, 126–130, 1968.

Toksöz, M. N., and A. T. Hsui, Numerical studies on back-arc convection and the formation of marginal basins, Numerical Modeling in Geodynamics, *Tectonophysics*, *50*, 177–196, 1978.

Toksöz, M. N., N. H. Sleep, and A. T. Smith, Evolution of the downgoing lithosphere and the mechanisms of deep focus earthquakes, *Geophys. J. R. Astron. Soc.*, *35*, 285–310, 1973.

Tomblin, J. F., Lesser Antilles, in *Mesozoic-Cenozoic Orogenic Belts*, edited by A. M. Spencer, pp. 663–670, Scottish Academic Press, Edinburgh, 1974.

Tovish, A., and G. Schubert, Island arc curvature, velocity of convergence and angle of subduction, *Geophys. Res. Lett.*, *5*, 329–332, 1978.

Tovish, A., G. Schubert, and B. P. Luyendyk, Mantle flow pressure and the angle of subduction: Non-Newtonian corner flows, *J. Geophys. Res.*, *83*, 5892–5898, 1978.

Udias, A., and W. Stauder, Application of numerical method for *S*-wave focal mechanism determinations to earthquakes of Kamchatka-Kurile Islands region, *Bull. Seismol. Soc. Am.*, *54*, 2049–2065, 1964.

Utsu, T., Distribution of earthquakes in and around Japan, *Kagaku Tokyo*, *44*, 739–746, 1974.

Uyeda, S., Subduction zones: Their diversity, mechanism and human impacts, *GeoJournal*, *8*, 381–406, 1984.

Uyeda, S., and Z. Ben-Avraham, Origin and development of the Philippine Sea, *Nature*, *240*, 176–178, 1972.

Uyeda, S., and K. Horai, Terrestrial heat flow in Japan, *J. Geophys. Res.*, *69*, 2121–2141, 1964.

Uyeda, S., and H. Kanamori, Back-arc opening and the mode of subduction, *J. Geophys. Res.*, *84*, 1049–1061, 1979.

Uyeda, S., and R. McCabe, A possible mechanism of episodic spreading of the Philippine Sea, in *Accretion Tectonics in the Circum-*

Pacific Regions, edited by M. Hashimoto and S. Uyeda, pp. 291–306, Terra Scientific Publishing, Tokyo, 1983.

Uyeda, S., and C. Nishiwaki, Stress field, metallogenesis and mode of subduction, The Continental Crust and Its Mineral Deposits, *Spec. Pap. Geol. Assoc. Can., 20*, 323–339, 1980.

Viniegra, F., Age and evolution of salt basins of southeastern Mexico, *Am. Assoc. Pet. Geol. Bull., 55*, 478–494, 1971.

Vink, G. E., W. J. Morgan, and W.-L. Zhao, Preferential rifting of continents: A source of displaced terranes, *J. Geophys. Res., 89*, 10,072–10,076, 1984.

Vlaar, N. J., and M. J. R. Wortel, Lithospheric aging, instability, and subduction, *Tectonophysics, 32*, 331–351, 1976.

von Huene, R., Tectonic processes along the front of modern convergent margins—Research of the past decade, *Annu. Rev. Earth Planet. Sci., 12*, 359–381, 1984.

von Huene, R., et al., Leg 67: The Deep Sea Drilling Project Mid-America Trench transect off Guatemala, *Geol. Soc. Am. Bull., 91*, 421–432, 1980.

von Huene, R., M. Langseth, N. Nasu, and H. Okada, Summary of Cenozoic tectonic history along the IPOD Japan Trench transect, *Geol. Soc. Am. Bull., 93*, 829–846, 1982.

Ward, P. L., J. Gibbs, D. Harlow, and A. Aburto Q., Aftershocks of the Managua, Nicaragua, earthquake and the tectonic significance of the Tiscapa Fault, *Bull. Seismol. Soc. Am., 64*, 1017–1029, 1974.

Watts, A. B., J. K. Weissel, and R. L. Larson, Sea-floor spreading in marginal basins of the western Pacific, *Tectonophysics, 37*, 167–181, 1977.

Weaver, C. S., and S. W. Smith, The St. Helens seismic zone: A major crustal fault zone in western Washington (abstract), *Eos Trans. AGU, 62*, 966, 1981.

Weissel, J. K., Evidence for Eocene oceanic crust in the Celebes Basin, in *The Tectonic and Geologic Evolution of Southeast Asian Seas and Islands, Part 1, Geophys. Monogr. Ser.*, vol. 23, edited by D. E. Hayes, pp. 37–47, *AGU*, Washington, D. C., 1980*a*.

Weissel, J. K., Evolution of the Lau Basin by the growth of small plates, in *Island Arcs, Deep Sea Trenches, and Back-Arc Basins, Maurice Ewing Ser.*, vol. 1, edited by M. Talwani and W. C. Pitman III, pp. 429–436, AGU, Washington, D. C., 1980*b*.

Weissel, J. K., Magnetic lineations in marginal basins of the west Pacific, *Philos. Trans. R. Soc. London, Ser. A., 300*, 223–247, 1981.

Weissel, J. K., and R. N. Anderson, Is there a Caroline plate?, *Earth Planet. Sci. Lett., 41*, 143–158, 1978.

Weissel, J. K. B. Taylor, and G. D. Karner, The opening of the Woodlark Basin, subduction of the Woodlark spreading system, and the evolution of northern Melanesia since mid-Pliocene time, *Tectonophysics, 87*, 253–277, 1982.

Wellman, H. W., Age of Alpine Fault, New Zealand, *Int. Geol. Congr. 22nd, Part IV*, 148–162, 1964.

White, R. S., Deformation of the Makran continental margin, in *Geodynamics of Pakistan*, edited by A. Farah and K. A. DeJong, pp. 295–304, Geological Survey of Pakistan, Quetta, 1979.

Wilson, D. S., R. N. Hey, and C. E. Nishimura, Propagation as a mechanism of ridge reorientation in the Juan de Fuca area (abstract), *Eos Trans. AGU, 65*, 330, 1984.

Wilson, J. T., and K. Burke, Two types of mountain building, *Nature, 239*, 448–449, 1972.

Wortel, M. J. R., and N. J. Vlaar, Age-dependent subduction of oceanic lithosphere beneath western South America, *Phys. Earth Planet. Inter., 17*, 201–208, 1978.

Yoshii, T., A detailed cross section of the deep seismic zone beneath northeastern Honshu, Japan, *Tectonophysics, 55*, 349–360, 1979.

Zoback, M. L., and M. Zoback, State of stress in the coterminous United States, *J. Geophys. Res., 85*, 6113–6156, 1980.

R. D. Jarrard, Lamont-Doherty Geological Observatory, Palisades, NY 10964.

(Received June 28, 1985;
accepted December 9, 1985.)